Uniwersytet Łódzki

Wydział Chemii

Katedra Chemii Nieorganicznej i Analitycznej

Zakład Analizy Instrumentalnej

WYKORZYSTANIE TECHNIK WOLTAMPEROMETRYCZNYCH W ELEKTROANALIZIE I BADANIACH INTERAKCJI DNA

mgr Kamila Morawska

ROZPRAWA DOKTORSKA

Promotor: prof. dr hab. Witold Ciesielski

Promotor pomocniczy: dr Sylwia Smarzewska

Łódź 2021

Podziękowania

Na powstanie niniejszej pracy doktorskiej i jej ostateczny kształt miało wpływ wiele osób, którym chciałabym w tym miejscu podziękować.

*Dziękuję mojemu promotorowi Panu **prof. dr hab. Witoldowi Ciesielskiemu** za opiekę, cenne uwagi i sugestie, a także za stworzenie niezwykle miłej atmosfery w trakcie przygotowywania niniejszej pracy.*

*Szczególne wyrazy wdzięczności składam **dr Sylwii Smarzewskiej**, bez której moja praca doktorska nie mogłaby powstać. Dziękuję Pani Doktor za wsparcie i przyjaźń, wyrozumiałość i nigdy niekończącą się cierpliwość. Dziękuję za zaangażowanie, życzliwość, za niezliczone godziny dyskusji, a także za inspiracje do badań i dalszych poszukiwań.*

*Pragnę podziękować również **pracownikom Zakładu Analizy Instrumentalnej** za życzliwość, wszelką pomoc i ciepłą atmosferę.*

Moim Najbliższym natomiast dziękuję za okazaną cierpliwość, wsparcie i wiarę w moje możliwości.

*Niniejszą rozprawę doktorską dedykuję **Mojej Mamie**.*

Spis treści

Wykaz skrótów stosowanych w tekście:

BDDE – elektroda diamentowa domieszkowana borem

bufor BR – bufor Brittona-Robinsona

CAS - Chemical Abstract System

CV – woltamperometria cykliczna

cv - współczynnik zmienności

D_f – współczynnik dyfuzji

DNA – kwas deoksyrybonukleinowy

dsDNA – dwuniciowy DNA

ΔG^0 - zmiana entalpii swobodnej Gibbsa

GCE – elektroda z węgla szklistego

GPES - General Purpose Electrochemical System

Hg(Ag)FE - elektroda srebrna z odnawialnym filmem amalgamatu srebra

HPLC-UV – wysokosprawna chromatografia cieczowa z detektorem UV

I_p – natężenie prądu piku

K- stała wiązania

k^0 - heterogeniczna stała szybkości reakcji

Lct - laktofen

Lmt – lamotrygina

LOD – granica wykrywalności

LOQ – granica oznaczalności

Met – metoksyfenozyd

PBS - roztwór chlorku sodu buforowany fosforanami (z ang. *Phosphate-buffered saline*)

Sez – sezamol

ssDNA – jednoniciowy DNA

SWSV – woltamperometria fali prostokątnej, z zatężaniem

SWV – woltamperometria fali prostokątnej

v – szybkość skanowania

Autoreferat

Wstęp

W roku 2015, w bazie *Chemical Abstract System* (CAS) sklasyfikowanych było łącznie około 100 milionów substancji chemicznych [1, 2]. Obecnie, w roku 2021, baza ta liczy już ponad 176 milionów substancji [2]. Dane te, bezsprzecznie wskazują na prędkość z jaką następuje chemizacja naszego otoczenia, co więcej, należy przypuszczać, iż tendencja ta nie zmieni się na przestrzeni najbliższych dekad. Szacuje się, że to każdy z nas, w ciągu swojego życia, może mieć styczność z około milionem związków chemicznych na poziomie stężeń powyżej 10^{-12}% [3]. Masowa produkcja nowych substancji chemicznych jest niebezpieczna zarówno dla organizmów żywych jak i dla środowiska, gdyż mimo badań towarzyszących syntezom i wprowadzaniu produktów na rynek, nigdy nie możemy być pewni skutków długotrwałego narażenia. Co więcej, gwałtowny rozwój przemysłu jest ściśle powiązany z wytwarzaniem ogromnych ilości ścieków i odpadów chemicznych, których częściowej emisji do otoczenia, nie jesteśmy w stanie uniknąć. Odpady te, po wniknięciu do ekosystemów naturalnych, mogą być szkodliwe dla środowiska i organizmów w nim żyjących, nadto, mogą ulegać migracjom i przekształceniom, trudnym do przewidzenia i w przebiegu i w skutkach. Powszechne narażenie na szeroko rozumiane chemikalia oraz ich potencjalna toksyczność sprawiają, iż chemia analityczna odgrywa niezwykle ważną rolę i wszystko wskazuje na to, że w ciągu najbliższych lat jej znaczenie będzie, niestety, dynamicznie rosnąć. Współczesna chemia analityczna jest nauką interdyscyplinarną, wykorzystującą metody chemiczne, fizyczne i biologiczne [4], do ilościowego i jakościowego analizowania materii. Trudno jest obecnie wskazać dziedziny nauki bądź techniki, które nie korzystają z osiągnięć chemii analitycznej. Złożone, chemiczne procesy przemysłowe wymagają stałego monitorowania, medycyna natomiast, szybkiej i wiarygodnej diagnostyki. Analiza gleb, wód czy ścieków daje możliwość oceny poziomu zanieczyszczeń środowiska a analiza żywności pozwala na określenie jakości danego produktu, poprzez oznaczenie ilości substancji o charakterze prozdrowotnym.

Dynamiczny wzrost ilości związków chemicznych dopuszczonych do powszechnego użytku, sprawia, iż niezwykle istotne staje się opracowanie nowych procedur analitycznych o odpowiednich parametrach walidacyjnych. W tym celu wykorzystuje się szereg technik analitycznych, na czele z technikami chromatograficznymi. Dużą popularnością cieszą się także techniki elektrochemiczne, co jest związane z ich wysoką czułością, krótkim czasem analiz oraz stosunkowo niedrogą aparaturą o dużym potencjale

miniaturyzacyjnym. Technika woltamperometrii fali prostokątnej (SWV) jest jedną z najczęściej stosowanych i najbardziej zaawansowanych technik woltamperometrycznych. Łączy ona zalety woltamperometrii cyklicznej (CV) jak i technik impulsowych, wskutek czego odgrywa znaczącą rolę w badaniach analitycznych, gwarantując wysoką czułość pomiarów, nawet do 10^{-12} mol L^{-1} [5]. Ze względu na swoje szczególne właściwości techniki woltamperometryczne mogą być wykorzystywane nie tylko w analizie chemicznej. W literaturze znaleźć można liczne doniesienia opisujące ich wykorzystanie np. do badań kinetyki czy mechanizmów reakcji elektrodowych [6, 7]. Mając na względzie temat niniejszej dysertacji nie można nie wspomnieć o wykorzystaniu technik elektrochemicznych w badaniach interakcji jakim ulega kwas deoksyrybonukleinowy [8, 9]. Oceniając wpływ DNA na sygnały pochodzące od danej substancji można wyciągnąć wiele wartościowych wniosków. W przypadku leków, konkluzje te mogą przyczynić się do syntezy leków bardziej specyficznych i/lub wykazujących mniejszą ilość efektów ubocznych. W przypadku środków ochrony roślin, wiedza na temat interakcji z DNA, może pomóc ograniczyć stosowanie preparatów wykazujących toksyczność względem organizmów żywych. Zasadność wykorzystania technik woltamperometrycznych w badaniach interakcji opiera się głównie na podobieństwach występujących pomiędzy reakcjami elektrochemicznymi a biologicznymi. Podobieństwa te, dały podstawy do założenia, że mechanizm utleniania na powierzchni elektrody odbywa się na podobnych zasadach co w organizmach żywych. Badania elektrochemiczne oddziaływań DNA z farmaceutykami czy pestycydami dostarczają wielu użytecznych informacji i stanowią cenne uzupełnienie powszechnych badań spektroskopowych. Wyjaśnienie mechanizmu interakcji zachodzących pomiędzy danym związkiem chemicznym a DNA opiera się na analizie różnic obserwowanych pomiędzy aktywnością elektrochemiczną związku rejestrowaną, przed i po dodatku DNA. Wykorzystując techniki woltamperometryczne w tego typu analizach można uzyskać informacje o typie zachodzących interakcji, a także oszacować wartości stałych wiązania czy stabilność powstających kompleksów analit-DNA.

Tematyka i cel badań

Niniejsza dysertacja opisuje badania prowadzone w ramach dwóch postawionych celów. Pierwszy cel pracy można zdefiniować jako opracowanie elektrochemicznych metod oznaczania wybranych związków chemicznych zaliczanych do różnych klas (pestycydy, lek oraz naturalnie występujący antyoksydant), drugi zaś jako uzupełnienie tych badań o analizę interakcji związek-DNA przeprowadzoną dla substancji przenikających do środowiska.

Analizowane substancje przenikające, były szczególnie niebezpieczne dla organizmów wodnych, za zasadne uznano zatem, by wyjaśnić mechanizm interakcji między wybranymi związkami a materiałem genetycznym narażonych organizmów. Badania elektrochemiczne prowadzono wykorzystując woltamperometrię fali prostokątnej oraz woltamperometrię cykliczną. W toku badań wykorzystano różne materiały elektrodowe (węgiel szklisty, srebro i jego amalgamat, diament domieszkowany borem). Realizacja opisanych celów wymagała opracowania metod oznaczania badanych związków, ich walidacji, określenia wpływu substancji potencjalnie przeszkadzających oraz analizy interakcji z DNA.

Obiekty badań

W niniejszej rozprawie doktorskiej obiektami badań były cztery związki, których wzory strukturalne przedstawiono na Rysunku 1.
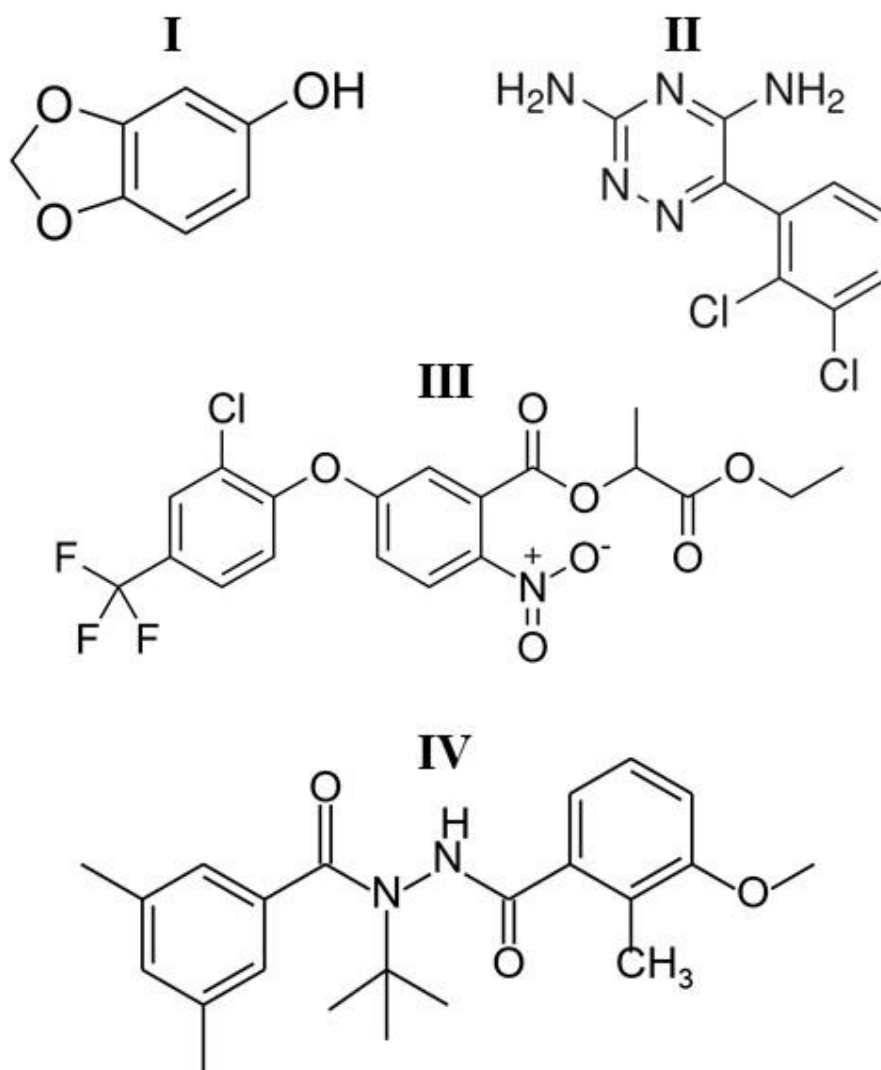
*Rys. 1 (**I**) sezamol; (**II**) lamotrygina; (**III**) laktofen; (**IV**) metoksyfenozyd.*

Sezamol (*Sez*) jest naturalnym antyoksydantem występującym w oleju sezamowym, gdzie jego zawartość waha się od 50 do 100 mg kg^{-1} oleju [10]. Sezamol efektywnie neutralizuje wolne rodniki, co sprawia, że przypisuje mu się szereg właściwości prozdrowotnych. Wykazuje on przede wszystkim ochronne działanie na komórki wątroby, stanowi także ochronę przeciwnowotworową. Ponadto, zawartość sezamolu wywiera istotny wpływ na smak oraz barwę oleju sezamowego, przez co stanowi ważny czynnik warunkujący jakość tłoczonego oleju [11, 12]. Po wnikliwym

przeglądzie literatury można stwierdzić, że opracowane dotychczas metody oznaczania *Sez* wykorzystują głównie techniki chromatograficzne [13, 14]. Pojawiły się także nieliczne doniesienia opisujące elektrochemiczne badania tego związku [15, 16], m.in. woltamperometryczna metoda oznaczania sezamolu w próbkach chałwy sezamowej [17]. Artykuł opublikowany przez autora niniejszej dysertacji w czasopiśmie Food Chemistry, zatytułowany „*Rapid electroanalytical procedure for sesamol determination in real samples*" [18], stanowi natomiast pierwszą elektrochemiczną procedurę oznaczania *Sez* w próbkach oleju sezamowego.

Lamotrygina jest lekiem przeciwpadaczkowym o szerokim spektrum aktywności. Mechanizm działania *Lmt* polega na stabilizacji błon neuronalnych poprzez blokowanie potencjałozależnych kanałów sodowych, co w konsekwencji hamuje uwalnianie pobudzających neuroprzekaźników [19, 20]. Lamotryginę stosuje się w leczeniu napadów toniczno−klonicznych czy zespołu Lennoxa−Gestauta. Dodatkowo, jest wykorzystywana jako lek normotymiczny u osób z chorobą afektywną dwubiegunową oraz w zapobieganiu atakom migreny. W literaturze opisuje się szereg działań niepożądanych, które mogą wystąpić w trakcie terapii, w tym m.in: gorączkę, zawroty i bóle głowy, biegunkę czy zmęczenie [19].

Na podstawie przeprowadzonej analizy bibliograficznej można stwierdzić, iż opublikowano dotychczas szereg procedur oznaczania lamotryginy, w tym kilka, wykorzystujących techniki woltamperometryczne [21-23]. Mając na względzie powyższe, uznano za bezcelowe opracowanie kolejnej elektrochemicznej metody oznaczania *Lmt*. Badając ten związek, za priorytet uznano zatem analizę interakcji *Lmt*-DNA. Wyniki wspomnianych badań opublikowano w artykule „*Interactions of lamotrigine with single- and double-stranded DNA under physiological conditions*" w czasopiśmie Bioelectrochemistry [24].

Laktofen (*Lct*) to herbicyd należący do grupy eterów difenylowych. Jest on powszechnie stosowany do zwalczania chwastów szerokolistnych w uprawie soi, zbóż oraz ziemniaków. Związek ten wykazuje niewielką toksyczność po wniknięciu do organizmu człowieka, drogą pokarmową lub oddechową. Powoduje natomiast podrażnienia skóry, w tym jej zaczerwienienie i obrzęk. Laktofen, stanowi ponadto czynnik drażniący dla oczu, a częsta ekspozycja na jego opary może prowadzić nawet do trwałego uszkodzenia wzroku. Na podstawie licznych badań wykazano, że *Lct* nie jest toksyczny dla ptaków i pszczół. Niekorzystnie wpływa natomiast na ekosystemy wodne [25].

Metoksyfenozyd (*Met*), podobnie jak laktofen, zaliczany jest do środków ochrony roślin. Jest to powszechnie stosowany insektycyd, który znalazł zastosowanie w uprawie winogron, kukurydzy, pomidorów, a także wybranych zielonych warzyw liściastych [26]. *Met* wykazuje bardzo wysoką skuteczność owadobójczą przeciwko szerokiej gamie gąsienic szkodliwych gatunków motyli. Na skutek wysokiego powinowactwa do receptora ekdyzonu tych owadów, wywołuje on przedwczesne linienie, a tym samym śmierć szkodnika [27]. Metoksyfenozyd nie jest toksyczny dla ssaków, ptaków czy pszczół miodnych. Udowodniono jednakże, iż stanowi poważne zagrożenie dla organizmów wodnych i dżdżownic. Mając na względzie właściwości chemiczne i fizyczne metoksyfenozydu, istnieje znaczące ryzyko przenikania tego związku do wód gruntowych i innych zbiorników wodnych, co stwarza bezpośrednie zagrożenie dla bytujących tam organizmów.

Obydwa badane pestycydy (laktofen oraz metoksyfenozyd) analizowano dotychczas głównie z wykorzystaniem technik chromatograficznych [28-30]. Dokonując przeglądu literatury nie znaleziono metod oznaczania żadnego z tych związków opartych na technikach woltamperometrycznych. Artykuły składające się na niniejszą rozprawę doktorską („*Lactofen – electrochemical sensing and interaction with dsDNA*" [31] oraz „*First electroanalytical studies of methoxyfenozide and its interactions with dsDNA*" [32]), opisują zatem pierwsze, elektrochemiczne metody oznaczania *Lct* oraz *Met* w próbkach wody. Dodatkowo, ze względu na potencjalną toksyczność tych związków dla organizmów wodnych, w niniejszych pracach przedstawiono również analizę ich interakcji z DNA wyizolowanym ze spermy łososia.

Układ pomiarowy

Badania woltamperometryczne prowadzono z wykorzystaniem potencjostatu µAutolab Typ III (Metrohm−EcoChemie, Holandia), sterowanego oprogramowaniem GPES (General Purpose Electrochemical System, wersja 4.9). W pomiarach wykorzystano klasyczny układ trójelektrodowy, gdzie:

- ✓ nasycona elektroda chlorosrebrowa Ag/AgCl (3 mol L^{-1} KCl) stanowiła elektrodę odniesienia,
- ✓ drut platynowy pełnił funkcję elektrody pomocniczej,
- ✓ elektrodę pracującą stanowiła:
    - ▪ elektroda z węgla szklistego (GCE_1) (BASi, USA, $\phi = 3$ mm),
    - ▪ elektroda z węgla szklistego (GCE_2) (Mineral, Polska, $\phi = 3$ mm),
    - ▪ elektroda diamentowa domieszkowana borem (BDDE) (Windsor Scientific Ltd., UK, $\phi = 3$ mm),
    - ▪ elektroda srebrna z odnawialnym filmem amalgamatu srebra (Hg(Ag)FE) (mtm anko, Polska)

Badania interakcji z DNA prowadzono także z wykorzystaniem spektrofotometru Cary 100 Bio (Agilent, USA).

Woltamperometryczna analiza wybranych związków biologicznie czynnych

Analizę badanych związków prowadzono stosując technikę SWV [18, 24, 31, 32] oraz technikę woltamperometrii fali prostokątnej, z zatężaniem (SWSV) [31]. Dodatkowo, w celu wyjaśnienia natury zachodzących procesów elektrodowych wykorzystano technikę woltamperometrii cyklicznej [18, 24, 31, 32].

Badania wstępne

Woltamperometryczne oznaczanie badanych związków rozpoczynano od doboru elektrolitu podstawowego, nie ulega bowiem wątpliwości, że jego skład i pH jest jednym z głównych czynników warunkujących optymalne ukształtowanie sygnałów. W toku badań testowano różne elektrolity podstawowe tj. bufory Brittona−Robinsona (BR), bufory cytrynianowe, bufory cytrynianowo−fosforanowe, bufory chlorkowe, bufory boranowe, TRIS, bufory fosforanowe oraz roztwory kwasów solnego i siarkowego. Ze względu na szeroki zakres dostępnych wartości pH (2−10), bufor Brittona−Robinsona był elektrolitem pierwszego wyboru, umożliwiającym znalezienie optymalnego stężenia jonów wodorowych dla konkretnej analizy. Po znalezieniu optymalnego pH buforu BR, sprawdzano wpływ innych buforów bądź kwasów o zbliżonym stężeniu jonów wodorowych, na rejestrowane sygnały pochodzące od analizowanego związku. Mając na względzie kształt oraz wysokość rejestrowanych prądów pików dokonywano wyboru optymalnego elektrolitu podstawowego. Uzyskane rezultaty zestawiono w tabeli 1. Wyjątek stanowiły badania lamotryginy, których celem była przede wszystkim analiza interakcji z DNA. W badaniach *Lmt* nie przeprowadzano zatem optymalizacji pH, użyto natomiast buforu zalecanego do tego typu badań, tj. roztworu chlorku sodu buforowanego fosforanami (PBS, z ang. *Phosphate−buffered saline*). Warto w tym miejscu nadmienić, że w zastosowanym elektrolicie uzyskane sygnały pochodzące od redukcji *Lmt* były dobrze ukształtowane oraz cechowały się dużą wartością natężenia prądu piku.

Tabela 1. Zestawienie wybranych elektrolitów podstawowych

Badany związek	Elektroda pracująca	Potencjał piku V	Elektrolit podstawowy	pH elektrolitu podstawowego
Lct	GCE$_1$	−0.25	bufor BR	2.0
	Hg(Ag)FE	−0.48	bufor boranowy	8.5
Sez	GCE$_2$	0.69	HCl$_{aq}$	0.7
Lmt	GCE$_1$	−1.05	PBS	7.4
Met	BDDE	1.51	bufor BR	3.0

Dobór parametrów technik SWV oraz SWSV

W kolejnym kroku, tuż po doborze elektrolitu podstawowego, prowadzono optymalizację parametrów techniki pomiarowej. Etap ten pozwalał na poprawę morfologii i wysokości rejestrowanych sygnałów, przyczyniając się do zwiększania czułości analizy. Procesowi optymalizacji poddawano parametry takie jak: amplituda, częstotliwość, krok potencjału. Dodatkowo w trakcie analizy laktofenu na elektrodzie Hg(Ag)FE zoptymalizowano potencjał zatężania oraz czas zatężania. W trakcie tych analiz zmieniano wartość jednego z wyżej wymienionych parametrów, podczas gdy wartości pozostałych utrzymywano na stałym poziomie. Otrzymane wyniki zebrano w tabeli 2.

Tabela 2. Zestawienie wybranych parametrów technik pomiarowych

Badany związek	Elektroda pracująca	Amplituda mV	Krok potencjału mV	Częstotliwość Hz	Potencjał zatężania V	Czas zatężania s
Lct	GCE$_1$	50	3	40	−	−
	Hg(Ag)FE	50	7	100	−0.25	30
Sez	GCE$_2$	30	6	10	−	−
Lmt	GCE$_1$	30	6	25	−	−
Met	BDDE	30	4	25	−	−

<u>Walidacja opracowanych metod analitycznych</u>

Wykorzystując zoptymalizowane uprzednio warunki eksperymentu, wyznaczano zakres liniowej zależności natężenia prądu piku od stężenia dla każdego z badanych związków. Na podstawie wykreślonych prostych wzorcowych wyznaczano granice wykrywalności (LOD, z ang. *limit of detection*) oraz granice oznaczalności (LOQ, z ang. *limit of quantification*), korzystając z następującego wzoru: kSD/b, gdzie b − nachylenie krzywej kalibracyjnej, SD − odchylenie standardowe wyrazu wolnego, k=3 dla LOD, k=10 dla LOQ [33]. Otrzymane zależności zestawiono w tabeli 3. W tym miejscu warto przypomnieć, iż badania laktofenu wykonywano zarówno techniką SWV jak i SWSV, wykorzystując dwie elektrody robocze. Rezultaty uzyskane na elektrodzie z węgla szklistego w połączeniu z techniką woltamperometrii fali prostokątnej były niezadowalające. Cechował je bardzo wąski zakres liniowej odpowiedzi, co przedstawiono w tabeli 3. W konsekwencji nie wykorzystano tej metody w dalszych badaniach tego związku. Najniższą granicę wykrywalności dla laktofenu uzyskano na elektrodzie Hg(Ag)FE przy użyciu techniki SWSV, w związku z tym ta procedura została wykorzystana do analizy próbek rzeczywistych.

Tabela 3.Zestawienie wyników uzyskanych podczas woltamperometrycznego oznaczania badanych związków

Badany związek	Elektroda pracująca	Zakres liniowości mol L^{-1}	LOD mol L^{-1}	LOQ mol L^{-1}
Lct	GCE$_1$	$1.0 \times 10^{-6} - 4.0 \times 10^{-6}$	2.8×10^{-7}	9.5×10^{-7}
	Hg(Ag)FE (SWSV)	$1.0 \times 10^{-8} - 1.0 \times 10^{-7}$	2.0×10^{-9}	6.5×10^{-9}
	Hg(Ag)FE (SWV)	$5.0 \times 10^{-8} - 2.5 \times 10^{-7}$	9.5×10^{-9}	3.2×10^{-8}
Sez	GCE$_2$	$3.0 \times 10^{-6} - 1.4 \times 10^{-4}$	7.1×10^{-7}	2.4×10^{-6}
Lmt	GCE$_1$	$1.0 \times 10^{-6} - 1.6 \times 10^{-4}$	2.1×10^{-7}	7.0×10^{-7}
Met	BDDE	$5.0 \times 10^{-7} - 7.0 \times 10^{-5}$	1.4×10^{-7}	4.8×10^{-7}

Analityczne zastosowanie opracowanych procedur

Opracowane metody woltamperometryczne wykorzystano do oznaczania badanych związków w różnorodnych próbkach rzeczywistych. W przypadku oznaczeń analizowanych pestycydów obiektami badań były próbki wody wodociągowej i rzecznej, z dodatkiem analitu [31, 32]. Dodatkowo, mając na uwadze fakt, że metoksyfenozyd jest wykorzystywany w uprawach winogron, wykonano również analizy soku winogronowego wzbogaconego o analit [32]. Do oznaczeń sezamolu wykorzystano próbki oleju sezamowego, gdyż związek ten jest naturalnym składnikiem tego oleju [18]. Próbki oleju poddawano uprzednio procesowi ekstrakcji [13]. Stężenia badanych związków wyznaczano stosując metodę wielokrotnego dodatku wzorca, uzyskane rezultaty zestawiono w tabeli 4.

Jako metodę porównawczą do oznaczania sezamolu w próbkach oleju zastosowano wysokosprawną chromatografię cieczową z detektorem UV (HPLC−UV), uzyskując zgodne wyniki [18].

Mając na względzie liczne doniesienia literaturowe dotyczące woltamperometrycznego oznaczania lamotryginy, nie przeprowadzono analizy tego związku w próbkach rzeczywistych.

Tabela 4. Zestawienie rezultatów woltamperometrycznego oznaczania badanych związków

w próbkach rzeczywistych

Badany związek	Próbka z dodatkiem analitu	$c_{deklarowane}$ mol L^{-1}	$c_{znalezione}$ mol L^{-1}	Precyzja (cv) %	Odzysk %
Lct	Woda z rzeki Mszanka (Polska)	3.00×10^{-8}	$3.12 \pm 0.13 \times 10^{-8}$	4.3	104
	Woda wodociągowa	3.00×10^{-8}	$3.06 \pm 0.24 \times 10^{-8}$	8.0	102
Met	Woda z rzeki Ljubljanica (Słowenia)	1.00×10^{-5}	$1.05 \pm 0.06 \times 10^{-5}$	4.7	105
		5.00×10^{-6}	$5.09 \pm 0.40 \times 10^{-6}$	7.0	102
		1.00×10^{-6}	$1.05 \pm 0.08 \times 10^{-6}$	6.7	104
	Woda wodociągowa	1.00×10^{-5}	$1.04 \pm 0.01 \times 10^{-5}$	1.0	103
		5.00×10^{-6}	$5.18 \pm 0.29 \times 10^{-6}$	5.0	104
		1.00×10^{-6}	$0.96 \pm 0.04 \times 10^{-6}$	3.7	95.6
	Sok winogronowy	1.00×10^{-5}	$1.05 \pm 0.10 \times 10^{-5}$	8.6	105
		5.00×10^{-6}	$5.19 \pm 0.16 \times 10^{-6}$	2.8	104
		2.50×10^{-6}	$2.57 \pm 0.07 \times 10^{-6}$	2.5	103

Badany związek	Nr próbki	Technika	$c_{znalezione}$ mg kg oleju^{-1}	$c_{znalezione}$ mol L^{-1}	Precyzja (cv) %	E_1^* %
Sez	1	SWV	73.9 ± 4.6	$1.12 \pm 0.07 \times 10^{-4}$	5.6	1.9
		HPLC−UV	72.5 ± 1.9	$1.09 \pm 0.03 \times 10^{-4}$	2.6	
	2	SWV	66.5 ± 2.5	$1.00 \pm 0.04 \times 10^{-4}$	3.4	−1.3
		HPLC−UV	67.4 ± 1.6	$1.02 \pm 0.02 \times 10^{-4}$	2.3	
	3	SWV	n/a	n/a	n/a	n/a
		HPLC−UV	2.2 ± 0.2	$3.4 \pm 0.3 \times 10^{-6}$	7.6	

*Błąd względny $= ((c_{znalezione\ SWV} - c_{znalezione\ HPLC})/\ c_{znalezione\ HPLC}) \times 100.$

Selektywność opracowanych procedur pomiarowych

W toku badań sprawdzono również wpływ obecności innych substancji elektroaktywnych tj. kationów metali i pestycydów, na możliwość oznaczania laktofenu i metoksyfenozydu [31, 32]. Procedura polegała na analizie sygnału pochodzącego od badanego związku (*Lct* lub *Met*), po dodaniu do analizowanego roztworu substancji potencjalnie przeszkadzającej. Stężenia analitów w trakcie badań pozostawały niezmienione ($c_{Lct} = 1.0 \times 10^{-7}$ mol L^{-1}; $c_{Met} = 5.0 \times 10^{-6}$ mol L^{-1}), zmieniano natomiast stężenia interferentów, tak aby odpowiadały one założonemu uprzednio stosunkowi stężeń c_{Lct}/c_{Met} : $c_{Interferent}$. Substancje, testowane jako interferenty, wybrano z uwagi na możliwość ich występowania w badanych próbkach rzeczywistych. W przypadku laktofenu, większość badanych pestycydów nie wykazywała znaczącego wpływy na sygnały pochodzące od redukcji tego związku. Jedynie metam sodu znacząco utrudniał analizę *Lct*, prawdopodobnie ze względu na silną adsorpcję na powierzchni elektrody. Aklonifen natomiast, wpływał na wysokość prądów pochodzących od redukcji laktofenu jedynie przy wyższych stężeniach. Dodatkowo jony Ni^{2+} oraz Cu^{2+} niekorzystnie wpływały na kształt sygnałów analitu w całym zakresie stosowanych stężeń. Selektywność procedury oznaczania metoksyfenozydu testowano w obecności 11 substancji potencjalnie przeszkadzających. Obecność 7 z nich nie wpływała znacząco na sygnały pochodzące od utleniania *Met*. Jony Pb^{2+} i Cu^{2+} w stężeniach większych bądź równych 2.5×10^{-5} mol L^{-1}, a także fenton i profluralin w stężeniach większych bądź równych 5.0×10^{-6} mol L^{-1}, przyczyniały się do obniżenia wartości natężenia prądów pików *Met*.

<u>Badania procesów elektrodowych</u>

W kolejnym etapie, tuż po opracowaniu woltamperometrycznych metod oznaczania wybranych związków, przeprowadzono elektrochemiczne badania procesów zachodzących na elektrodach pracujących, wykorzystując technikę woltamperometrii cyklicznej. W tym celu, sprawdzano wpływ szybkości skanowania na rejestrowane sygnały pochodzące od utleniania bądź redukcji analizowanych substancji. Zestawienie uzyskanych rezultatów przedstawiono w tabeli 5. Zastosowanie przemiatania potencjałem pozwala na scharakteryzowanie rejestrowanych prądów, w tym ustalenie odwracalności procesu utleniania/redukcji badanego związku. W przypadku uzyskania liniowej zależności natężenia prądu piku (I_p) od wartości pierwiastka z szybkości skanowania ($v^{1/2}$) ($I_p = f(v^{1/2})$) uważa się, że etapem limitującym w badanym mechanizmie jest proces dyfuzji depolaryzatora do powierzchni elektrody roboczej. Wzrost wykładniczy funkcji $I_p = f(v^{1/2})$ bądź liniowy funkcji $I_p = f(v)$ świadczy natomiast o zachodzącej adsorpcji depolaryzatora na powierzchni elektrody [34, 35]. Potwierdzeniem dla powyższych korelacji jest analiza nachylenia krzywej zależności logarytmu z natężenia prądu piku od logarytmu z szybkości skanowania ($\log I_p = f(\log v)$). Dla mechanizmów gdzie etapem limitującym jest proces dyfuzji bądź adsorpcji, wartość współczynnika nachylenia prostej $\log I_p = f(\log v)$ powinna wynosić odpowiednio 0.5, 1 [34, 35].

Tabela 5. Charakterystyka procesów zachodzących na elektrodach pracujących

Badany związek	Elektroda pracująca	Odwracalność procesu	Charakter zachodzącego procesu elektrodowego	Wartość nachylenia $\log I_p = f(\log v)$
Lct	GCE$_1$	proces nieodwracalny	dyfuzyjno-adsorpcyjny	
			I_p (μA)= 2.22v (V s^{-1}) + 0.0641 $R^2 = 0.999$	0.80
Sez	GCE$_2$	proces nieodwracalny	dyfuzyjny	
			I_p (μA)= 6.08 $v^{1/2}$ (mV s^{-1})$^{1/2}$ + 0.316 $R^2 = 0.999$	0.44
Lmt	GCE$_1$	proces nieodwracalny	dyfuzyjny	
			I_p (μA)= 5.65 $v^{1/2}$ (mV s^{-1})$^{1/2}$ + 0.178 $R^2 = 0.999$	0.55
Met	BDDE	proces nieodwracalny	dyfuzyjny	
			I_p (μA)= 8.90 $v^{1/2}$ (mV s^{-1})$^{1/2}$ + 0.190 $R^2 = 0.995$	0.49

Badania interakcji DNA

Badania interakcji DNA prowadzono wykorzystując techniki woltamperometryczne (SWV, CV) oraz spektroskopowe (spektrofotometrię UV-Vis). We wszystkich analizach stosowano dwuniciowy kwas deoksyrybonukleinowy wyizolowany ze spermy łososia (dsDNA) [24, 31, 32], a dodatkowo w przypadku lamotryginy analizy urozmaicono o badania interakcji z jednoniciowym DNA (ssDNA) [24]. Roztwór ssDNA przygotowywano poprzez poddanie odpowiedniej obróbce termicznej roztworu dsDNA [36]. Buforem stosowanym w badaniach DNA jest bufor PBS o fizjologicznym pH, w związku z tym został on wykorzystany w analizach interakcji *Lmt*-DNA oraz *Lct*-DNA. Badania interakcji metoksyfenozydu z dsDNA przeprowadzono w środowisku buforu fosforowego o pH 4.5. Było to podyktowane głównie faktem, iż dla wartości pH powyżej 6.0 nie zaobserwowano sygnałów pochodzących od utleniania *Met*, a dodatkowo bufory o pH zbliżonym do 4.5 są również stosunkowo często wykorzystywane w tego typu analizach [37, 38]. Ze względu na fakt, iż badania laktofenu prowadzano z wykorzystaniem różnych elektrod roboczych, warto nadmienić, iż badania interakcji *Lct* z DNA przeprowadzono na elektrodzie Hg(Ag)FE, wykorzystując technikę woltamperometrii fali prostokątnej.

Wykorzystując różnice w elektrochemicznym zachowaniu analizowanych związków w obecności i bez DNA, można dokonać charakterystyki zachodzących interakcji. W tym celu przeprowadza się analizę wartości prądów oraz potencjałów pików pochodzących od utleniania/redukcji badanych związków, w obecności kwasów nukleinowych. Obserwowane obniżenie wartości natężenia prądu piku badanego związku, po dodatku DNA, z dużym prawdopodobieństwem wynika z przyłączenia dużej, wolno dyfundującej cząsteczki DNA do analitu. Powinno to skutkować znaczącym spadkiem współczynnika dyfuzji (D_f). W związku z tym wykorzystując technikę woltamperometrii cyklicznej oszacowano wartości D_f dla analitów w obecności i przy braku obecności DNA [35]. Woltamperogramy cykliczne rejestrowano przy różnych szybkościach skanowania, a stężenia wszystkich reagentów pozostawały niezmienione. D_f w obecności kwasów nukleinowych malał zarówno w przypadku lamotryginy jak i metoksyfenozydu, co potwierdza wcześniejsze założenie o powstawaniu kompleksów pomiędzy badanymi związkami a DNA. Obliczone wartości współczynników dyfuzji dla kompleksów *Lmt* i *Met* z DNA umieszczono w tabeli 6. Dodatkowo, wykorzystując oszacowane wartości D_f, policzono heterogeniczne stałe szybkości reakcji (k^o), na podstawie których można

wnioskować o ewentualnym wpływie DNA na kinetykę reakcji elektrodowej badanego analitu. Wartości k^0 umieszczono w tabeli 6. Na ich podstawie można stwierdzić, iż obecność kwasów nukleinowych wpływa na zdolność przenoszenia elektronów przez wszystkie z badanych związków.

Tabela 6. Zestawienie obliczonych wartości współczynników dyfuzji oraz stałych szybkości reakcji

Badany związek/kompleks	D_f cm^2 s^{-1}	k^0 s^{-1}
Lmt	2.32×10^{-6}	1.1×10^{-2}
Lmt-dsDNA	1.76×10^{-6}	9.0×10^{-3}
Lmt-ssDNA	1.44×10^{-6}	9.1×10^{-3}
Met	6.91×10^{-6}	2.1×10^{-3}
Met-dsDNA	2.09×10^{-6}	1.1×10^{-3}
Lct	−	6.3
Lct-dsDNA	−	2.4

Zmiany wartości natężenia prądów mogą posłużyć także do oszacowania stałej wiązania (*K*), podczas gdy przesunięcia potencjałów pików do określenia typu zachodzących interakcji [39, 40]. Wykorzystując technikę woltamperomterii fali prostokątnej rejestrowano sygnały przy stałym stężeniu analitu i wzrastającym stężeniu DNA. W przypadku wszystkich analizowanych związków (*Lmt*, *Met*, *Lct*) zaobserwowano stopniowe obniżenie wartości rejestrowanych prądów wraz ze wzrostem stężenia DNA. Na podstawie uzyskanych w ten sposób rezultatów oszacowano wartości stałych wiązania powstających kompleksów *Lmt*-dsDNA, *Lmt*-ssDNA oraz *Met*-dsDNA [24, 32]. Procedura pomiaru wyglądała analogicznie przy wykorzystaniu techniki spektrofotometrycznej, co pozwoliło uzyskać wartości stałej wiązania dla celów porównawczych. Obliczone wartości stałych umieszczono w tabeli 7. Wykorzystując uzyskane wartości *K* obliczono energię swobodną Gibbsa ($\Delta G^o = -RT\ln K$)), która to odzwierciedla stabilność powstających kompleksów. Otrzymano ujemne wartości ΔG^o (tab. 7), co świadczy o spontanicznym tworzeniu się kompleksów *Lmt* i *Met* z DNA. W przypadku laktofenu zbadano natomiast, czy obserwowany stopniowy spadek natężenia prądów pików wraz ze wzrastającym stężeniem dsDNA, może zostać wykorzystany w analizie ilościowej dsDNA. Wykazano, że pośrednie oznaczanie dwuniciowego DNA jest możliwe w zakresie jego stężeń 1.0−10.0 ppm. Obliczone wartości granicy wykrywalności i oznaczalności wynosiły odpowiednio 0.3 i 1.0 ppm.

Tabela 7. Zestawienie obliczonych wartości stałych wiązania oraz energii swobodnej Gibbsa

Badany związek	Rodzaj DNA	K_{SWV} M^{-1}	K_{UV-Vis} M^{-1}	ΔG^0_{SWV} $kJ\ mol^{-1}$
Lmt	dsDNA	6.46×10^5	6.93×10^5	-32.59
	ssDNA	1.81×10^6	1.19×10^6	-35.70
Met	dsDNA	3.47×10^7	2.34×10^7	-42.29

W przypadku wszystkich trzech badanych związków zaobserwowano przesunięcia potencjałów pików po dodaniu do naczynka woltamperometrycznego roztworu DNA, co daje możliwość oszacowania typu zachodzących interakcji. Bazując na danych literaturowych, przesunięcie potencjału piku w kierunku potencjałów bardziej dodatnich może świadczyć o zachodzącej interkalacji analitu pomiędzy zasady azotowe kwasu nukleinowego. Przesunięcie natomiast w kierunku potencjałów bardziej ujemnych, daje podstawy do stwierdzenia interakcji na drodze elektrostatycznej [38, 41]. Podczas badań lamotryginy zaobserwowano przesunięcie pików w kierunku potencjałów ujemnych, co pozwoliło na wyciągnięcie wniosku, iż zachodzące interakcje *Lmt*-ds/ssDNA mają głównie charakter elektrostatyczny. Sygnały pochodzące od metoksyfenozydu ulegały przesunięciu w kierunku potencjałów bardziej dodatnich, wskazując na dominujący udział oddziaływań interkalacyjnych. W przypadku badań laktofenu obserwowano przesunięcie potencjałów pików w kierunku potencjałów bardziej ujemnych przy wzrastającym stężeniu dsDNA, co na podstawie aktualnej wiedzy należałoby opisać jako dominujące oddziaływania elektrostatyczne, jednakże artykuł ten stanowił pierwszą pracę z danej tematyki, przez co oddziaływania *Lct*-dsDNA przyporządkowano do typu interkalacyjnego na podstawie znalezionej wówczas literatury. Celem potwierdzenia typu zachodzących interakcji sprawdzono wpływ siły jonowej na oddziaływania pomiędzy lamotryginą a ss/dsDNA i metoksyfenozydem a dsDNA [24, 32]. Taka analiza stanowi

niezwykle cenne uzupełnienie informacji o zachodzących interakcjach [37, 42]. W trakcie tego eksperymentu zwiększano stopniowo stężenie chlorku sodu, podczas gdy stężenia analitów (*Lmt* lub *Met*) i DNA (dsDNA lub ssDNA) pozostawały niezmienione. W przypadku badań interakcji lamotryginy z DNA, zaobserwowano znaczny spadek sygnałów pochodzących od kompleksów *Lmt*-ss/dsDNA wraz ze wzrostem siły jonowej, co potwierdza jednoznacznie elektrostatyczny charakter interakcji. Wzrost siły jonowej nie powodował natomiast znaczących zmian rejestrowanych sygnałów pochodzących od kompleksu *Met*-dsDNA, co również potwierdziło, iż dominującym typem oddziaływań pomiędzy metoksyfenozydem a DNA jest interkalacja. Ostatnim już zagadnieniem było oszacowanie liczby koordynacyjnej powstających kompleksów przy użyciu techniki woltamperometrii fali prostokątnej [43, 44]. Badania takie przeprowadzono dla laktofenu oraz lamotryginy. W przeciwieństwie do poprzednich eksperymentów, w trakcie pomiaru utrzymywano stałe stężenie DNA, podczas gdy stężenia analitów stopniowo zwiększano. Na podstawie uzyskanych zależności, stwierdzono iż na jednostkę budulcową DNA przypada 1 cząsteczka lamotryginy a 2 cząsteczki laktofenu [24, 31].

Podsumowanie

Przedstawione w niniejszej pracy doktorskiej badania, które zostały opisane cyklem publikacji, ukazują dwa odrębne kierunki praktycznego wykorzystania technik woltamperometryczych. Pierwszy z nich dotyczy opracowania elektrochemicznych metod oznaczania badanych związków, drugi natomiast ukazuje możliwość analizy interakcji z DNA przy użyciu technik woltamperometrycznych. Obiektami badań, w omawianym cyklu publikacji, były związki o znaczeniu biologicznym, takie jak: sezamol, lamotrygina, laktofen oraz metoksyfenozyd. Badania sezamolu opisują wykorzystanie technik woltamperometrycznych w celach analitycznych. W przypadku lamotryginy, przedstawione rezultaty dotyczą głównie analizy interakcji z DNA. Badania laktofenu i metoksyfenozydu łączą natomiast obydwa zagadnienia, to znaczy opracowano dla nich metody oznaczania jak i przeprowadzono analizę interakcji DNA.

Do opracowania analitycznych metod oznaczania powyższych związków wykorzystano technikę woltamperometrii fali prostokątnej. Badania prowadzono z wykorzystaniem różnych elektrod roboczych. Dla każdego z badanych związków zoptymalizowano warunki oraz parametry pomiaru, następnie wykreślono zakres liniowej odpowiedzi natężenia prądu piku od stężenia każdego analitu. Wyznaczono granice wykrywalności i oznaczalności opracowanych procedur a ich poprawność zweryfikowano poprzez oznaczenie badanych związków w różnorodnych próbkach rzeczywistych (olej sezamowy, woda rzeczna, woda wodociągowa, sok winogronowy). Dodatkowo, celem uzyskania szczegółowych informacji dotyczących charakteru zachodzących procesów elektrodowych, wykonano szereg badań z wykorzystaniem techniki woltamperometrii cyklicznej. Podsumowując część analityczną pracy, można stwierdzić, iż opracowane procedury elektroanalityczne są szybkie, łatwe, stosunkowo tanie oraz pozwalają na monitorowanie stężeń omawianych związków w różnorodnych próbkach rzeczywistych.

Badania interakcji z DNA cieszą się ostatnio dużym zainteresowaniem w świecie nauki. Techniki spektroskopowe bez wątpienia wiodą prym w tego typu analizach, niemniej jednak z roku na rok pojawia się coraz więcej publikacji wykorzystujących techniki elektrochemiczne. W niniejszej pracy doktorskiej przedstawiono praktyczne podejście wykorzystujące techniki woltamperometryczne do analizy interakcji DNA. W tym celu, wykorzystano technikę woltamperometrii cyklicznej jak i fali prostokątnej. Badania polegały na analizie sygnałów pochodzących od omawianych związków po dodaniu

do naczynka woltamperometrycznego roztworu DNA. Uzyskane rezultaty pozwoliły oszacować typ zachodzących interakcji oraz obliczyć stałą wiązania analit-DNA. Na podstawie przeprowadzonych analiz można stwierdzić z całą pewnością, iż techniki woltampetrometryczne dają możliwość analizy interakcji z DNA, a sama procedura takich badań nie jest skomplikowana.

Bibliografia

(kolorem niebieskim zaznaczono publikacje stanowiące treść rozprawy doktorskiej)

[1] J. Namiesnik, Rola i zadania chemii analitycznej w zakresie technologii chemicznej, Przemysl Chemiczny, 94 (2015) 117-119.

[2] Chemical Abstracts Service, CAS content. http://www.cas.org/about/cas−content (dostęp 04.02.2021).

[3] Z. Witkiewicz, J. Kałużna-Czaplinska, Podstawy chromatografii i technik elektromigracyjnych, 5 ed., Wydawnictwo WNT, Warszawa, 2012.

[4] E. Hywel, M. Foulkes, Chemia analityczna : podejście praktyczne, Wydawnictwo Naukowe PWN, Warszawa, 2020.

[5] V. Mirceski, S. Komorsky-Lovric, M. Lovric, Square-Wave Voltammetry: Theory and Applications, Springer, Heidelberg, 2007.

[6] V. Mirceski, D. Guziejewski, M. Bozem, I. Bogeski, Characterizing electrode reactions by multisampling the current in square-wave voltammetry, Electrochimica Acta, 213 (2016) 520-528.

[7] D. Guziejewski, V. Mirceski, D. Jadresko, Measuring the Electrode Kinetics of Surface Confined Electrode Reactions at a Constant Scan Rate, Electroanalysis, 27 (2015) 67-73.

[8] Y. Temerk, M. Ibrahim, H. Ibrahim, M. Kotb, Interactions of an anticancer drug lomustine with single and double stranded DNA at physiological conditions analyzed by electrochemical and spectroscopic methods, Journal of Electroanalytical Chemistry, 769 (2016) 62-71.

[9] Y. Temerk, H. Ibrahim, Electrochemical studies and spectroscopic investigations on the interaction of an anticancer drug flutamide with DNA and its analytical applications, Journal of Electroanalytical Chemistry, 736 (2015) 1-7.

[10] Y. Wan, H. Li, G. Fu, X. Chen, F. Chen, M. Xie, The relationship of antioxidant components and antioxidant activity of sesame seed oil, Journal of the Science of Food and Agriculture, 95 (2015) 2571-2578.

[11] S. Hemalatha, Ghafoorunissa, Sesame lignans enhance the thermal stability of edible vegetable oils, Food Chemistry, 105 (2007) 1076-1085.

[12] A. Shah, R. Lobo, N. Krishnadas, R. Surubhotla, Sesamol and health - A comprehensive review, Indian Journal of Pharmaceutical Education and Research, 53 (2019) S28-S42.

[13] W. Liu, K. Zhang, Y. Qin, J. Yu, A simple and green ultrasonic-assisted liquid-liquid microextraction technique based on deep eutectic solvents for the HPLC analysis of sesamol in sesame oils, Analytical Methods, 9 (2017) 4184-4189.

[14] W. Sun, R. Xiao, Determination of sesamol in sesame oil by anion exchange solid phase extraction coupled with HPLC, Analytical Methods, 6 (2014) 6432-6436.

[15] R.E. Brito, J.M.R. Mellado, P. Maldonado, M.R. Montoya, A. Palma, E. Morales, Elucidation of the electrochemical oxidation mechanism of the antioxidant sesamol on a glassy carbon electrode, Journal of the Electrochemical Society, 161 (2014) G27-G32.

[16] J.H.Q. Lee, B.K. Tay, R. Ganguly, R.D. Webster, The Electrochemical Oxidation of Sesamol in Acetonitrile Containing Variable Amounts of Water, Electrochimica Acta, 184 (2015) 392-402.

[17] B. Aslışen, Ç.C. Koçak, S. Koçak, Electrochemical Determination of Sesamol in Foods by Square Wave Voltammetry at a Boron-Doped Diamond Electrode, Analytical Letters, 53 (2020) 343-354.

[18] K. Morawska, N. Festinger, G. Chwatko, R. Głowacki, W. Ciesielski, S. Smarzewska, Rapid electroanalytical procedure for sesamol determination in real samples, Food Chemistry, 309 (2020) 125789.

[19] K. Beattie, G. Phadke, J. Novakovic, H.G. Brittain, Chapter 6 - Lamotrigine, Profiles of Drug Substances, Excipients and Related Methodology, Academic Press2012, pp. 245-285.

[20] R.T. Wechsler, R. Leroy, A. Van Cott, A.E. Hammer, A. Vuong, R. Huffman, K. VanLandingham, J.A. Messenheimer, Lamotrigine extended-release as adjunctive therapy with optional conversion to monotherapy in older adults with epilepsy, Epilepsy Research, 108 (2014) 1128-1136.

[21] A. Hanawa, K. Asai, G. Ogata, H. Hibino, Y. Einaga, Electrochemical measurement of lamotrigine using boron-doped diamond electrodes, Electrochimica Acta, 271 (2018) 35-40.

[22] H. Wang, D. Qian, X. Xiao, S. Gao, J. Cheng, B. He, L. Liao, J. Deng, A highly sensitive and selective sensor based on a graphene-coated carbon paste electrode modified with a computationally designed boron-embedded duplex molecularly imprinted hybrid membrane for the sensing of lamotrigine, Biosensors and Bioelectronics, 94 (2017) 663-670.

[23] S. Smarzewska, D. Guziejewski, A. Leniart, W. Ciesielski, Nanomaterials vs Amalgam in Electroanalysis: Comparative Electrochemical Studies of Lamotrigine, Journal of The Electrochemical Society, 164 (2017) B321-B329.

[24] K. Morawska, T. Popławski, W. Ciesielski, S. Smarzewska, Interactions of lamotrigine with single- and double-stranded DNA under physiological conditions, Bioelectrochemistry, 136 (2020) 107630.

[25] F. Wang, D. Liu, H. Qu, L. Chen, Z. Zhou, P. Wang, A full evaluation for the enantiomeric impacts of lactofen and its metabolites on aquatic macrophyte Lemna minor, Water Research, 101 (2016) 55-63.

[26] A. European Food Safety, M. Arena, D. Auteri, S. Barmaz, G. Bellisai, A. Brancato, D. Brocca, L. Bura, H. Byers, A. Chiusolo, D. Court Marques, F. Crivellente, C. De Lentdecker, M. De Maglie, M. Egsmose, Z. Erdos, G. Fait, L. Ferreira, M. Goumenou, L. Greco, A. Ippolito, F. Istace, S. Jarrah, D. Kardassi, R. Leuschner, C. Lythgo, J.O. Magrans, P. Medina, I. Miron, T. Molnar, A. Nougadere, L. Padovani, J.M. Parra Morte, R. Pedersen, H. Reich, A. Sacchi, M. Santos, R. Serafimova, R. Sharp, A. Stanek, F. Streissl, J. Sturma, C. Szentes, J. Tarazona, A. Terron, A. Theobald, B. Vagenende, A. Verani, L. Villamar-Bouza, Peer review of the pesticide risk assessment of the active substance methoxyfenozide, EFSA Journal, 15 (2017) e04978.

[27] G.R. Carlson, T.S. Dhadialla, R. Hunter, R.K. Jansson, C.S. Jany, Z. Lidert, R.A. Slawecki, The chemical and biological properties of methoxyfenozide, a new insecticidal ecdysteroid agonist, Pest Management Science, 57 (2001) 115-119.

[28] S. Song, C. Zhang, Z. Chen, F. He, J. Wei, H. Tan, X. Li, Simultaneous determination of neonicotinoid insecticides and insect growth regulators residues in honey using LC–MS/MS with anion exchanger-disposable pipette extraction, Journal of Chromatography A, 1557 (2018) 51-61.

[29] J.D. Berset, S. Mermer, A.E. Robel, V.M. Walton, M.L. Chien, J.A. Field, Direct residue analysis of systemic insecticides and some of their relevant metabolites in wines by liquid chromatography – mass spectrometry, Journal of Chromatography A, 1506 (2017) 45-54.

[30] P. Wang, S. Jiang, D. Liu, W. Shan, H. Zhang, Z. Zhou, Chiral Separations of Pesticide Enantiomers by High- Performance Liquid Chromatography Using Cellulose Triphenylcarbamate Chiral Stationary Phase, Journal of Chromatographic Science, 44 (2006) 602-606.

[31] D. Guziejewski, K. Morawska, T. Popławski, R. Metelka, W. Ciesielski, S. Smarzewska, Lactofen – Electrochemical Sensing and Interaction with dsDNA, Electroanalysis, 30 (2018) 94-100.

[32] K. Morawska, W. Ciesielski, S. Smarzewska, First electroanalytical studies of methoxyfenozide and its interactions with dsDNA, Journal of Electroanalytical Chemistry, 882 (2021) 115030.

[33] L.B.O. dos Santos, G. Abate, J.C. Masini, Determination of atrazine using square wave voltammetry with the Hanging Mercury Drop Electrode (HMDE), Talanta, 62 (2004) 667-674.

[34] D.K. Gosser, Cyclic Voltammetry, VCH, New York, 1994.

[35] A.J. Bard, L.R. Faulkner, Electrochemical Methods: Fundamentals and Applications, John Wiley & Sons, New York, 2000.

[36] S.S. Kalanur, U. Katrahalli, J. Seetharamappa, Electrochemical studies and spectroscopic investigations on the interaction of an anticancer drug with DNA and their analytical applications, Journal of Electroanalytical Chemistry, 636 (2009) 93-100.

[37] Y. Temerk, M. Ibrahim, H. Ibrahim, M. Kotb, Interactions of an anticancer drug Formestane with single and double stranded DNA at physiological conditions, Journal of Photochemistry and Photobiology B: Biology, 149 (2015) 27-36.

[38] S. Shahzad, B. Dogan-Topal, L. Karadurmus, M.G. Caglayan, T. Taskin Tok, B. Uslu, A. Shah, S.A. Ozkan, Electrochemical, spectroscopic and molecular docking studies on the interaction of calcium channel blockers with dsDNA, Bioelectrochemistry, 127 (2019) 12-20.

[39] X. Wang, L. Sun, N. Zou, Z. Yu, Electrochemical study on the interaction between dopamine and deoxyribonucleic acid using a glassy carbon electrode modified with silver-doped poly cysteine membrane, International Journal of Electrochemical Science, 10 (2015) 7320-7330.

[40] E. Jabeen, N.K. Janjua, S. Ahmed, I. Tahiri, M. Kashif, A. Javed, DNA binding interaction studies of flavonoid complexes of Cu(II) and Fe(II) and determination of their chemotherapeutic potential, Inorganica Chimica Acta, 496 (2019).

[41] M.T. Carter, A.J. Bard, Voltammetric studies of the interaction of tris(1,10-phenanthroline)cobalt(III) with DNA, Journal of the American Chemical Society, 109 (1987) 7528-7530.

[42] Y. Temerk, M. Ibrahim, H. Ibrahim, W. Schuhmann, Comparative studies on the interaction of anticancer drug irinotecan with dsDNA and ssDNA, RSC Advances, 8 (2018) 25387-25395.

[43] X. Tian, Y. Song, H. Dong, B. Ye, Interaction of anticancer herbal drug berberine with DNA immobilized on the glassy carbon electrode, Bioelectrochemistry, 73 (2008) 18-22.

[44] K. Morawska, K. Jedlińska, S. Smarzewska, R. Metelka, W. Ciesielski, D. Guziejewski, Analysis and DNA interaction of the profluralin herbicide, Environmental Chemistry Letters, 17 (2019) 1359-1365.

Abstract

The studies presented in this Ph.D. dissertation were focused on two distinct issues. The first goal of the discussed series of publications was to develop electroanalytical assays for determining chosen electroactive compounds. The second was to evaluate the possible mechanisms of interactions between selected bioactive substances and DNA, using voltammetric techniques. Four different compounds were analyzed, i.e., sesamol, lamotrigine, lactofen, and metoxyfenozide.

To develop analytical methods for determination of the above-mentioned compounds, square wave voltammetry was used. The analyses were carried out using different working electrodes. In the first step, the optimization of the experimental conditions and parameters were made, afterwards, the linear relationship between the peak currents and concentration of each compound were found, and finally, the validation of the methods was carried out. The correctness of the proposed procedures was verified by the determination of selected compounds in various spiked samples. Additionally, to explain the nature of the processes taking place at the working electrodes, detailed studies were performed using the cyclic voltammetry technique. The obtained results clearly demonstrate the potential utility of voltammetric techniques for sensitive determination of selected compounds. Furthermore, the proposed methodologies are fast, have high precision, and can be employed for quantification of chosen compounds in various natural samples.

In the second part of the thesis, the characterization of the interaction mechanisms between analytes and DNA was presented. These interactions were studied by cyclic and square wave voltammetry. The observed differences in the electrochemical behavior of the analyzed compounds after the addition of DNA enabled the evaluation of binding constants, and allowed for an examination of the nature of the formed complexes. The obtained results show the usefulness of the voltammetric techniques for simple investigation of analyte-DNA interactions.

Sylwetka autora

Życiorys i przebieg pracy naukowej

Urodziłam się 13 listopada 1991 r. w Kole. Po ukończeniu gimnazjum, rozpoczęłam naukę w I Liceum Ogólnokształcącym im. Kazimierza Wielkiego w Łęczycy, wybierając klasę o profilu biologiczno-chemicznym. W roku 2010 zakończyłam naukę we wspomnianym liceum, zdając egzamin dojrzałości.

Pierwszym wybranym przeze mnie kierunkiem studiów była dietetyka na Wydziale Nauk o Zdrowiu, Uniwersytetu Medycznego w Łodzi. Studia te rozpoczęłam w roku 2010 i ukończyłam z wyróżnieniem w roku 2015. W roku 2012 rozpoczęłam równolegle studia na kierunku analityka chemiczna, na Wydziale Chemii Uniwersytetu Łódzkiego. Studia te zakończyłam terminowo w 2017 roku, uzyskując medal za chlubne studia. Od roku 2014 realizowałam indywidualny program studiów pod opieką dr Sylwii Smarzewskiej. Pracę magisterską zatytułowaną „*Elektroanaliza związków biologicznie czynnych*", wykonałam w Zakładzie Analizy Instrumentalnej pod kierunkiem dr Sylwii Smarzewskiej. Po zdaniu egzaminu magisterskiego w lipcu 2017 roku uzyskałam tytuł magistra analityki chemicznej. Na podstawie uzyskanych wyników powstała publikacja w czasopiśmie *Bioelectrochemistry*.

Na początku października 2017 roku rozpoczęłam studia doktoranckie pod opieką prof. dra hab. Witolda Ciesielskiego oraz dr Sylwii Smarzewskiej, w Zakładzie Analizy Instrumentalnej, w Katedrze Chemii Nieorganicznej i Analitycznej, Wydziału Chemii, Uniwersytetu Łódzkiego. Tematyka prowadzonych przeze mnie badań w dalszym ciągu skupiała się na analitycznym wykorzystaniu technik woltamperometrycznych a dodatkowo zakres zainteresowań badawczych poszerzyłam o elektrochemiczne badania interakcji z DNA.

W roku 2018 odbyłam miesięczny staż w laboratorium prof. Mihaela Badea (Transilvania University of Brasov, Brasov, Romania). Wynikiem wspólnej pracy był materiał doświadczalny, który został zaprezentowany na międzynarodowej konferencji naukowej (The 4th International Conference New Trends on Sensing-Monitoring-Telediagnosis for Life Sciences, Brasov, Romania).

W trakcie trwania studiów doktoranckich miałam możliwość uczestniczenia w 2 międzynarodowych szkołach letnich o tematyce "*Food Safety and Healthy Living*". Uczestniczyłam także w licznych konferencjach krajowych oraz międzynarodowych, prezentując łącznie 14 wystąpień ustnych oraz 11 wystąpień posterowych.

Wyniki badań własnych elektrochemicznych metod oznaczania wybranych związków biologicznie czynnych oraz analizy ich interakcji z DNA zawarte są w cyklu publikacji stanowiących podstawę niniejszej pracy doktorskiej.

Działalność naukowa, organizacyjna i dydaktyczna

Publikacje stanowiące podstawę Dysertacji Doktorskiej (wraz z wkładem procentowym współautorów):

1.	**Kamila Morawska*** (80%), Witold Ciesielski (5%), Sylwia Smarzewska* (15%) "*First electroanalytical studies of methoxyfenozide and its interactions with dsDNA*" Journal of Electroanalytical Chemistry (**2021**), 882, 115030.	IF_{2019}*= 3.807 5-year IF*= 3.519 $MNiSW_{2021}$= 70
2.	**Kamila Morawska*** (70%), Tomasz Popławski (5%), Witold Ciesielski (5%), Sylwia Smarzewska (20%) "*Interactions of lamotrigine with single- and double-stranded DNA under physiological conditions*" Bioelectrochemistry (**2020**), 136, 107630.	IF_{2019}*= 4.722 5-year IF*= 4.034 $MNiSW_{2021}$= 100
3.	**Kamila Morawska*** (50%), Natalia Festinger (5%), Grażyna Chwatko (15%), Rafał Głowacki (5%), Witold Ciesielski (5%), Sylwia Smarzewska* (20%) "*Rapid electroanalytical procedure for sesamol determination in real samples*" Food Chemistry (**2020**), 309, 125789.	IF_{2019}*= 6.306 5-year IF*= 6.219 $MNiSW_{2021}$= 200
4.	Dariusz Guziejewski* (25%), **Kamila Morawska** (35%), Tomasz Popławski (5%), Radovan Metelka (5%), Witold Ciesielski (5%), Sylwia Smarzewska* (25%) "*Lactofen – electrochemical sensing and interaction with dsDNA*" Electroanalysis (**2018**), 30 (1), 94-100.	IF_{2019}*= 2.544 IF_{2018}*= 2.691 5-year IF*= 2.623 $MNiSW_{2021}$= 70

*Dane na dzień 08.04.2021r., wg bazy Web of Science.

Publikacje uzupełniające, nie stanowiące podstawy Dysertacji Doktorskiej:

	CZASOPISMA Z LISTY FILADELFIJSKIEJ	
1.	Natalia Festinger*, **Kamila Morawska**, Vladimir Ivanovski, Magdalena Ziąbka, Katarzyna Jedlińska, Witold Ciesielski, Sylwia Smarzewska "*Comparative Electroanalytical Studies of Graphite Flake and Multilayer Graphene Paste Electrodes*" Sensors (**2020**), 20, 1684.	IF_{2019}*= 3.275 5-year IF*= 3.427 $MNiSW_{2021}$= 100
2.	**Kamila Morawska**, Katarzyna Jedlińska, Sylwia Smarzewska*, Radovan Metelka, Witold Ciesielski, Dariusz Guziejewski* "*Analysis and DNA interaction of the profluralin herbicide*" Environmental Chemistry Letters (**2019**), 17 (3), 1359-1365.	IF_{2019}*= 5.922 5-year IF*= 5.249 $MNiSW_{2021}$= 100
3.	**Kamila Morawska***, Tomasz Popławski, Witold Ciesielski, Sylwia Smarzewska* "*Electrochemical and spectroscopic studies of the interaction of antiviral drug Tenofovir with single and double stranded DNA*" Bioelectrochemistry (**2018**), 123, 227-232.	IF_{2019}*= 4.722 IF_{2018}*= 4.474 5-year IF*= 4.034 $MNiSW_{2021}$= 100
4.	**Kamila Morawska***, Witold Ciesielski, Sylwia Smarzewska* "*First electrochemical approach to voltammetric behavior and sensing of anticancer drug ponatinib*" Publikacja przygotowana do druku.	

*Dane na dzień 08.04.2021r., wg bazy Web of Science.

ROZDZIAŁY W MONOGRAFIACH

1.	Sylwia Smarzewska, **Kamila Morawska** "*Wastewater treatment technologies*" w "Handbook of Advanced Approaches Towards Pollution Prevention and Control 1st Edition" (red. R.O. A. Rahman, C. Hussain), Elsevier, 2021, ISBN 9780128221211.
2.	**Kamila Morawska**, Natalia Festinger, Witold Ciesielski, Sylwia Smarzewska "*Elektrochemiczne biosensory DNA*" w "Kwadrans dla chemii", wyd. Oficyna Edukacyjna Krzysztof Pazdro, Warszawa 2019, ISBN 978-83-7594-191-3, s. 68-78.
3.	Natalia Festinger, **Kamila Morawska**, Witold Ciesielski "*Właściwości elektrochemiczne elektrod wykonanych z wysoce zorientowanego grafitu pirolitycznego*" w "Kwadrans dla chemii", wyd. Oficyna Edukacyjna Krzysztof Pazdro, Warszawa 2019, ISBN 978-83-7594-191-3, s. 42-54.
4.	**Kamila Morawska**, Sylwia Smarzewska, Radovan Metelka, Natalia Festinger, Witold Ciesielski "*Woltamperometryczne badania 1,3-benzodioksol-5-olu*" w "Kwadrans dla chemii", wyd. Oficyna Edukacyjna Krzysztof Pazdro, Warszawa 2018, ISBN 978-83-7594-170-8, s. 88-97.
5.	**Kamila Morawska**, Tomasz Popławski, Radovan Metelka, Witold Ciesielski, Sylwia Smarzewska "*Woltamperometria jako narzędzie do badania biointerakcji na przykładzie leku antywirusowego*"

w "Współczesne metody i sensory elektrochemiczne" (red. B. Baś, M. Jakubowska, W.W. Kubiak), Wydawnictwo Naukowe AKAPIT, Kraków 2018, ISBN 978-83-65995-09-8, str. 265-273.

6.	**Kamila Morawska**, Sylwia Smarzewska, Dariusz Guziejewski, Katarzyna Jedlińska, Witold Ciesielski "*Elektrochemiczne badania tolbanu*" w "Współczesne metody i sensory elektrochemiczne" (red. B. Baś, M. Jakubowska, W.W. Kubiak), Wydawnictwo Naukowe AKAPIT, Kraków 2018, ISBN 978-83-65995-09-8, str. 155-165.

Sumaryczne zestawienie danych bibliograficznych[1]:

Publikacje stanowiące podstawę Dysertacji Doktorskiej	
Liczba publikacji	4
Sumaryczny IF_{2019}	17.379
Średni IF	4.345

Publikacje uzupełniające, nie stanowiące podstawy Dysertacji Doktorskiej	
Liczba publikacji	3
Sumaryczny IF_{2019}	13.919
Średni IF	4.640

Wszystkie publikacje	
Liczba publikacji	7
Sumaryczny IF_{2019}	31.298
Średni IF	4.471
Liczba cytowań (bez autocytowań)[2]	20
Liczba cytowań (z autocytowaniami)[2]	24
Indeks Hirsha(H):	3

[1] Dane odnoszą się do publikacji z listy filadelfijskiej

[2] Dane na dzień 08.04.2021r., wg bazy Web of Science, odnoszą się do 6 publikacji.

Nagrody naukowe:

1.	Nagroda I Stopnia Dziekana Wydziału Chemii za najlepszą publikację naukową w roku 2020 w kategorii prac oryginalnych (2021).
2.	Nagroda I Stopnia Rektora Uniwersytetu Łódzkiego dla doktorantów w dziedzinie nauk ścisłych (2019).
3.	Stypendium Rektora Uniwersytetu Łódzkiego dla najlepszych doktorantów w roku akademickim 2017/2018, 2018/2019, 2019/2020, 2020/2021.
4.	Zwiększenie stypendium doktoranckiego z dotacji podmiotowej na dofinansowanie zadań projakościowych w roku akademickim 2017/2018, 2018/2019, 2019/2020, 2020/2021.
5.	Nagroda im. "Profesora Romualda Skowrońskiego" za najlepszą pracę magisterską przygotowaną na Wydziale Chemii Uniwersytetu Łódzkiego w roku akademickim 2016/2017 (2018).
6.	Nagroda wyróżnienia w konkursie Metrohm Young Chemist Award 2018 za najlepszą pracę magisterską, licencjacką, inżynierską lub doktorską (2018).
7.	Medal za chlubne studia przyznany Uchwałą Senatu Uniwersytetu Łódzkiego z dnia 13.11.2017 (2017).
8.	Nagroda II stopnia Dziekana Wydziału Chemii UŁ za wyróżniający się poster na VIII Sesji Magistrantów i Doktorantów Łódzkiego Środowiska Chemików (2017).

Spis doniesień konferencyjnych:

	WYSTĄPIENIA USTNE
1.	**Kamila Morawska**, Sylwia Smarzewska, Witold Ciesielski "*Woltamperometryczne badania Metoksyfenozydu i jego interakcji z dsDNA*" XVII Konferencja "Elektroanaliza w Teorii i Praktyce", Kraków, 19-20.11.2020, Materiały: K4 str. 26.
2.	**Kamila Morawska**, Witold Ciesielski, Sylwia Smarzewska "*Zastosowanie technik woltamperometrycznych do analizy interakcji DNA*" I Ogólnopolska Konferencja Online Sekcji Studenckiej Polskiego Towarzystwa Chemicznego, Ustroń, 10-12.09.2020, Materiały str. 44.
3.	**Kamila Morawska** "*Electrochemical sensing of the diacylhydrazine insecticide and interaction with dsDNA*" 16th International Students Conference "Modern Analytical Chemistry", Praga, (Czechy), 17-18.09.2020, Materiały str. 6.
4.	**Kamila Morawska** "*Assays for guanine damage by hydroxyl radical and its protection by sesamol*" 15th International Students Conference "Modern Analytical Chemistry", Praga, (Czechy), 19-20.09.2019, Materiały str. 8.
5.	**Kamila Morawska**, Sylwia Smarzewska, Dariusz Guziejewski, Tomasz Popławski, Katarzyna Jedlińska, Witold Ciesielski "*Application of silver amalgam film electrode to study DNA-herbicides interactions*" 26th Young Investigators' Seminar on Analytical Chemistry, Pardubice (Czechy), 24-27.06.2019, Materiały str. 40.

6.	Natalia Festinger, **Kamila Morawska**, Ewelina Skowron, Sylwia Smarzewska, Witold Ciesielski
	"*Zastosowanie różnych materiałów węglowych do produkcji elektrod pastowych wykorzystywanych w woltamperometrii*"
	Zjazd Wiosenny SSPTChem, Ustroń, 10-14.04.2019, Materiały: O6 str. 56.
7.	**Kamila Morawska**, Sylwia Smarzewska, Natalia Festinger, Grażyna Chwatko, Witold Ciesielski
	"*Zastosowanie technik woltamperometrycznych do analizy wybranych olejów spożywczych*"
	Zjazd Wiosenny SSPTChem, Ustroń, 10-14.04.2019, Materiały: O9 str. 59.
8.	**Kamila Morawska**
	"*Electroanalytical and microscopic examination of screen-printed gold electrodes modified with graphene oxide*"
	14th International Students Conference 'Modern Analytical Chemistry', Praga (Czechy), 20-21.09.2018. Materiały str. 7.
9.	Natalia Festinger, Sylwia Smarzewska, **Kamila Morawska**, Witold Ciesielski
	"*Carbon paste electrode for determination of nonsteroidal anti-inflammatory drug used in osteoarthritis treatment*"
	The 4th International Conference New Trends on Sensing-Monitoring-Telediagnosis for Life Sciences, Braszów (Rumunia), 30.08-1.09.2018, Materiały: O1.8 str. 29.
10.	**Kamila Morawska**, Sylwia Smarzewska, Natalia Festinger, Witold Ciesielski
	"*Properties and application of glassy carbon electrode modified with B-cyclodextrin*" The 4th International Conference New Trends on Sensing-

	Monitoring-Telediagnosis for Life Sciences, Braszów (Rumunia), 30.08-1.09.2018, Materiały: O3.3 str. 90.
11.	**Kamila Morawska**, Natalia Festinger, Sylwia Smarzewska, Witold Ciesielski, D.Casoni, C.S.A Cobzac, Mihaela Badea "*Electroanalytical studies of L-DOPA*" The 4th International Conference New Trends on Sensing-Monitoring-Telediagnosis for Life Sciences, Braszów (Rumunia), 30.08-1.09.2018, Materiały: O1.10 str. 31.
12.	Natalia Festinger, **Kamila Morawska**, Sylwia Smarzewska, Witold Ciesielski, D.Casoni, C.S.A Cobzac, Mihaela Badea "*Voltammetric determination of D-DOPA on screen-printed carbon electrodes*" The 4th International Conference New Trends on Sensing-Monitoring-Telediagnosis for Life Sciences, Braszów (Rumunia), 30.08-1.09.2018, Materiały: O1.11 str. 32.
13.	**Kamila Morawska**, Sylwia Smarzewska, Radovan Metelka, Witold Ciesielski "*Electroanalytical studies of sesamol*" 9th Central European Congress on Food (CEFood), Sibiu (Rumunia), 24-26.05.2018, Materiały str. 66.
14.	**Kamila Morawska**, Sylwia Smarzewska, Radovan Metelka, Witold Ciesielski "*Woltamperometryczne badania 1,3-benzodioksol-5-olu*" Zjazd Wiosenny SSPTChem, Skorzęcin, 25-29.04.2018, Materiały: O20 str. 76.

WYSTĄPIENIA POSTEROWE

1.	**Kamila Morawska**, Witold Ciesielski, Sylwia Smarzewska "*Electroanalytical studies of methoxyfenozide*"

	The 5th International Conference New Trends on Sensing- Monitoring-Telediagnosis for Life Sciences, Bukareszt (Rumunia), 3-4.07.2020, Materiały: P.2.12 str. 92.
2.	**Kamila Morawska**, Sylwia Smarzewska, Natalia Festinger, Witold Ciesielski "*Techniques used to study drug-DNA interactions*" Zjazd Zimowy SSPTChem, Gdańsk, 14.12.2019, Materiały str. 50.
3.	Natalia Festinger, **Kamila Morawska**, Sylwia Smarzewska, Witold Ciesielski "*Carbon paste electrodes in voltammetry*" Zjazd Zimowy SSPTChem, Gdańsk, 14.12.2019, Materiały str. 36.
4.	Adrianna Lemiesz, Natalia Festinger, **Kamila Morawska**, Sylwia Smarzewska, Witold Ciesielski "*Wykorzystanie elektrody z węgla pirolitycznego do oznaczania mandipropamidu*" I Konferencja MŁodzi Zdolni, Łódź, 20.02.2019, Materiały: P04 str. 12.
5.	**Kamila Morawska**, Sylwia Smarzewska, Natalia Festinger, Witold Ciesielski "*Generation of reactive oxygen species for electrochemical antioxidant biosensors*" Zjazd Zimowy SSPTChem, Warszawa, 8.12.2018, Materiały str. 44.
6.	Adrianna Lemiesz, Natalia Festinger, **Kamila Morawska**, Sylwia Smarzewska, Witold Ciesielski "*Woltamperometryczne oznaczanie mandipropamidu*" Zjazd Zimowy SSPTChem, Warszawa, 8.12.2018r, Materiały str. 101.
7.	Natalia Festinger, Sylwia Smarzewska, **Kamila Morawska**, Witold Ciesielski "*Edge- and basal-plane pyrolytic graphite electrodes in voltammetry*" Zjazd Zimowy SSPTChem, Warszawa, 8.12.2018, Materiały str. 34.

8.	Witold Ciesielski, Natalia Festinger, C. Fernandez, Monika Skowron, Dariusz Guziejewski, **Kamila Morawska**, Katarzyna Ranoszek-Soliwoda, Jarosław Grobelny, Sylwia Smarzewska
	"*Elektrochemiczne właściwości elektrod złotych modyfikowanych tlenkiem grafenu*" X Polska Konferencja Chemii Analitycznej "Od chemii wszystko się zaczyna" Lublin, 1-5.07.2018, Materiały: P-12 str. 201.
9.	**Kamila Morawska**, Sylwia Smarzewska
	"*Elektroanaliza związków biologicznie czynnych*"
	VIII Sesja Magistrantów i Doktorantów Łódzkiego Środowiska Chemików, Łódź, 22.06.2017, Materiały: S01-P06 str. 23.
10.	Sylwia Smarzewska, Tomasz Popławski, **Kamila Morawska**, Dariusz Guziejewski, Witold Ciesielski
	"*Interaction study of lactofen with DNA and voltammetric determination of DNA in aqueous solutions*"
	New Trends on Sensing - Monitoring - Telediagnosis for Life Sciences, Bukareszt (Rumunia), 7-9.09.2017, Materiały: P.1.18 str. 10.
11.	Sylwia Smarzewska, Tomasz Popławski, **Kamila Morawska**, Dariusz Guziejewski, Witold Ciesielski
	"*Electrochemical and spectroscopic studies of the interaction between the antiviral drug tenofovir and DNA*"
	New Trends on Sensing - Monitoring - Telediagnosis for Life Sciences, Bukareszt (Rumunia), 7-9.09.2017, Materiały: P.1.19 str. 11.

Spis publikacji pokonferencyjncyh:

1.	Natalia Festinger, **Kamila Morawska**, Sylwia Smarzewska, Witold Ciesielski "*Voltammetric studies of acemetacin*" Proceedings of the 14th International Students Conference 'Modern Analytical Chemistry', Praga (Czechy) 2018, ISBN: 978-80-7444-059-5, str. 77-81.

Udział w projektach badawczych: *Pełniona funkcja:*

2018	Grant dla młodych naukowców Uniwersytetu Łódzkiego pt. „*Innowacyjne techniki instrumentalne odpowiedzią na potrzeby współczesnej analizy chemicznej*" (nr projektu B1811100001859.02)	wykonawca

Staże i szkolenia naukowe:

05.07-08.07.2020	Międzynarodowa szkoła letnia "*Food Safety and Healthy Living*" (Transilvania University of Brasov, Brasov, Romania) - online
24.08-09.09.2018	Stypendium w ramach programu CEEPUS (CIII-RO-1111-02-1718): 26.08 - 30.08.2018 – międzynarodowa szkoła letnia "*Food Safety and Healthy Living*" (Transilvania University of Brasov, Brasov, Romania)
10.05-31.05.2018	Stypendium w ramach programu CEEPUS (CIII-RO-1111-02-1718): Staż naukowy w laboratorium prof. Mihaela Badea (Transilvania University of Brasov, Faculty of Medicine,

	Fundamental, Prophylactic and Clinical Specialties Department, Romania)	
26.03-30.03.2018	e-MINDS training course 2018 "*Electrochemical processing methodologies and corrosion protection for device and systems miniaturization*", Siófok (Węgry)	

Działalność organizacyjna: *Pełniona funkcja:*

2018-2021	Wydziałowa Rada Samorządu Doktorantów Wydziału Chemii UŁ	sekretarz
2018-2020	Sąd Koleżeński Doktorantów UŁ	sekretarz
21.02.2020	2. Konferencja Naukowa Studentów MŁodzi Zdolni, Łódź	współorganizator
9.05.2019	VII Łódzkie Sympozjum Doktorantów Chemii, Łódź	współorganizator
20.02.2019	1. Konferencja Naukowa Studentów MŁodzi Zdolni, Łódź	współorganizator
10.05.2018	VI Łódzkie Sympozjum Doktorantów Chemii, Łódź	współorganizator

Działalność dydaktyczna: *Pełniona funkcja:*

2020/2021	„Podstaw analizy kryminalistycznej i sądowej" dla II roku II stopnia Analityki Chemicznej	prowadzenie zajęć
2019/2020	„Podstawy metod analizy instrumentalnej A, B" dla II roku I stopnia Chemii w Nauce i Gospodarce oraz Chemii kosmetyków i farmaceutyków z elementami biznesu	prowadzenie zajęć
2019/2020	„Podstaw analizy kryminalistycznej i sądowej" dla II roku II stopnia Analityki Chemicznej	prowadzenie zajęć
2018-2019	„Podstawy analizy instrumentalnej" dla II roku I stopnia Chemii w Nauce i Gospodarce	prowadzenie zajęć
2018/2019	„Podstawy analizy kryminalistycznej i sądowej" dla II roku II stopnia Analityki Chemicznej	prowadzenie zajęć
2017/2018	„Podstawy Technik nieseparacyjnych" dla II roku I stopnia Analityki Chemicznej	prowadzenie/ współprowadzenie zajęć
2017/2018	„Podstawy metod instrumentalnych" dla II roku I stopnia Chemii Kosmetycznej	prowadzenie zajęć

Recenzja artykułów naukowych:

1.	JELECHEM-D-20-01486	Journal of Electroanalytical Chemistry
2.	JELECHEM-D-20-02020	Journal of Electroanalytical Chemistry

Publikacje stanowiące podstawę

Dysertacji Doktorskiej

Oświadczenia współautorów

Lactofen – Electrochemical Sensing and Interaction with dsDNA

Dariusz Guziejewski,*[a] Kamila Morawska,[a] Tomasz Popławski,[b] Radovan Metelka,[c] Witold Ciesielski,[a] and Sylwia Smarzewska*[a]

Abstract: The electrochemical reduction of lactofen (LCT) at the glassy carbon (GCE) and silver amalgam film electrode (AMFE) is investigatedin detail by the means of square wave voltammetry (SWV), square wave stripping voltammetry (SWSV) and cyclic voltammetry. The influence of various factors such as supporting electrolyte composition and SW parameters were studied. The AMFE electrode showed an excellent electrochemical activity toward the electro-reduction of LCT, leading to a significant improvement in sensitivity as compared to the glassy carbon electrode.The SWSV detection limits for GCE and AMFE were 285.0 nM and 2.0 nM, respectively. The applicability of the developed voltammetric method for analysis of tap water and river water is illustrated with spiked samples analysis. Moreover, as lactofen is highly toxic to fish and other aquatic organisms, its interaction with dsDNA isolated from salmon sperm was tested. The intercalative mode of LCT binding to dsDNA was estimated. The heterogeneous rate constants were calculated for the free LCT and the LCT-dsDNA complex. Moreover, LCT-dsDNA complex binding ratio and equilibrium constant were determined. The decrease in the SWV peak current of LCT in the presence of dsDNA was used for the determination of dsDNA.

Keywords: Lactofen · square-wave voltammetry · glassy carbon electrode · silver amalgam film electrode · herbicide determination · DNA · intercalation

1 Introduction

There are many synthetic organic compounds that are biologically active and useful, but possessing toxic side effects and being potentially dangerous for human health. Therefore, the demand for methods of determination and monitoring of hazardous compounds in environmental samples and for studies of their interaction with important biological molecules, such as DNA, is increasing. Electrochemical techniques offer inexpensive methods for environmental analysis [1–3]. There are several methods for the investigation of interaction between DNA and organic compounds [4–7]. Modern electrochemical techniques represent a very useful tool for this purpose [8], and mercury [9], amalgam [2], and carbon [10] electrodes are most often applied in such experiments.

Lactofen ((1-ethoxy-1-oxopropan-2-yl) 5-[2-chloro-4-(trifluoromethyl)phenoxy]-2-nitrobenzoate, LCT, Figure 1) is a derivative of acifluorfen, popular herbicide of selective mode of action. It is widely prepared for post emergence applications to a certain resistant cropsto control broadleaved weeds in potatoes, soybean, peanuts and cereals. LCT is slightly to non-toxic to humans after ingestion or inhalation but it can be harmful when getting in contact with a skin or an eye. It is non-poisonous to birds and what is more important practically it doesn't exhibit any kind of toxicity towards bees. This herbicide unfortunately exhibits rather highly undesirable effects to fish, like bluegill or trout as well as aquatic invertebrate species [11 and ref. therein].
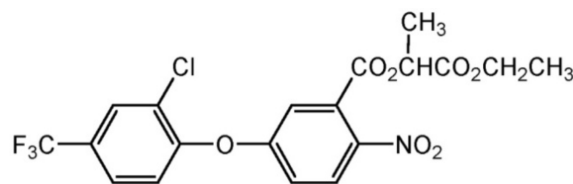
Fig. 1. Chemical structure of lactofen.

Determination methods developed for lactofen are rather of scarce. Only few chromatographic methods were reported in the literature. Most of them use solid phase extraction along with gas chromatography and ECD detection [12], HPLC [13,14] or LC/MS/MS [15]. To the best of our knowledge no study has been devoted for the

[a] D. Guziejewski, K. Morawska, W. Ciesielski, S. Smarzewska
Department of Inorganic and Analytical Chemistry, University of Lodz, Tamka 12, 91-403 Lodz, Poland
E-mail: dguziejewski@uni.lodz.pl
smarzewskasylwia@uni.lodz.pl

[b] T. Popławski
Department of Molecular Genetics, Faculty of Biology and Environmental Protection, University of Lodz, Pomorska 141/143, 90-237 Lodz, Poland

[c] R. Metelka
Department of Analytical Chemistry, Faculty of Chemical Technology, University of Pardubice, Studentska 573, 53210 Pardubice, Czech Republic

voltammetric assessment of LCT. In this manuscript we report the development of lactofen determination method using square-wave voltammetry (SWV) and square-wave stripping voltammetry (SWSV). Its application for herbicide quantification in spiked environmental samples is described. Therefore the aims of this study were, first, to demonstrate the usefulness of GC and AMF electrodes to characterize the LCT voltammetric behaviour, and second, to study interaction of LCT with DNA using electrochemical techniques.

2 Experimental

A conventional three-electrode system was used with a saturated Ag/AgCl reference electrode, a Pt wire counter electrode, and a GCE or AMFE as working electrode. GC electrode was purchased from BASi (USA), while AMFE [16] from MTM-Anko (Poland). Before measurements GCE was polished on abrasive paper with different meshes. The construction and parameters of the AMFE, used in our experiments, were described previously [17–19]. Silver amalgam film was freshly prepared before each experiment. Voltammetric experiments at GCE were performed using a microAutolab type III potentiostat operated with GPES software (version 4.9) while those at AMFE with multiAutolab M101 and Nova v. 1.10 (all Metrohm-EcoChemie, The Netherlands).

Lactofen (PESTANAL, Fluka, Poland) was of 96.7 % purity. LCT stock solution (1.0×10^{-3} mol L^{-1}) was prepared by dissolving 0.01545 g of the substance in acetone, and the solution was stored in a refrigerator when not used. Lower concentrations of LCT were received by proper dilution of stock LCT solution. All other chemicals used were of analytical reagent grade and purchased from Sigma-Aldrich if not stated otherwise. The analytical standards of possible interferences were of analytical reagent grade, and the concentration of stock solutions of interfering agents was 1.0×10^{-3} mol L^{-1}. The supporting electrolytes were Clark-Lubs, Britton-Robinson (BR), citrate and TRIS as well as borate buffers. The 0.02 M Clark-Lubs buffer was prepared by combining portions of stock solution with standard solution of hydrochloric acid. The stock solution contained potassium chloride and potassium hydrogen phthalate. The Britton-Robinson buffer solution was prepared by mixing the same concentrations (0.04 mol L^{-1}) of H_3PO_4, H_3BO_3 and CH_3COOH (POCh SA, Gliwice, Poland), and 0.20 mol L^{-1} NaOH (POCh SA, Gliwice, Poland) solution to obtain the desired pH values. 0.1 M citrate buffer required mixing of 0.1 M sodium citrate and 0.1 M citric acid and adjusting the pH to the proper value. TRIS and borate buffers at the concentration 0.1 M were prepared from the stock solutions and addition of sodium hydroxide solution. dsDNA standard solutions (low molecular weight isolated from salmon sperm) were prepared with PBS buffer (0.01 M phosphate buffer, 0.0027 M potassium chloride and 0.137 M sodium chloride). Distilled and deionized water was used throughout the experiments. A digital pH/mV/

ion meter (Elmetron, Poland) was used for preparation of the buffer solutions. All electrochemical measurements were carried out at the ambient temperature of the laboratory (20–22 °C).

The general procedure used to obtain voltammograms was as follows: to record the voltammograms of the blank solution, 10 mL of the supporting electrolyte solution was mixed for 10 min under open circuit and argon stream passage. Further, to obtain the voltammograms of LCT, a known volume of LCT solution was pipetted into an electrochemical cell and then a voltammogram was recorded under the inert atmosphere. If consecutive voltammograms were necessary the required volumes of the compound solution were added to the cell by means of a micropipette. The tap and river water sample preparation procedure was as follows: the spiked samples collected from local water supplier and the Mszanka river (Lubomierz, Poland) were prepared in a 50 mL volumetric flasks by mixing a 1.0×10^{-5} mol L^{-1} solution of LCT (1.5 mL) with the tap or river water. To obtain the SWV of the blank solution, 9 mL of the supporting electrolyte solution and 1 mL of the river water sample (without analyte) were transferred to the voltammetric cell. Next, to record the SWV of the spiked river water sample, 1 mL of the prepared spiked solution was poured into the cells with 9 mL of the supporting electrolyte solution. Successive additions of 1.0×10^{-5} mol L^{-1} LCT solution were added to the cell with a micropipette. If any reagents were added, the solution was mixed for further 30 s under open circuit and argon deoxidation, and the SWVs were recorded after each addition using the standard addition method.

3 Results and Discussion

3.1 Electrochemical Studies of Lactofen at Glassy Carbon Electrode

Electrochemical behavior of lactofen on GCE was initially studied in BR buffer (pH range from 1.6 to 10.0). As the highest LCT signals were observed in acidic pH other supporting electrolytes as citrate and Clark-Lubs buffers were examined. Nevertheless, best shape and height of analyte signal was received in BR buffer pH 2.0 (Figure 2). Following the standard rules this composition was chosen for further studies as a supporting electrolyte. Dependence between lactofen peak potential and BR buffer pH (2.0-5.0) was linear and can be described with the equation $E_p = 0.028$ pH $+ 0.173$, $R^2 = 0.993$ (Figure S2). LCT signal position shifts towards more negative potential with acidity decrease. The slope of the presented dependence suggests twice higher number of electrons involved in the molecule reduction process in compare to the number of participating protons.

Next, optimization of the square-wave voltammetric signal concentrated upon varying the square-wave parameters such as the step potential, frequency and pulse amplitude (Figure S3–S5). The influence of step potential
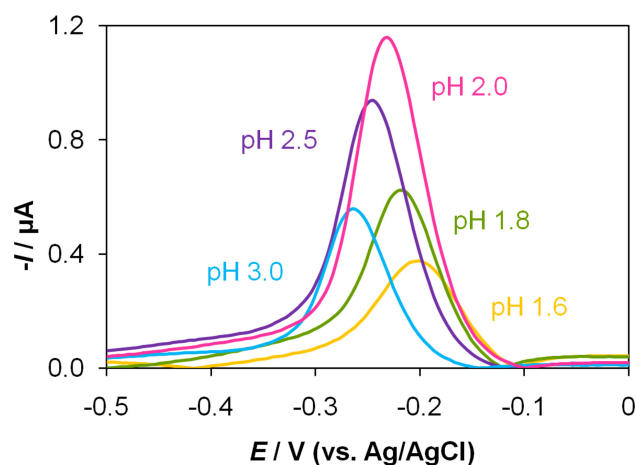
Fig. 2. SW voltammograms of lactofen recorded in BR buffer, $c(\text{LCT}) = 4.0 \times 10^{-6} \, \text{mol} \, \text{L}^{-1}$. The other experimental conditions were: SW amplitude 25 mV, step potential 5 mV and frequency 25 Hz.
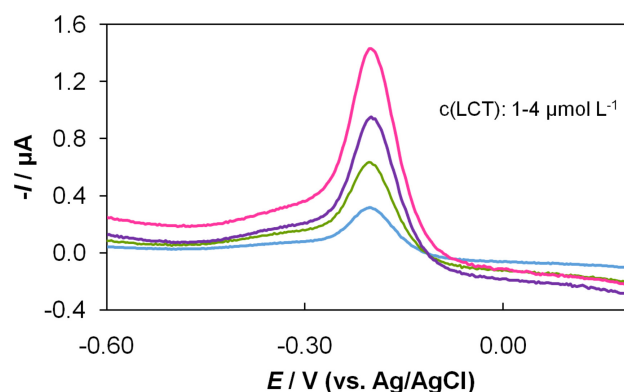

Fig. 3. SW voltammograms recorded in BR buffer pH 2.0 with increasing lactofen concentration $c(\text{LCT}) = 1.0$, 2.0, 3.0, 4.0 µmol L^{-1}. The other experimental conditions were SW amplitude 50 mV, step potential 3 mV and frequency 40 Hz.

was investigated between 1 and 11 mV. The peak height increased up to 3 mV and then decreased. Therefore step potential of 3 mV was chosen for further experiments. Then, the effect of frequency was studied in the range 10–100 Hz. A linear relationship was obtained between the peak current and frequency due to the increase in the effective scan rate but at higher frequency values, peak shape was distorted. Hence the frequency 40 Hz was chosen for entire analysis. The analytical signal was also depended on the pulse amplitude. Square-wave pulse amplitude was examined in the range from 10 to 80 mV. Dependence of LCT peak current on SW amplitude exhibited parabolic course with maximum located at amplitude equal to 50 mV. Thus 50 mV was chosen as the optimum pulse amplitude for all subsequent works. Due to lactofen chemical structure adsorption at the working electrode surface can take place. Hence effect of scan rate (in the range 30–600 mV s^{-1}) in cyclic voltammetry on the recorded LCT peak current was checked (Figure S1). Linear dependence between peak current and scan rate was observed $(I_p(A) = 2.22 \times 10^{-6} \nu (\text{Vs}^{-1}) - 6.36 \times 10^{-8}(A)$, $R^2 = 0.999)$ indicating adsorption-controlled nature of electrode processes. This evidence was acknowledged with the logarithmic plot I_p vs. log ν construction. Received slope for this dependence was equal to 0.801, where value close 1.0 is specific for processes controlled by adsorption.

The applicability of the proposed square-wave voltammetric (SWV) procedure for the determination of lactofen, was examined by measuring the LCT peak current as a function of its concentration under the optimized conditions (n = 3). The calibration plot of the peak current vs. the concentration was found to be linear over the range 1.0 µM–4.0 µM (Figure 3).

The linear regression equation is expressed with equation $I_p = a + b \times c(\text{LCT})$ (correlation coefficient 0.99), where the intercept and slope are $7.37 \times 10^{-7} \, \text{A}$ and $0.75 \, \text{A L mol}^{-1}$, respectively. The limit of detection was

calculated with the equation: (LOD = 3S/b), while the quantitation limit was estimated from LOQ = 10S/b, where S is the standard deviation of intercept and b is the slope of the regression line (here S = 7.13×10^{-8} A and b given in the text above). The evaluated detection and quantitation limits were 0.28 µM and 0.95 µM, respectively. As these result were unsatisfactory (due to high LOD, LOQ values and narrow linear concentration range) and introduction of stripping step did not give any improvement, we decided to check whether better analytical characteristics might be obtained with the silver amalgam film electrode, as many literature positions report excellent usefulness of this electrode in biologically active compounds determination [1,19–21].

3.2 Voltammetric Behavior of Lactofen at Silver Amalgam Film Electrode

First, significant difference between LCT behavior at GC and AMF electrode were observed during preliminary studies in BR buffer. As at GCE there is only one reduction signal at around −0.2 V, at AMFE two reduction signals are observed. First signal (signal I) is located at about −0.2 V, and its magnitude is similar to the one obtained at glassy carbon electrode. Second and third signal (signal II and III), caused by nitro group reduction are placed around −0.45 and −0.70 V, respectively.

The LCT electrochemical behavior seems to be different at those two presented electrodes. The reason of it may be a result of supporting electrolyte pH but also due to different character of surface for glassy carbon and silver amalgam film electrode. It seems that at GCE, which disfavor adsorption phenomena, we observe the reduction process related with the cleavage in the ester section (acid or base-induced) first. On the other hand AMFE allow us to observe both the former reduction but also two step reduction of a nitro group. Further detailed studies should be performed in order to clarify those hypotheses.

According to signal shape and height, signal II was chosen for analytical purposes. Since this signal was much higher in basic medium TRIS and borate buffers were also tested as supporting electrolytes. For further studies borate buffer pH 8.5 was chosen according to LCT signal height (Figure 4).
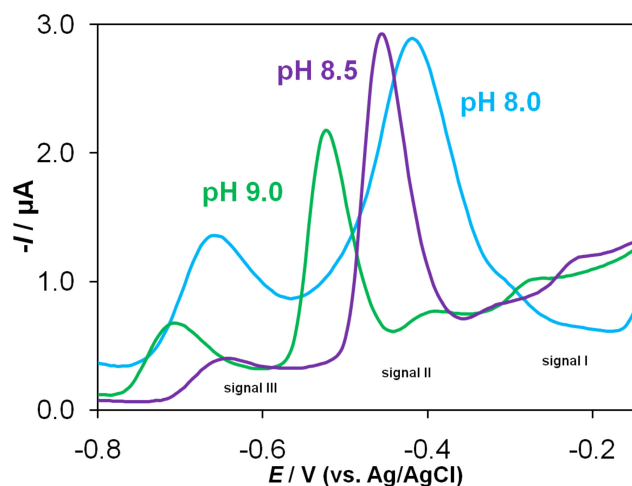

Fig. 4. SW voltammograms of lactofen recorded in borate buffer, $c(\text{LCT}) = 5.0 \times 10^{-5} \text{ mol L}^{-1}$. The other experimental conditions were: conditioning potential -1 V, conditioning time 5 s; SW amplitude 50 mV, step potential 5 mV and frequency 25 Hz.

Subsequently, the impact of instrumental parameters, such as amplitude, step potential, frequency, and accumulation time and potential, was investigated (Figure S3-S6). During optimization of the above-mentioned parameters, one parameter was changed while the others were kept constant. For step potentials from 1 to 20 mV, the peak current increased linearly but step potentials higher than 7 mV caused significant peak deterioration. Step potential of 7 mV was applied in further work. Influence of

amplitude was tested in the range from 10 to 200 mV. Since amplitudes higher than 50 mV caused a non-linear growth of the peak (plateau), this value was chosen as optimal. The influence of frequency (10–160 Hz) on the peak current was also studied. The highest LCT signals were obtained when frequency was 100 Hz. The influences of the accumulation potential E_{acc} on the reduction peak of LCT was studied over the potential range of 0 to -0.4 V. The plot of stripping peak current as a function of accumulation potential indicated the maximum peak current when $E_{\text{acc}} = -0.25$ V. Thus, this parameter value was chosen for subsequent uses. The influence of accumulation time (t_{acc}) was also investigated (0–180 s). Variation of the accumulation time showed that the lactofen peak current increased initially with the accumulation time elongation, and consecutively gradually level off at period longer than 30 s, presumably due to the saturation of the electrode surface with the LCT adsorbed layer. Thus deposition time of 30 s was used throughout. Quantification of LCT was based on the dependence of peak current upon its concentration in the chosen supporting electrolyte solution under the optimal procedural conditions. Validation of the proposed voltammetric procedures for trace assay of lactofen was examined *via* linearity and sensitivity. Calibration curves for LCT were constructed using both SWV and SWSV technique (Figure 5).

The regression equation associated with the calibration curves (Table 1) exhibited a good linearity that supported the proposed procedure. LCT limit of detection (LOD) and limit of quantification (LOQ) were estimated from the same equations as listed in section 3.1 (here, $S = 1.6 \times 10^{-9}$ and 6.9×10^{-9} A for SWV and SWSV, respectively and b given in the Table 1). Both LOD and LOQ values in (Table 1) confirmed improved sensitivity of the proposed method compared with those calculated when GCE electrode was used.

The presence of heavy metal ions and other pesticides may influence the recorded signal of the analyte. There-
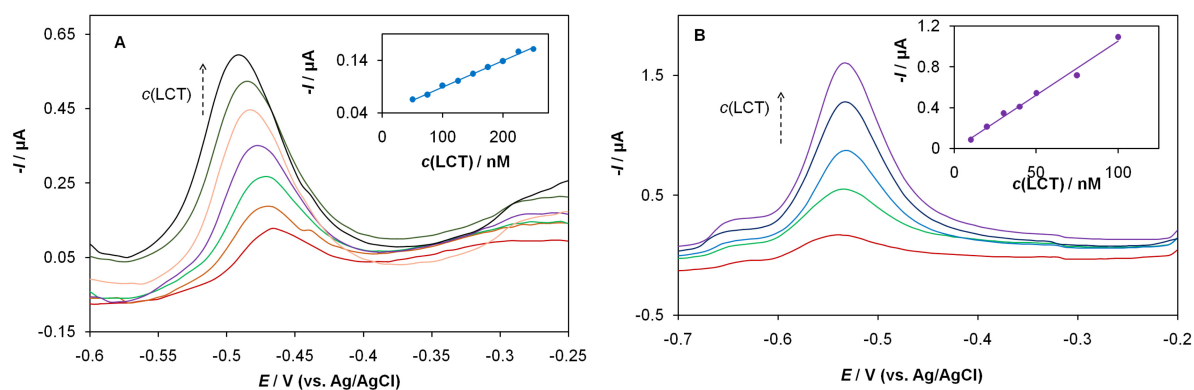

Fig. 5. **(A)** SW voltammograms recorded in borate buffer pH 8.5 with increasing lactofen concentration $c(\text{LCT}) = 50, 75, 100, 150, 175, 200$ and 250 nmol L^{-1}. **(B)** Square-wave stripping voltammograms recorded under the same conditions with increasing lactofen concentration $c(\text{LCT}) = 10, 30, 50, 75$ and 100 nmol L^{-1}. Insets: corresponding calibration lines. Curves presented after blank subtraction. The other experimental conditions were SW amplitude 50 mV, step potential 7 mV and frequency 100 Hz, for SWSV accumulation potential and time -0.25 V and 30 s, respectively.

Table 1. Characteristic of the calibration plots of LCT in borate buffer, pH = 8.5, n = 6.

Technique	SWV	SWSV
Linearity range (nM)	50.0–250.0	10.0–100.0
Regression equation (slope in $\mu A \times nM^{-1}$)	$I_p = 3.89 \times 10^{-2} + 5.02 \times 10^{-4} c$	$I_p = -6.66 \times 10^{-3} + 1.06 \times 10^{-2} c$
Correlation coefficient	0.996	0.998
LOD (nM)	9.5	2.0
LOQ (nM)	32.0	6.5

fore we have additionally performed selectivity studies and evaluated the effect of possible contaminants. The interferent concentration was changed in the concentration range from 5.0×10^{-9} up to 1.0×10^{-6} mol L^{-1}, what corresponds to interferent/analyte ratios: 0.05, 0.1, 0.5, 1, 5 and 10. The recorded signals were evaluated along with LCT only solution (concentration 1.0×10^{-7} mol L^{-1}). The effect of nickel and copper ions caused significant deterioration in the analyte signal in the whole studied concentration range. Increasing concentration of Co^{2+} bring about a linear decrease in the LCT response what suggest formation of a stable complex and possible application for indirect determination of cobalt ions. On the contrary zinc ions didn't influence LCT signal at all. Cimetidine, dinotefuran and blasticidine S had no interference action in the studied concentration range. Aclonifen ruled out lactofen analysis only at the concentrations higher than 5.0×10^{-8} mol L^{-1}. Only presence of metam sodium probably due to strong adsorption processes didn't allow to record stable LCT voltammetric signal.

The adequacy of the developed SWSV method was evaluated by quantifying LCT in environmental samples of tap and river water. No signal deterioration or matrix effects were observed. The nominal content of the LCT in spiked samples were equal to 30 nM. Samples were analyzed with standard addition method. A sample water solution was subjected to six successive additions of LCT standard solution. SWV curves were recorded before and after each addition and standard addition dependence was plotted. The concentration of LCT determined in water samples with the proposed method is reported in Table 2. The mean results for the LCT determination using the proposed method were found close to the declared value. The mean recoveries were found to be 107 and 105 % for tap and river water, respectively. The obtained results showed that the proposed method could be applied with great success to LCT assay in water samples without any interference.

Table 2. Results of LCT determination in spiked environmental samples with SWSV.

Sample	Added [nM]	Found [nM]	CV [%]
Tap water	30.0	30.6 ± 2.4	8.0
River water		31.2 ± 1.3	4.3

3.3 Voltammetric Studies of LCT-dsDNA Interaction

The interaction of lactofen with double stranded DNA was investigated with cyclic voltammetry (Figure 6) and square wave voltammetry.
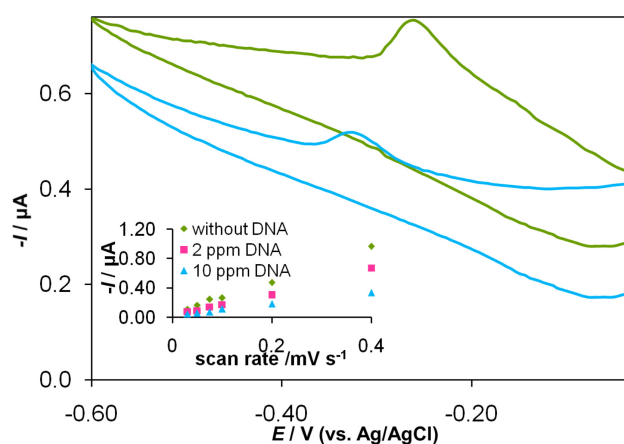
Fig. 6. CV voltammograms of lactofen (c(LCT) = 5.0×10^{-6} mol L^{-1}) recorded in absence (green) and presence (blue) of DNA (10 ppm). Inset: Dependence between lactofen peak current and scan rate in absence and presence of DNA.

In the absence of dsDNA, CV studies revealed one irreversible cathodic peak caused by lactofen reduction. In the presence of dsDNA, LCT signals decreases and shifts to more negative potentials suggesting that dsDNA-LCT interaction can be described as intercalation mode [22]. This causes decrease of LCT peak current as large molecular weight adduct has always lower diffusion coefficient. This is emphasized from the decrease in the slope of the linear $I_p - \nu$ as depicted in Figure 6 (inset). Cyclic voltammetry was also used to examine whether presence of dsDNA influence kinetic parameters of LCT. For a totally irreversible and an adsorption-controlled electrode process, the relationship between E_p and scan rate ν can be expressed by the Laviron's [23] equation: $E_p = E^\circ - (RT)/(\alpha nF) \ln(\alpha nF/RTk_s) - (RT/\alpha nF) \ln \nu$, where α is the charge transfer coefficient, k_s is the standard heterogeneous electron transfer rate constant, n is the number of electrons transferred, ν is the scan rate, and E° is the formal redox potential (other symbols have their usual meanings). Calculated standard heterogeneous elec-

tron transfer rate constants were equal to 6.3 and 2.4 s^{-1} for LCT and LCT-dsDNA, respectively, and proven that dsDNA altered the electrochemical kinetics of LMT reduction [7,24]. As can be seen on Figure 6, no new voltammetric signals appeared after dsDNA-LCT interaction (the same situation was observed when LCT and LCT-dsDNA was examined with SWV). This suggest that interaction between lactofen and double stranded DNA produces single complex [25,26]: m(LCT) + DNA↔DNA(LCT)$_m$, where m is the binding ratio. Therefore, the equilibrium constant β can be described as: β = [c(DNA LCT))$_m$]/[c(DNA)][c(LCT)]^m. Then, to estimate the change in the square wave current caused by presence of constant concentration of DNA (10 ppm) over different concentrations of lactofen, the following equation may be used: $\log[\Delta I_{p}/(\Delta I_{p,max}-\Delta I_p)] = m\log\beta + m\log[c(LCT)]$, where $\Delta I_p = I_{p,0}-I_p$ (Figure 7). Based on these, the relationship between $\log[c(LCT)]$ and $\log[\Delta I_p/(\Delta I_{p,max}-\Delta I_p)]$ can be constructed (inset on Figure 8). The slope of mentioned dependence is equal to 2.1 (~2), which means that dsDNA can bind two LCT molecules. Using the relationship between $\log[c(LCT)]$ and $\log[\Delta I_p/(\Delta I_{p,max}-\Delta I_p)]$ equilibrium constant was calculated as 1.55×10^7 M^{-1}.
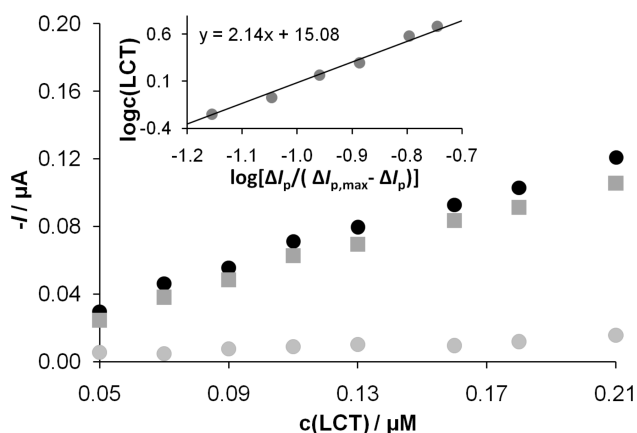
Fig. 7. Relationships between LCT peak current and its concentration in the absence (black dots) and presence of dsDNA (grey dots). Gray squares - separation of the peak currents ΔI_p as a function of LCT concentration; inset: relationship between $\log[c(LCT)]$ and $\log[\Delta I_p/(\Delta I_{p,max}-\Delta I_p)]$.

Since LCT signal significantly decreased upon dsDNA addition, we decide to check analytical aspects of LCT-dsDNA interaction. It was stated, that LCT intercalation into dsDNA can be employed to determine the concentration of dsDNA using the LCT reduction peak current in the SWV. Under optimum experimental conditions, the decrease in peak current of LCT was linearly correlated to dsDNA concentration in the range of 1.0 to 10.0 ppm (Figure 8). The variation of decrease in peak current versus the dsDNA concentration was represented by a straight line followed by the equation I_p (µA) = -0.43(µA ×
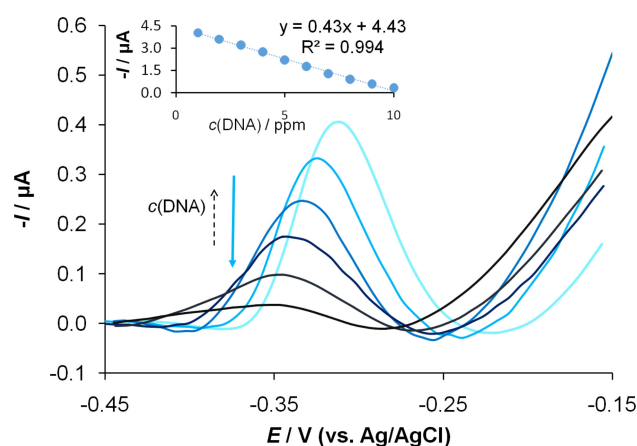
Fig. 8. SW voltammograms of LCT (c(LCT) = 2.5×10^{-6} mol L^{-1}) recorded in presence of DNA. c(DNA) = 2.0, 4.0, 6.0, 8.0, 10.0 ppm, inset: corresponding calibration curve.

ppm^{-1}) × c(dsDNA, ppm) + 4.43 (µA). Limit of detection and quantification were 0.3 and 1.0 ppm, respectively.

4 Conclusions

We have presented first voltammetric methods of lactofen determination using glassy carbon and silver amalgam film electrodes. The above results clearly demonstrate the potential utility of the bare GCE for square-wave voltammetric determination but first of all the applicability of SWSV at the AMFE. Moreover, the proposed methodology is fast, precise and accurate. The presented lactofen determination method at AMFE proved to be extremely sensitive, reaching nanomoles per liter level. We have demonstrated that the elaborated procedure can be employed for evaluation of LCT quantity in water samples. The results showed no influence of the matrices on the recorded response. The delivered procedure ensures a new instrument for lactofen determination in contaminated samples. The developed sensors were found to be electrochemically stable, reusable, and economically effective due to their extremely low operational cost.

Moreover, in the present work interaction between lactofen and double stranded DNA was investigated for the first time. The electrochemical studies showed that LCT can intercalate through dsDNA. The binding ratio and equilibrium constant for formed LCT-DNA complex were determined. It was also stated that dsDNA influence kinetics of electrochemical reduction LCT. Since, LCT signal decreases linearly in the presence of DNA, we have proposed new electrochemical probe for determination of dsDNA.

References

[1] S. Smarzewska, R. Metelka, N. Festinger, D. Guziejewski, W. Ciesielski, *Electroanalysis* **2017**, *2*, 1154–1160.

[2] K. Kucharikova, L. Novotny, B. Yosypchuk, M. Fojta, *Electroanalysis* **2004**, *16*, 410–414.

[3] D. Guziejewski, A. Nosal-Wiercińska, S. Skrzypek, W. Ciesielski, S. Smarzewska, *J. Chem.* **2016**, article ID 6045347.

[4] E. Horakova, V. Vyskocil, J. Barek, *Monatsh. Chem.* **2016**, *147*, 119–126.

[5] N. Li, Y. Ma, C. Yang, L. Guo, X. Yang, *Biophys. Chem.* **2005**, *116*, 199–205.

[6] M. Aslanoglu, *Anal. Sci.* **2006**, *22*, 439–443.

[7] Y. Temerk, M. Ibrahim, H. Ibrahim, M. Kotb, *J. Electroanal. Chem.* **2016**, *769*, 62–71.

[8] J. Vacek, L. Havran, M. Fojta, *Chem. Listy* **2011**, *105*, 15–26.

[9] W. Sun, Z. Shang, Q. Li, K. Jiao, *J. Chin. Chem. Soc.* **2005**, *52*, 1269–1274

[10] A. Hajkova, J. Barek, V. Vyskocil, *Electroanalysis* **2015** *27*, 101–110.

[11] http://pmep.cce.cornell.edu/profiles/extoxnet/haloxyfop-methylparathion/lactofen-ext.html, accessed 2017.08.01

[12] H.-L. Sheu, Y.-H. Sung, M. B. Melwanki, S.-D. Huang, *J. Sep. Sci.* **2006**, *29*, 2647–2652.

[13] A. Lagana, G. Fago, L. Fasciani, A. Marino, M. Mosso, *Anal. Chim. Acta* **2000**, *414*, 79–94.

[14] P. Wang, S. Jiang, D. Liu, W. Shan, H. Zhang, Z. Zhou, *J. Chromatogr. Sci.* **2006**, *44*, 602–606,

[15] M. Takino, T. Tanaka, application note available at *https://www.agilent.com/cs/library/applications/5989-5459EN.pdf*, accessed 2017.08.01

[16] D. Guziejewski, S. Smarzewska, R. Metelka, A. Nosal-Wiercińska, W. Ciesielski, *Monatsh. Chem.* **2017**, *148*, 555.

[17] B. Baś, Z. Kowalski, AGH University of Science and Technology, PL Patent No. P–319984, *Method of and apparatus for making a thin-layer mercury electrode*, **1997**.

[18] B. Baś, Z. Kowalski, *Electroanalysis* **2002**, *14*, 1067–1071.

[19] S. Smarzewska, S. Skrzypek, W. Ciesielski, *Electroanalysis* **2012**, *24*, 1591–1596.

[20] S. Smarzewska, N. Festinger, M. Skowron, D. Guziejewski, R. Metelka, M. Brycht, W. Ciesielski, *Turk. J. Chem.* **2017**, *47*, 116–124.

[21] S. Smarzewska, D. Guziejewski, A. Leniart, W. Ciesielski, *J. Electrochem. Soc.* **2017**, *164*, B321–B329.

[22] Y. M. Temerk, M. S. Ibrahim, M. Kotb, W. Schuhmann, *Anal. Bioanal. Chem.* **2013**, *405*, 3839–3846.

[23] E. Laviron, *J. Electroanal. Chem.* **1979**, *101*, 19–28.

[24] L. Fotouhi, Z. Atoofi, M. M. Heravi, *Talanta* **2013**, *103*, 194–200.

[25] X. Tian, Y. Song, H. Dong, B. Ye, *Bioelectrochem.* **2008**, *73*, 18–22.

[26] L. Fang, W. Wang, P. He, L. Du, Y. Yuan, *Symposium on Sensors for Biomedical Applications/219th Meeting of the Electrochemical-Society (ECS)* **2011**, 3.

Supplementary Information

Lactofen- electrochemical sensing and interaction with dsDNA

Dariusz Guziejewski[1]*, Kamila Morawska [1], Tomasz Popławski[2], Radovan Metelka[3], Witold Ciesielski [1],Sylwia Smarzewska[1]*

[1] Department of Inorganic and Analytical Chemistry, University of Lodz, Tamka 12, 91-403 Lodz, Poland

[2] Department of Molecular Genetics, Faculty of Biology and Environmental Protection, University of Lodz, Pomorska 141/143, 90-237 Lodz, Poland

[3] Department of Analytical Chemistry, Faculty of Chemical Technology, University of Pardubice, Studentska 573, 53210 Pardubice, Czech Republic

* e-mails: dguziejewski@uni.lodz.pl and smarzewskasylwia@uni.lodz.pl
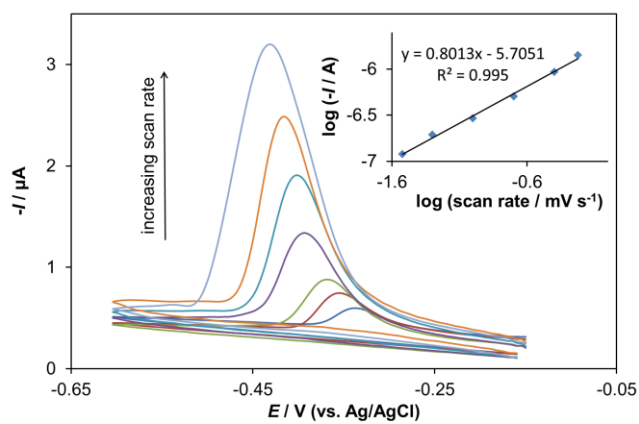
Fig. S1 CVs of LCT (5.0×10^{-6} mol L^{-1}) in BR buffer, pH 2.0, at scan rates: 50, 100, 200, 400, 600, 800 and 1000 mV s^{-1}.
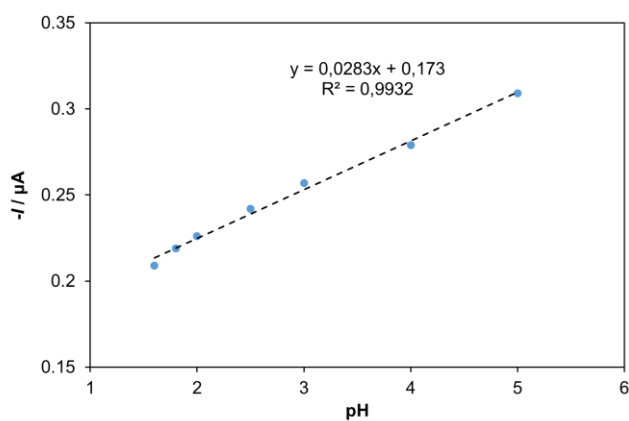
Fig. S2 The pH effect on 4.0 µmol L^{-1} LCT response recorded at GCE in BR buffer.
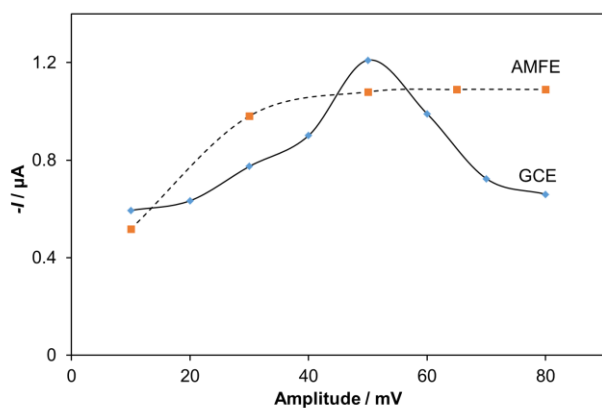
Fig. S3 The optimization effect of the SW amplitude on 1.0 µmol L^{-1} LCT response recorded at GCE in BR buffer, pH 2.0 and 0.1 µmol L^{-1} LCT recorded at AMFE in borate buffer, pH 8.5.
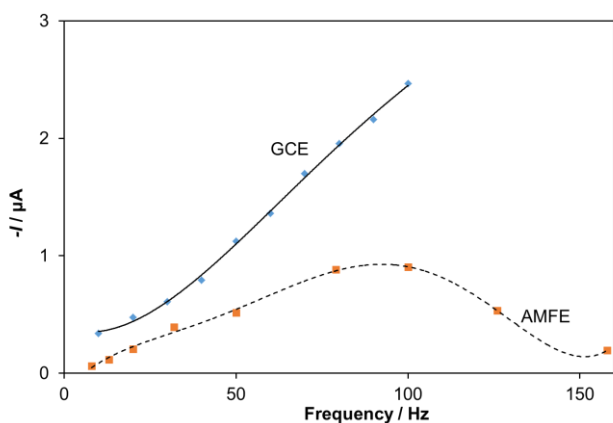
Fig. S4 The effect of the optimization of the SW frequency of 1.0×10^{-6} mol L^{-1} LCT recorded at GCE in BR buffer, pH 2.0 and 0.1 µmol L^{-1} LCT recorded at AMFE in borate buffer, pH 8.5.
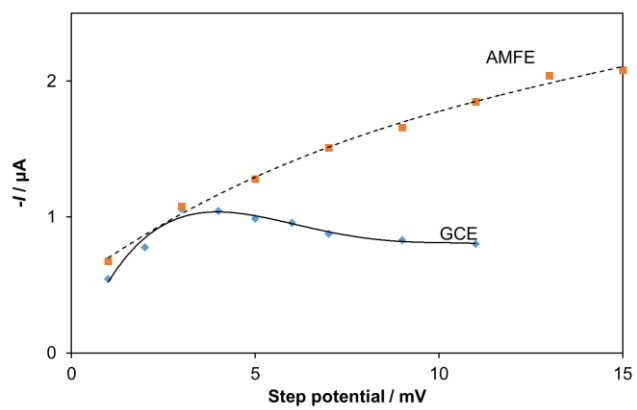
Fig. S5 The effect of the optimization of the SW step potential of 1.0×10^{-6} mol L^{-1} LCT recorded at GCE in BR buffer, pH 2.0 and 0.1 μmol L^{-1} LCT recorded at AMFE in borate buffer, pH 8.5.
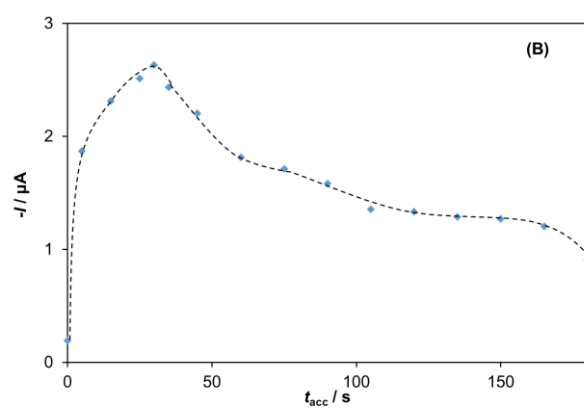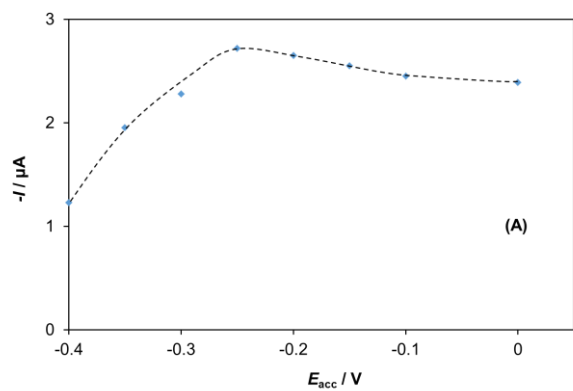
Fig. S6 The effect of the accumulation potential (A) and time (B) optimization of 2.0×10^{-8} mol L^{-1} LCT response recorded at AMFE in borate buffer, pH 8.5.
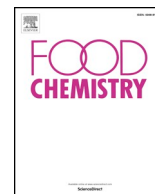
Rapid electroanalytical procedure for sesamol determination in real samples

Kamila Morawska[a],[*], Natalia Festinger[a], Grażyna Chwatko[b], Rafał Głowacki[b], Witold Ciesielski[a], Sylwia Smarzewska[a],[*]

[a] *University of Lodz, Department of Inorganic and Analytical Chemistry, 12 Tamka Str, Lodz 91-403, Poland*
[b] *University of Lodz, Department of Environmental Chemistry, 163 Pomorska Str, Lodz 90-236, Poland*

ARTICLE INFO

ABSTRACT

In this study, the development of an electroanalytical assay based on square wave voltammetry technique for determining sesamol (*Ses*) in sesame oil samples is described. The influence of various factors such as pH of the supporting electrolyte, its composition, and SW (square wave) parameters was studied. Linearity of the peak current depended on the concentration of *Ses* in the range from 3.0 to 140.0 $\mu mol\,L^{-1}$ with a limit of detection of 0.71 $\mu mol\,L^{-1}$. Furthermore, the cyclic voltammetric behavior of *Ses* and the effects of scan rate and pH on the peak current and peak potential of *Ses* were determined. Moreover, the electrode process was found to be diffusion-controlled. The proposed methodology was successfully applied for determining *Ses* in commercial sesame oil samples. The obtained results were in good agreement with the results from the HPLC-UV reference method.

1. Introduction

Sesame is an oilseed crop derived from *Sesamum indicum* L., and it is popular because of its many beneficial effects on human health (Hemalatha, Raghunath, and Ghafoorunissa (2004); Shah, Lobo, Krishnadas, & Surubhotla, 2019; Shasmitha, 2015; Sun & Xiao, 2014; Liu, Zhang, Yang, & Yu, 2019; Liu et al., 2013). Tahini and sesame oil are the most popular products derived from sesame. Sesame seed oil (SSO) is a high-quality, high-priced edible oil that has a unique flavor. Although it contains high levels of unsaturated fatty acids, SSO is one of the most stable vegetable oils (Dar & Arumugam, 2013; Hemalatha & Ghafoorunissa, 2007; Lee, Tay, Ganguly, & Webster, 2015). The good stability of sesame oil has been primarily ascribed to the presence of lignans and tocopherols. The most abundant tocopherol in SSO is γ-tocopherol (from 0.4 to 0.7 $g\,kg^{-1}$) (Liu et al., 2019; Pokkanta et al., 2019). The entire content of lignans in SSO varies from 6.5 to 17.3 $g\,kg^{-1}$ (Wan et al., 2015). Lignans in SSO mainly comprise sesamolin, sesamin, and sesamol (1,3-benzodioxo-5-ol). Sesamol (*Ses*) is primarily formed during the oil production process; thus, the content of *Ses* in roasted oil is significantly higher (50–100 $mg\,kg^{-1}$) than its original level in the unroasted oil (< 7 $mg\,kg^{-1}$) (Dachtler, Van De Put, Stijn, Beindorff, & Fritsche, 2003; Fukuda, Nagata, Osawa, & Namiki, 1986). Because of its phenolic structure, sesamol is able to act as a free

radical scavenger by transferring its hydrogen atom to the reactive radical species (Joshi, Kumar, Satyamoorthy, Unnikrisnan, & Mukherjee, 2005; Suja, Jayalekshmy, & Arumughan, 2004). This ability of *Ses* allows sesame oil to be less vulnerable to harmful effects of free radicals, increases the stability of the oil and shelf life, and curtails its rancidity (Johnson & Decker, 2015; Lee et al., 2015). Based on these characteristics, sesamol is particularly important because of its anti-oxidant activity (Fhaner, Hwang, Winkler-Moser, Bakota, & Liu, 2016; Na, Mok, & Lee, 2020; Prevc, Šegatin, Poklar Ulrih, & Cigić, 2013). Moreover, *Ses* exhibits many therapeutic properties such as anti-aging, antimutagenic, antitumor, anticarcinogenic, and hepatoprotective properties (Hemalatha et al., 2004; Kapadia et al., 2002; Kaur & Saini, 2000; Liu et al., 2013, 2019; Reshma et al., 2010; Sun & Xiao, 2014).

Because of the influence of *Ses* content on the bioproperties and flavor of SSO, numerous studies on the determination of *Ses* in oil samples have been reported. Various analytical methods have been developed for analyzing sesamol in oils such as high-performance liquid chromatography (HPLC), which is the most widely used analytical tool for sesamol determination (Liu, Zhang, Qin, & Yu, 2017; Sun & Xiao, 2014; Wu et al., 2017); UV spectroscopy (Bhatnagar, Hemavathy, & Gopala Krishna, 2015); FTIR spectroscopy (Mirghani, Che Man, Jinap, Baharin, & Bakar, 2003); HPTLC (Sukumar, Arimboor, & Arumughan, 2008); and other techniques (Liu et al., 2015). However, there are very

few detailed electrochemical studies of sesamol (Brito et al., 2014; Keene, Ruddy, & Fhaner, 2019; Lee et al., 2015; Shiragami, Kim, & Kusuda, 1994). To our knowledge, there have been no attempts for the development of an electroanalytical procedure of sesamol determination directly from sesame oil to date. Note that, prior to each analysis, oil samples needed to be pre-treated to remove interfering components and/or to concentrate the inherent lignans. Commonly, solid phase extraction and liquid–liquid extraction were used for extracting phenolics from SSO (Dar & Arumugam, 2013; Khezeli, Daneshfar, & Sahraei, 2016; Liu et al., 2017; Reshma et al., 2010; Sun & Xiao, 2014; Wu et al., 2017; Yu & Yang, 2017; Yu, Ang, Yang, Zheng, & Zhang, 2017).

The goal of this study was to develop a precise, reproducible, simple and fast method for sesamol determination. The analytical performance of proposed methodology was verified by analyzing sesame oil samples. The results were compared with those obtained via high-performance liquid chromatography with UV detection (HPLC-UV), which is commonly used as comparative technique in case of analysis of real samples (Ali, Abdullah, Pınar, Yardım, & Şentürk, 2017; Sunyer et al., 2019).

2. Material and methods

2.1. Apparatus and instrumentation

Electrochemical experiments were performed using an μAutolab type III (Metrohm-EcoChemie, The Netherlands) potentiostat/galvanostat with an M164 electrode stand (mtm-anko, Cracow, Poland) operated with the GPES software (version 4.9). A classical three-electrode system was used with a glassy carbon working electrode (GCE; Mineral, Poland; diameter: 3 mm), a Pt wire as an auxiliary electrode, and a saturated Ag/AgCl as a reference electrode. All studies were carried out using a 10 mL voltammetric cell. The electrode surface was polished on the alumina slurry before each new sample. After polishing, the electrode surface was carefully rinsed with water. The HPLC studies of sesamol were performed using the 1220 Infinity LC system (Agilent Technologies), which was equipped with an autosampler, a binary pump integrated with a degasser, a column oven, and a diode array detector. Data acquisition and analysis were performed using OpenLAB CDS ChemStation Edition software. All measurements were conducted at ambient temperature of the laboratory (20–22 °C).

2.2. Chemicals and reagents

Sesamol was purchased from Acros Organics (Finland). Stock solution of *Ses* (1.0×10^{-3} mol L^{-1}) was prepared by dissolving the required mass of *Ses* in water or methanol, and then stored in a refrigerator at 4 °C when not in use. Lower concentrations were received by proper dilution of the stock *Ses* solution. Various supporting electrolytes, namely, Britton–Robinson (BR), citrate, and chloride buffers, and hydrochloric acid solutions were used. Buffer components were purchased in Avantor (Poland). All reagents that were employed were of analytical grade. For HPLC experiments, acetic acid was purchased from Chempur (Piekary Śląskie, Poland) and HPLC-grade acetonitrile was purchased from J.T. Baker (Deventer, The Netherlands). All aqueous solutions were prepared with distilled and deionized water. A digital pH/mV/ion meter purchased from Elmetron (Poland), which was used for preparing the buffer solutions. Finally, a sesame seed oils (Blue Dragon, Taiwan and Eco Spa, Poland) were obtained from a local market.

2.3. Experimental procedures and samples preparation

Preliminary studies on the electrochemical behavior of *Ses* were performed using cyclic and square wave voltammetry. Voltammograms were initially recorded in the blank solution of the supporting electrolyte, and then in the supporting electrolyte solution containing

appropriate amount of sesamol. After optimizing the SW parameters (frequency, step potential, and pulse amplitude), the calibration curve was constructed by successive addition of aliquots of a standard solution of *Ses* into the measurement cell with the supporting electrolyte. Voltammograms were recorded after each aliquot addition of the compound. Next, square wave voltammetry technique was used for determining sesamol in real samples. During real samples analysis addition of methanolic extract to electrochemical cell was equal to 2.5% of the total volume. All voltammetric measurements were performed in triplicate. The HPLC separations, after automatic injection of 5 μl of the clear extract or standard solution of sesamol, were performed with an analytical column Zorbax C-18 (150 × 4.6 mm, 5 μm) (Agilent Technologies, Waldbronn, Germany) with 0.5% acetic acid solution (A) and acetonitrile (B) as the mobile phase components. The elution profile was as follows: 0–6 min, 20%–80% B; 6–8 min, 80%–90% B; 8–11 min, 90%–20% B. An additional 2 min were required for re-equilibration with a mobile phase composed of 0.5% acetic acid/acetonitrile (80:20, v/v). The temperature of the column was 25 °C, and the flow rate of the mobile phase was 1 mL/min. The detection and quantification were completed by absorbance set at 395 nm as the analytical wavelength. The identification of sesamol peak was based on comparing retention times and DAD spectra with a parallel set of data obtained from authentic compounds. Commercial sesame seed oils were analyzed shortly after opening (Blue Dragon oil – sample 1, sample 2; Eco Spa oil – sample 3). Each sample of SSO was prepared using a conventional liquid–liquid extraction. The general extraction procedure was as follows: 5.0 g of sesame oil was extracted three times with 8 mL of methanol (Liu et al., 2017). The methanolic solution was then collected and analyzed by a voltammetric (SWV) or reference (HPLC) method.

3. Results and discussion

3.1. Voltammetric behavior of sesamol on the GC electrode

The electrochemical behavior of *Ses* was initially studied in the broad pH range offered by the Britton–Robinson buffer (1.1–9.0, Fig. 1A). The highest *Ses* signals were observed in acidic pH (lower than 2.0). At higher pH values, a diminution of the peak current was noticed. Moreover, the oxidation signals of *Ses* were not observed in pH higher than 6.0. The *Ses* peak potential shifted toward more negative values with increase in the pH. Dependence between the *Ses* peak potential and pH of the BR buffer was linear and could be described using the following equation: $E_p = -0.052$ pH $+ 0.803$, R^2 = 0.992 (Fig. 1B). The slope of the mentioned dependence was very close to the theoretical value of 0.059 V pH^{-1}; therefore, it could be presumed that equal numbers of protons and electrons were involved in the *Ses* oxidation process. Because the highest *Ses* signals were recorded in acidic pH, other electrolytes, such as citrate, chloride buffer, and hydrochloric acid solutions, were examined as supporting electrolytes. The best shape and height of sesamol signal was achieved in HCl (pH 0.7; Fig. 1C and D), which was selected for further studies.

Next, the influence of square wave parameters on sesamol signal was examined. Experimental parameters such as amplitude (10–100 mV), frequency (10–100 Hz), and step potential (1–10 mV) were optimized. During these experiments, one of the above mentioned parameters was changed while the others were kept constant. We attempted to optimize the accumulation time and potential to examine sesamol behavior under conditions of square-wave stripping voltammetry (SWSV); however, the stripping procedure exerted no influence over the recorded sesamol signals. The optimized SW parameters, which were selected with respect to shape and height of *Ses* peaks, were as follows: amplitude of 30 mV, frequency of 10 Hz, and step potential of 6 mV. All further voltammetric experiments were performed using these optimized parameters.

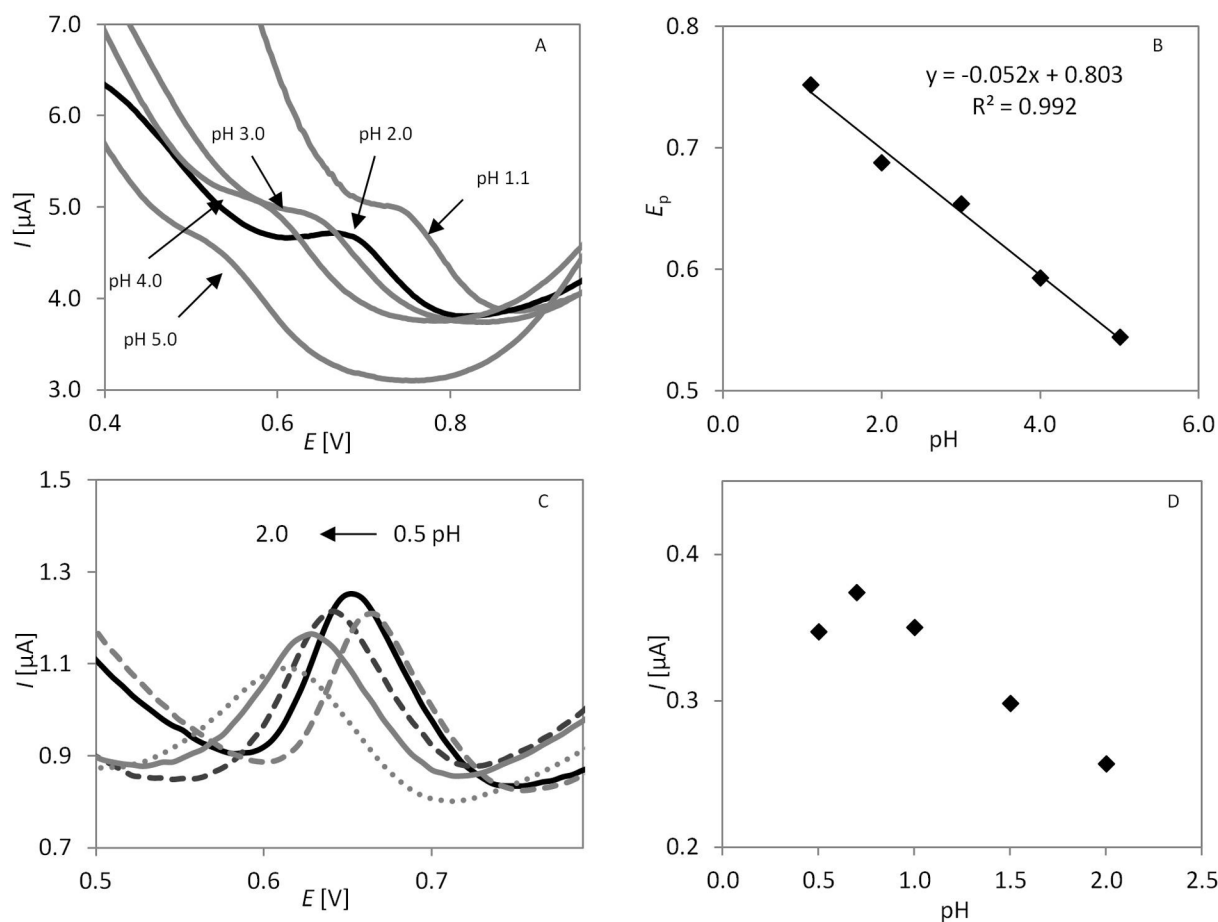In the next experimental step, the oxidation process of sesamol was

Fig. 1. (A) SW voltammograms of 1.0×10^{-5} mol L^{-1} sesamol in Britton–Robinson buffer at different pH values; voltammograms are presented without background subtraction (B) Dependence between sesamol peak potential and pH of BR buffer; (C) SW voltammograms of 1.0×10^{-5} mol L^{-1} sesamol in hydrochloric acid solutions of different pH: pH 0.5 (dashed gray line), pH 0.7 (straight black line), pH 1.0 (dashed dark gray line), pH 1.5 (straight gray line), and pH 2.0 (dotted gray line); (D) Dependence between sesamol (1.0×10^{-5} mol L^{-1}) peak currents and pH of hydrochloric acid. SW parameters: pulse amplitude 30 mV, frequency 25 Hz, and step potential 3 mV.
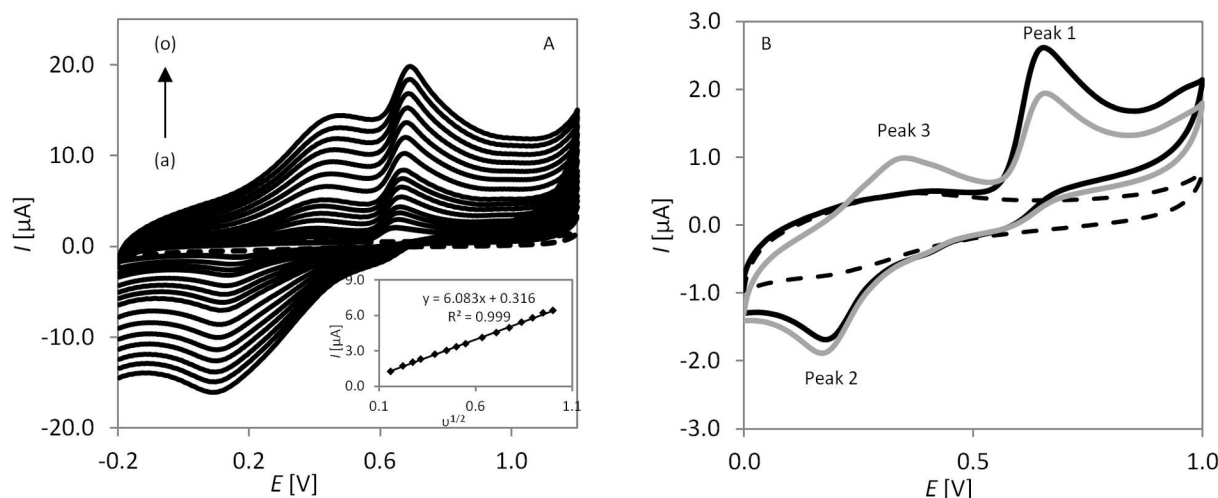
Fig. 2. (A) Cyclic voltammograms of sesamol (1.0×10^{-4} mol L^{-1}), obtained at different scan rates: (a) 25, (b) 50, (c) 75, (d) 100, (e) 150, (f) 200, (g) 250, (h) 300, (i) 400, (j) 500, (k) 600, (l) 700, (m) 800, (n) 900, (o) 1000 mV s^{-1} (the first cycle is depicted). Inset: the linear dependence of *Ses* peak current versus the square root of the scan rate; (B) Cyclic voltammogram of sesamol (1.0×10^{-4} mol L^{-1}) obtained using a scan rate of 50 mV s^{-1}, black line represents the first scan, and gray line the second scan. Dashed lines represent blanks.

investigated using cyclic voltammetry. Fig. 2A shows the CV curves of *Ses* recorded within the potential window from −0.2 to +1.2 V at different scan rates. Depending on whether one or two successive cycles

were recorded, sesamol exhibited two oxidation peaks and one reduction peak in the examined potential range (Fig. 2B). The first cycle (black line) shows one oxidation peak ($E = 0.65$ V, Peak 1) and one

reduction peak ($E = 0.2$ V, Peak 2). In the second cycle (gray line), a new oxidation peak appeared at potential 0.35 V (Peak 3). According to previous studies (Brito et al., 2014), the redox system formed by peaks 2 and 3 is related to the oxidation process that occurs at the potential of 0.65 V. As species oxidized at the potential of 0.35 V must be different from *Ses* but related to the *Ses* oxidation product (Brito et al., 2014), the oxidation occurring at the potential of 0.65 V must involve cleavage of the five-membered ring and affording 1,4-benzoquinone. Such a process involves two protons and two electrons, which is in good agreement with the data obtained from relationship between the *Ses* peak potential and pH. The formed 1,4-benzoquinone remains in the close proximity to the electrode surface and can be reduced to 1,4-dihydrobenzoquinone in the reverse scan (Peak 2). Subsequently, in the next scan, 1,4-dihydrobenzoquinone is oxidized to yield Peak 3.

To evaluate if the mass transfer of sesamol toward the electrode is adsorption or diffusion-controlled, the effect of scan rate within the range of 25–1000 mV s^{-1} on *Ses* signal was investigated. The linear relationship between peak current of *Ses* and the square root of the scan rate was found to be $I_p = 6.083v^{1/2} + 0.316$, $R^2 = 0.999$, indicating that the oxidation of *Ses* occurring on the GCE was a diffusion-controlled process (Fig. 2A inset). Next, the relationship between $\log I_p$ and $\log v$ was examined. The value of the slope of this dependence ($\log I_p = 0.441\log v - 5.201$) confirmed the diffusion characteristics of the registered sesamol currents because it is close to the theoretical value of 0.5.

3.2. Analytical application

The applicability of the proposed SWV procedure for determining sesamol was examined by measuring the peak current as a function of *Ses* concentration under optimal conditions. A linear dependence was observed between the *Ses* concentration and the corresponding peak current within the *Ses* concentration ranging from 3.0×10^{-6} to 1.4×10^{-4} mol L^{-1} (Fig. 3A). The calibration curve was constructed by plotting the *Ses* peak height against *Ses* concentration (Fig. 3B). Using the plotted calibration curve, the limit of detection (LOD) and limit of quantification (LOQ) were calculated using the equation kSD/b, where k = 3 for LOD, k = 10 for LOQ, b = slope of the calibration curve, and SD = standard deviation of the intercept. The characteristics of the calibration plot are listed in Table 1.

The intra-day precision of sesamol peak current was studied using successive assays (n = 10) in a solution containing 5.0×10^{-5} mol L^{-1} of *Ses*. The corresponding relative standard deviation of 5.4% was obtained. Furthermore, repetitive inter-day measurements (over a period
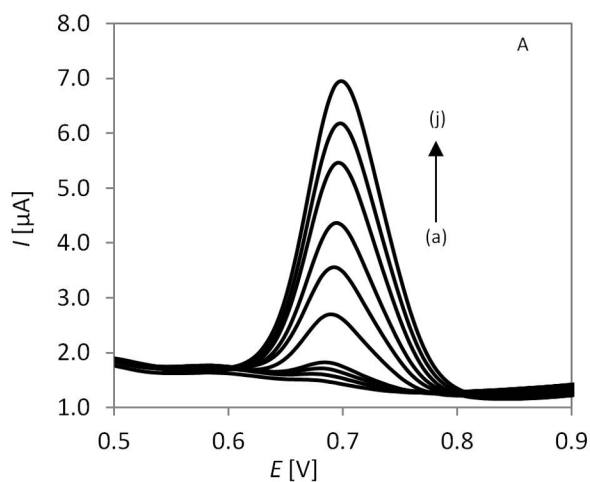
Table 1
Voltammetric determination of *Ses* – analytical characteristics of the calibration curve.

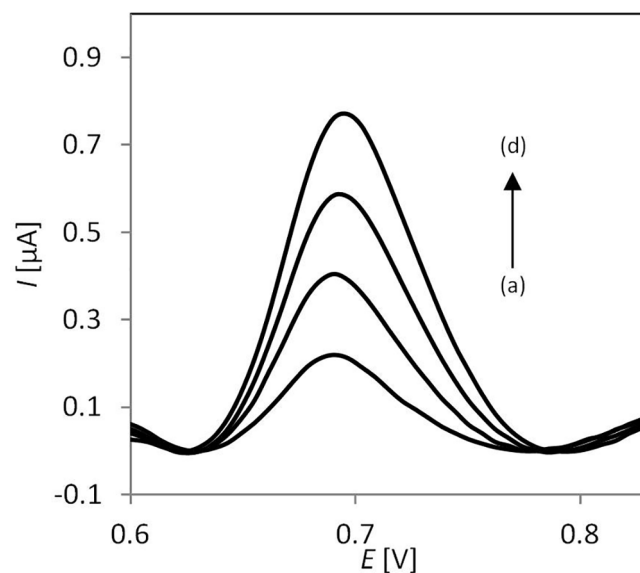| Analytical parameter	Value
Linear concentration range [μmol L^{-1}]	3.0–140.0
Slope of calibration curve [A L^{-1} μmol^{-1}]	0.0400
LOD [μmol L^{-1}]	0.71
LOQ [μmol L^{-1}]	2.37
Correlation coefficient R^2	0.9986
Intra-day precision (CV) [%]	5.4
Inter-day precision (CV) [%]	8.0

Fig. 4. SW voltammograms of sesamol determination in oil sample using the standard addition method, where a – sample; b–d – standard additions; supporting electrolyte: hydrochloric acid pH 0.7; The other experimental conditions were as follows: frequency 10 Hz, amplitude 30 mV and step potential 6 mV.

of 5 days) were performed by measuring the current response for similar freshly prepared sesamol solutions of the same molar concentration. The RSD was found to be 8.0%, which is acceptable for practical applications. Above results prove a high precision of the proposed methodology for the determination of sesamol.
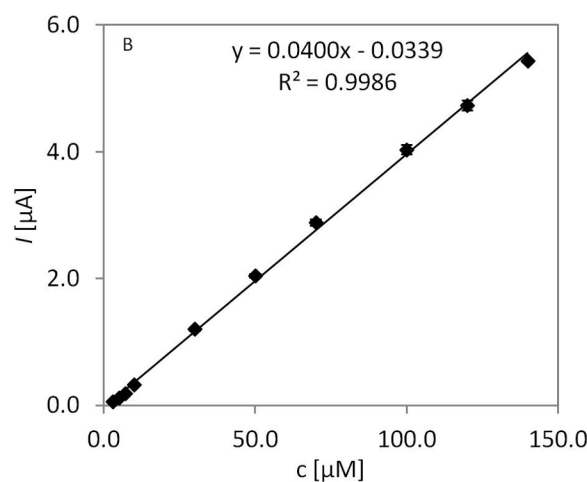

Fig. 3. (A) SW voltammograms for various concentrations of *Ses*, c (ses) = 3.0 (a), 5.0 (b), 7.0 (c), 10.0 (d), 30.0 (e), 50.0 (f), 70.0 (g), 100.0 (h), 120 (i), 140 (j) μmol L^{-1}; supporting electrolyte: hydrochloric acid pH 0.7; The other experimental conditions were as follows: frequency 10 Hz, amplitude 30 mV and step potential 6 mV. (B) A corresponding calibration curve.

Table 2
Determination of sesamol in sesame oil samples.

Sample	Technique	Detected concentration in sample [$\mu mol\,L^{-1}$]	Detected concentration in oil [$mg\,kg^{-1}$]	Precision [%]	E_1[a] [%]
Sample 1	SWV	111.5 ± 7.0	73.9 ± 4.6	5.6	1.9
	HPLC-UV	109.4 ± 2.8	72.5 ± 1.9	2.6	
Sample 2	SWV	100.3 ± 3.8	66.5 ± 2.5	3.4	−1.3
	HPLC-UV	101.6 ± 2.4	67.4 ± 1.6	2.3	
Sample 3	SWV	n/a	n/a	n/a	n/a
	HPLC-UV	3.4 ± 0.3	2.2 ± 0.2	7.6	

[a] Relative error = [(SWV − HPLC value)/HPLC value] × 100.

To verify the analytical performance of the developed procedure, sesamol was determined in the SSO samples. As described in the "Experimental procedures and samples preparation" section, sesame oil samples were prepared using a conventional liquid–liquid extraction. For determining *Ses* in the sesame oil samples, standard addition method was used (Fig. 4). The obtained data (Table 2) clearly demonstrate that the proposed procedure can be effectively used to determine sesamol in oil samples. The HPLC-UV method was used as a reference procedure. For determining sesamol in the SSO samples, the previously described chromatographic method (Chen et al., 2018) was adopted. In the present assay, methanol was changed for acetonitrile, and the column temperature was reduced from 40 °C to 25 °C and gradient elution was modified as described in Section 2.3. Under these conditions, sesamol was separated from other compounds of oil extract and detected after 4.6 min.

To evaluate the HPLC-UV method, a series of experiments were designed to assess the linearity, accuracy, precision, LOD, and LOQ. A seven-point calibration curve of sesamol in the range of 1–150 $\mu mol\,L^{-1}$ was obtained using least-squares linear regression analysis of peak area *vs.* concentration of standard solution. The linear regression equation was y = 1.036x + 0.0321 and showed good linearity with square correlation coefficients of 0.9999. Based on a signal-to-noise ratio of 3 and 10, the LOD and LOQ were 0.3 $\mu mol\,L^{-1}$ and 1 $\mu mol\,L^{-1}$, respectively. Moreover, the accuracy and precision of the method was in the range 91.2%–105.6% and 0.2%–3.7%, respectively. The results obtained using the reference method are also listed in Table 2.

The obtained data confirmed good agreement between the developed and reference method. Based on above results, it can be stated that the proposed voltammetric methodology can be applied for the rapid and inexpensive determination of sesamol in sesame oil samples.

4. Conclusion

A simple and rapid voltammetric method for determining sesamol in sesame oil samples was developed. For this purpose, GC electrode was employed along with the SWV technique. To improve the electroanalytical performance of the proposed procedure, several operational key parameters, such as pH and composition of supporting electrolyte and SW parameters, were optimized. The best shape and height of sesamol signal was achieved in HCl pH 0.7. The optimized SW parameters, were as follows: amplitude of 30 mV, frequency of 10 Hz, and step potential of 6 mV. The electrooxidation of sesamol was used as a sensitive procedure for the *Ses* determination in the concentration range from 3.0×10^{-6} to $1.4 \times 10^{-4}\,mol\,L^{-1}$ with a LOD of $7.1 \times 10^{-7}\,mol\,L^{-1}$. The practical use of voltammetric methodology was demonstrated by real samples analysis. The results were confirmed using the HPLC-UV reference method. The proposed voltammetric procedure is a fast, simple and cost-effective screening tool for determining *Ses* in oil samples. Hence, it is a good, environmentally friendly and inexpensive complement for the more accurate yet expensive chromatographic methodology that is usually employed for such types of analysis.

Declaration of Competing Interest

The authors declare that they have no known competing financial interests or personal relationships that could have appeared to influence the work reported in this paper.

References

Ali, H. S., Abdullah, A. A., Pınar, P. T., Yardım, Y., & Şentürk, Z. (2017). Simultaneous voltammetric determination of vanillin and caffeine in food products using an anodically pretreated boron-doped diamond electrode: Its comparison with HPLC-DAD. *Talanta, 170*, 384–391. https://doi.org/10.1016/j.talanta.2017.04.037.

Bhatnagar, A. S., Hemavathy, J., & Gopala Krishna, A. G. (2015). Development of a rapid method for determination of lignans content in sesame oil. *Journal of Food Science and Technology, 52*(1), 521–527. https://doi.org/10.1007/s13197-013-1012-0.

Brito, R. E., Mellado, J. M. R., Maldonado, P., Montoya, M. R., Palma, A., & Morales, E. (2014). Elucidation of the electrochemical oxidation mechanism of the antioxidant sesamol on a glassy carbon electrode. *Journal of the Electrochemical Society, 161*(5), G27–G32. https://doi.org/10.1149/2.028405jes.

Chen, J., Chen, Y., Tian, J., Ge, H., Liang, X., Xiao, J., et al. (2018). Simultaneous determination of four sesame lignans and conversion in Monascus aged vinegar using HPLC method. *Food Chemistry, 256*, 133–139. https://doi.org/10.1016/j.foodchem.2018.02.081.

Dachtler, M., Van De Put, F. H. M., Stijn, F. V., Beindorff, C. M., & Fritsche, J. (2003). On-line LC-NMR-MS characterization of sesame oil extracts and assessment of their antioxidant activity. *European Journal of Lipid Science and Technology, 105*(9), 488–496. https://doi.org/10.1002/ejlt.200300835.

Dar, A. A., & Arumugam, N. (2013). Lignans of sesame: Purification methods, biological activities and biosynthesis – A review. *Bioorganic Chemistry, 50*, 1–10. https://doi.org/10.1016/j.bioorg.2013.06.009.

Fhaner, M., Hwang, H.-S., Winkler-Moser, J. K., Bakota, E. L., & Liu, S. X. (2016). Protection of fish oil from oxidation with sesamol. *European Journal of Lipid Science and Technology, 118*(6), 885–897. https://doi.org/10.1002/ejlt.201500185.

Fukuda, Y., Nagata, M., Osawa, T., & Namiki, M. (1986). Contribution of lignan analogues to antioxidative activity of refined unroasted sesame seed oil. *Journal of the American Oil Chemists' Society, 63*(8), 1027–1031. https://doi.org/10.1007/BF02673792.

Hemalatha, S., & Ghafoorunissa (2007). Sesame lignans enhance the thermal stability of edible vegetable oils. *Food Chemistry, 105*(3), 1076–1085. https://doi.org/10.1016/j.foodchem.2007.05.023.

Hemalatha, S., Raghunath, M., & Ghafoorunissa, A. (2004). Dietary sesame (Sesamum indicum cultivar Linn) oil inhibits iron-induced oxidative stress in rats. *British Journal of Nutrition, 92*(4), 581–587. https://doi-1org-10041dadb09ed.han3.lib.uni.lodz.pl/10.1079/BJN20041239.

Johnson, D. R., & Decker, E. A. (2015). The role of oxygen in lipid oxidation reactions: A review. *Annual Review of Food Science and Technology, 6*, 171–190. https://doi.org/10.1146/annurev-food-022814-015532.

Joshi, R., Kumar, M. S., Satyamoorthy, K., Unnikrisnan, M. K., & Mukherjee, T. (2005). Free radical reactions and antioxidant activities of sesamol: Pulse radiolytic and biochemical studies. *Journal of Agricultural and Food Chemistry, 53*(7), 2696–2703. https://doi.org/10.1021/jf0489769.

Kapadia, G. J., Azuine, M. A., Tokuda, H., Takasaki, M., Mukainaka, T., Konoshima, T., et al. (2002). Chemopreventive effect of resveratrol, sesamol, sesame oil and sunflower oil in the Epstein-Barr virus early antigen activation assay and the mouse skin two-stage carcinogenesis. *Pharmacological Research, 45*(6), 499–505. https://doi.org/10.1006/phrs.2002.0992.

Kaur, I. P., & Saini, A. (2000). Sesamol exhibits antimutagenic activity against oxygen species mediated mutagenicity. *Mutation Research – Genetic Toxicology and Environmental Mutagenesis, 470*(1), 71–76. https://doi.org/10.1016/S1383-5718(00)00096-6.

Keene, K. A., Ruddy, R. M., & Fhaner, M. J. (2019). Investigating the relationship between

antioxidants and fatty acid degradation using a combination approach of GC-FID and square-wave voltammetry. *ACS Omega, 4*(1), 983–991. https://doi.org/10.1021/acsomega.8b02275.

Khezeli, T., Daneshfar, A., & Sahraei, R. (2016). A green ultrasonic-assisted liquid-liquid microextraction based on deep eutectic solvent for the HPLC-UV determination of ferulic, caffeic and cinnamic acid from olive, almond, sesame and cinnamon oil. [Article]. *Talanta, 150*, 577–585. https://doi.org/10.1016/j.talanta.2015.12.077.

Lee, J. H. Q., Tay, B. K., Ganguly, R., & Webster, R. D. (2015). The Electrochemical oxidation of sesamol in acetonitrile containing variable amounts of water. *Electrochimica Acta, 184*, 392–402. https://doi.org/10.1016/j.electacta.2015.10.068.

Liu, H., Wu, D., Liu, Y., Zhang, H., Ma, T., Aidaerhan, A., et al. (2015). Application of an optosensing chip based on molecularly imprinted polymer coated quantum dots for the highly selective and sensitive determination of sesamol in sesame oils. *Journal of Agricultural and Food Chemistry, 63*(9), 2545–2549. https://doi.org/10.1021/jf505790c.

Liu, W., Zhang, K., Qin, Y., & Yu, J. (2017). A simple and green ultrasonic-assisted liquid-liquid microextraction technique based on deep eutectic solvents for the HPLC analysis of sesamol in sesame oils. *Analytical Methods, 9*(28), 4184–4189. https://doi.org/10.1039/c7ay01033h.

Liu, W., Zhang, K., Yang, G., & Yu, J. (2019). A highly efficient microextraction technique based on deep eutectic solvent formed by choline chloride and p-cresol for simultaneous determination of lignans in sesame oils. *Food Chemistry, 281*, 140–146. https://doi.org/10.1016/j.foodchem.2018.12.088.

Liu, Z., Xiang, Q., Du, L., Song, G., Wang, Y., & Liu, X. (2013). The interaction of sesamol with DNA and cytotoxicity, apoptosis, and localization in HepG2 cells. *Food Chemistry, 141*(1), 289–296. https://doi.org/10.1016/j.foodchem.2013.02.105.

Mirghani, M. E. S., Che Man, Y. B., Jinap, S., Baharin, B. S., & Bakar, J. (2003). Application of FTIR spectroscopy in determining sesamol in sesame seed oil. *JAOCS, Journal of the American Oil Chemists' Society, 80*(1), 1–4. https://doi.org/10.1007/s11746-003-0640-1.

Na, H., Mok, C., & Lee, J. (2020). Effects of plasma treatment on the oxidative stability of vegetable oil containing antioxidants. *Food Chemistry, 302*, 125306. https://doi.org/10.1016/j.foodchem.2019.125306.

Pokkanta, P., Sookwong, P., Tanang, M., Setchaiyan, S., Boontakham, P., & Mahatheeranont, S. (2019). Simultaneous determination of tocols, γ-oryzanols, phytosterols, squalene, cholecalciferol and phylloquinone in rice bran and vegetable oil samples. *Food Chemistry, 271*, 630–638. https://doi.org/10.1016/j.foodchem.2018.07.225.

Prevc, T., Šegatin, N., Poklar Ulrih, N., & Cigić, B. (2013). DPPH assay of vegetable oils and model antioxidants in protic and aprotic solvents. *Talanta, 109*, 13–19. https://doi.org/10.1016/j.talanta.2013.03.046.

Reshma, M. V., Balachandran, C., Arumughan, C., Sunderasan, A., Sukumaran, D.,

Thomas, S., et al. (2010). Extraction, separation and characterisation of sesame oil lignan for nutraceutical applications. *Food Chemistry, 120*(4), 1041–1046. https://doi.org/10.1016/j.foodchem.2009.11.047.

Shah, A., Lobo, R., Krishnadas, N., & Surubhotla, R. (2019). Sesamol and health – A comprehensive review. *Indian Journal of Pharmaceutical Education and Research, 53*(2), S28–S42.

Shasmitha, R. (2015). Health benefits of sesamum indicum: A short review. *Asian Journal of Pharmaceutical and Clinical Research, 8*(6), 1–3.

Shiragami, S., Kim, O. S., & Kusuda, K. (1994). Direct survey of redox active compounds in sesame oil by cyclic voltammetry-studies on sesaminol, sesamol and hydroxyhydroquinone in nujol. *Journal of Electroanalytical Chemistry, 379*(1–2), 315–319. https://doi.org/10.1016/0022-0728(94)87153-1.

Suja, K. P., Jayalekshmy, A., & Arumughan, C. (2004). Free radical scavenging behavior of antioxidant compounds of sesame (Sesamum indicum L.) in DPPH system. *Journal of Agricultural and Food Chemistry, 52*(4), 912–915. https://doi.org/10.1021/jf0303621.

Sukumar, D., Arimboor, R., & Arumughan, C. (2008). HPTLC fingerprinting and quantification of lignans as markers in sesame oil and its polyherbal formulations. *Journal of Pharmaceutical and Biomedical Analysis, 47*(4–5), 795–801. https://doi.org/10.1016/j.jpba.2008.03.018.

Sun, W., & Xiao, R. (2014). Determination of sesamol in sesame oil by anion exchange solid phase extraction coupled with HPLC. *Analytical Methods, 6*(16), 6432–6436. https://doi.org/10.1039/c4ay00663a.

Sunyer, A., González-Navarro, A., Serra-Roig, M. P., Serrano, N., Díaz-Cruz, M. S., & Díaz-Cruz, J. M. (2019). First application of carbon-based screen-printed electrodes for the voltammetric determination of the organic UV filters oxybenzone and octocrylene. *Talanta, 196*, 381–388. https://doi.org/10.1016/j.talanta.2018.12.092.

Wan, Y., Li, H., Fu, G., Chen, X., Chen, F., & Xie, M. (2015). The relationship of antioxidant components and antioxidant activity of sesame seed oil. *Journal of the Science of Food and Agriculture, 95*(13), 2571–2578. https://doi.org/10.1002/jsfa.7035.

Wu, L., Yu, L., Ding, X., Li, P., Dai, X., Chen, X., et al. (2017). Magnetic solid-phase extraction based on graphene oxide for the determination of lignans in sesame oil. *Food Chemistry, 217*, 320–325. https://doi.org/10.1016/j.foodchem.2016.08.109.

Yu, X., Ang, H. C., Yang, H., Zheng, C., & Zhang, Y. (2017). Low temperature cleanup combined with magnetic nanoparticle extraction to determine pyrethroids residue in vegetables oils. *Food Control, 74*, 112–120. https://doi.org/10.1016/j.foodcont.2016.11.036.

Yu, X., & Yang, H. (2017). Pyrethroid residue determination in organic and conventional vegetables using liquid-solid extraction coupled with magnetic solid phase extraction based on polystyrene-coated magnetic nanoparticles. *Food Chemistry, 217*, 303–310. https://doi.org/10.1016/j.foodchem.2016.08.115.

Interactions of lamotrigine with single- and double-stranded DNA under physiological conditions

Kamila Morawska [a],*, Tomasz Popławski [b], Witold Ciesielski [a], Sylwia Smarzewska [a]

[a] University of Lodz, Faculty of Chemistry, Department of Inorganic and Analytical Chemistry, 12 Tamka Str, 91-403 Lodz, Poland
[b] University of Lodz, Faculty of Biology and Environmental Protection, Department of Molecular Genetics, 141/143 Pomorska Str, 90-237 Lodz, Poland

A B S T R A C T

This study presents evaluation of the possible mechanisms of interaction between the antiepileptic drug lamotrigine (LMT) and single- and double-stranded DNA (ssDNA and dsDNA, respectively). These interactions were studied in phosphate-buffered saline (PBS) at physiological pH 7.4 by cyclic voltammetry (CV) and square wave voltammetry (SWV) using a glassy carbon electrode (GCE) in a bulk incubated solution. The addition of both types of DNA to LMT solution decreased peak currents and led to a negative shift in peak potentials, thus indicating the dominance of electrostatic interactions. UV–Vis absorption spectroscopy was also used to assess the interaction between ds/ssDNA and LMT. The data obtained from spectroscopic analysis confirmed that electrostatic interaction is the predominant interaction between LMT and both types of DNA. The calculated binding constants for LMT-dsDNA and LMT-ssDNA complexes as determined by SWV were 6.46×10^5 and 1.81×10^6, respectively, while the values obtained from UV–Vis spectroscopy were 6.93×10^5 and 1.19×10^6, respectively. The obtained results indicated a higher affinity of LMT for ssDNA than for dsDNA.

© 2020 Elsevier B.V. All rights reserved.

1. Introduction

Nucleic acids play a vital role in cellular processes such as cell division and protein synthesis. The replication or transcription of DNA starts only when it receives a specific signal, for example, in the form of binding of a regulatory protein to a particular region of the nucleic acid strand [1,2]. The binding specificity of this regulatory protein can be mimicked by a small molecule, and hence, DNA functions can be artificially modulated, activated, or inhibited by interaction with this molecule. Thus, natural/synthetic molecules can act as drugs when modulation of the DNA function is required to cure or control the disease [1]. Recently, increasing attention has been given to the mechanism by which drugs interact with biological systems, with the main goal of understanding the therapeutic and toxic effects of these small molecules on the wellness/equilibria of biological systems [3]. Moreover, these studies are indispensable for understanding the structural properties of nucleic acids, the origin of some diseases, the mutation of genes, and the mechanism of action of some drugs [3]. Generally, drugs that interact with DNA can be classified as covalently or noncovalently bound molecules. The covalent mode of binding is irreversible due to high binding strength and thus directly leads to cell death [4]. The noncovalent mode of binding is reversible, although it can change DNA conformation, interrupt the process of transcription, and potentially lead to DNA strand breaks [2], [4]. Noncovalent binding includes intercalation, electrostatic interaction, and major/minor DNA groove binding interactions [3–5]. Binding may occur through hydrogen bonding and/or hydrophobic, allosteric, electrostatic, and van der Waals interactions [6].

The interaction of drugs with DNA has been extensively studied using various techniques, including high-performance liquid chromatography [7], UV–visible absorption spectroscopy [8–11], NMR [12], electrophoresis [13], X-ray crystallography [14], luminescence [15], fluorescence [16,17], structural modeling [18], and dynamic viscosity measurements [19]. In recent years, there has been an increasing interest in electrochemical investigations of interactions between drugs or other DNA-target molecules and DNA [1,2,4,20–30]. The electrochemical approach to drug-DNA interactions can provide valuable complement to the results obtained by spectroscopic techniques; thus, in practice, these techniques are often combined to obtain enhanced results [1,2,4,20]. Amongst the techniques used in drug-DNA interaction studies, electrochemical techniques are especially promising because of their high sensitivity and selectivity at relatively low cost. Moreover, because of similarity between electrochemical and biological reactions, it can be presumed that the redox processes occurring at

---

* Corresponding author.
 E-mail address: kamila.morawska@chemia.uni.lodz.pl (K. Morawska).

the working electrodes and in living organisms share very similar principles [20]. Hence, the observation of electrochemical signals reflecting drug-DNA interactions enables the evaluation of binding constants and allows examination of the nature of the formed complexes and study of the interaction mechanisms. The differences in the electrochemical behavior of the analyzed drugs after the addition of DNA can be investigated by monitoring the shift in peak potential or by observing the changes (decrease or increase) in peak current [1,4].

According to a model developed by Bard and co-workers [4,31,32] for DNA-binding metal (e.g. Co^{3+}, Fe^{2+}) chelates, the direction of the peak potential shifts of the binders can be used to evaluate the mode of interaction (a positive shift is expected if the intercalation mode of interaction is dominant, whereas a negative shift in peak potential is a characteristic of the electrostatic binding mode). In more recent literature, attempts were made to apply the same model on other types of compounds that may interact with DNA, including those not containing transition metals [32]. Generally, it is believed that positively charged (protonated) electroactive functional groups may alter the role of positively charged transition metal ions [32]. Lamotrigine (LMT, 3,5-diamino-6-(2,3-dichlorophenyl)-1,2,4-triazine, Fig. 1) is a new, broad-spectrum antiepileptic agent [33,34]. The anticonvulsive mechanism of LMT is based on blocking of Na^+ channel and inhibiting the release of excitatory neurotransmitters. Lamotrigine has been increasingly used to manage tonic-clonic seizures [34–36]. In addition, it is effective against childhood epilepsy and has been approved by the US Food and Drug Administration (FDA) for the treatment of bipolar disorder [35,37]. An overdose of LMT has been reported to cause Stevens-Johnson syndrome, which is often fatal [33,35,38]. Moreover, this drug may lead to less harmful side effects such as fever, dizziness, headache, diarrhea, or fatigue [37,39]. LMT is eliminated from the human body primarily through hepatic glucuronidation. Approximately 70% of oral dose is recovered in urine within 144 h of administration, of which 90% is in the form of 2-N-glucuronide and 10% as unchanged drug [34,40]. It is worth mentioning that some pharmaceutically active compounds originating from human or veterinary therapy may not be eliminated completely in municipal sewage treatment plants and therefore may be discharged into receiving waters, thereby causing immediate risk to aquatic organisms [41]. Therefore, there is an urgent need to develop sensitive methodologies to determine lamotrigine in pharmaceutical, biological, and environmental samples and to examine how LMT may interact with DNA of aquatic organisms. Conventional methods for determining LMT are spectrofluorometry [42], chromatographic techniques [43,44], and capillary zone electrophoresis [45]. However, these methods are time consuming, and most of them are limited by the need for expensive instrumentation. Therefore, because of their high efficiency,

relative simplicity, and low cost, electrochemical approaches have emerged as the pre-eminent analytical tool for the determination of lamotrigine [33,35,38,39,46,47].

To the best of our knowledge, there are no reports on electrochemical studies of the interaction between the antiepileptic drug lamotrigine and single- and double-stranded DNA (ssDNA and dsDNA, respectively) at physiological pH. In the present study, the binding mechanism through which LMT interacts with ds- and ssDNA was investigated for the first time by using cyclic voltammetry (CV), square wave voltammetry (SWV), and UV–Vis spectroscopy. The present study aimed to characterize the interaction mechanism between LMT and ds- and ssDNA.

2. Experimental

2.1. Apparatus and instrumentation

Electrochemical experiments were performed using a μAutolab type III (Metrohm-EcoChemie, The Netherlands) potentiostat in conjunction with an M164 electrode stand (mtm-anko, Poland), controlled by a PC with GPES software (version 4.9). A three-electrode system was used, which comprised glassy carbon as a working electrode (BASi, USA; diameter: 3 mm), saturated Ag/AgCl as a reference electrode, and a Pt wire as an auxiliary electrode. All studies were performed using a standard 10 mL voltammetric cell. Spectrophotometric measurements were conducted using a Cary 100 Bio UV–Vis spectrophotometer (Agilent, USA). A digital pH/mV/ion meter (Elmetron, Poland) was used to prepare the buffer solutions. Water was demineralized in PURELAB UHQ (Elga Lab-Water, UK). All the measurements were conducted at the ambient temperature of the laboratory (20–22 °C).

2.2. Chemicals and reagents

Lamotrigine was purchased from Sigma-Aldrich (Poland). Stock solutions of LMT were prepared weekly by dissolving the required mass of the analyte in water and then stored in a refrigerator at 4 °C, when not in use. Lower concentrations were obtained by appropriately diluting the stock LMT solution. In the present study, the supporting electrolyte was phosphate-buffered saline (PBS) at pH 7.4 (Sigma-Aldrich, Poland). Double-stranded salmon sperm DNA was obtained from Sigma-Aldrich (Germany). A standard stock solution of dsDNA was prepared by dissolving the appropriate amount of dsDNA in PBS. Denatured ssDNA was produced by heating the dsDNA solution in a water bath at 90–95 ℃ for 10 min, followed by rapid cooling in an ice bath [20]. All the reagents used were of analytical grade. All aqueous solutions were prepared with distilled and deionized water.

2.3. Voltammetric and absorption experiments

Voltammetric measurements (SWV and CV) of LMT (at fixed concentration) were conducted in the absence and presence of ds- and ssDNA in PBS at pH 7.4. Briefly, 10 mL of PBS was placed in a voltammetric cell and subsequently purged with argon for 10 min. After recording the voltammogram for the blank, appropriate volumes of LMT and ds/ssDNA were added using a micropipette. After each addition, the solution was again deoxygenated for 10 s, and voltammogram was then recorded. SWV was performed using an amplitude of 30 mV, a frequency of 25 Hz, and a step potential of 6 mV. Cyclic voltammograms were recorded at the scan rate of 10–600 mV s^{-1}.

The glassy carbon electrode (GCE) surface was polished on an alumina slurry before each new sample until a mirror-shine surface was obtained. After polishing, the surface of the electrode
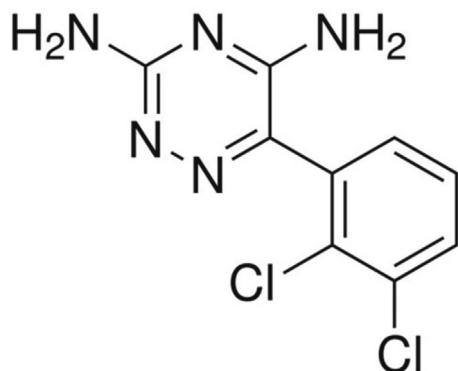

Fig. 1. Chemical structure of lamotrigine.

was carefully rinsed with distilled and deionized water. The absorption spectra of LMT were recorded in PBS at pH 7.4 in the absence and presence of an increasing amount of dsDNA or ssDNA in the wavelength range of 200–500 nm. All measurements were performed in triplicate.

3. Results and discussion

3.1. Voltammetric behavior of lamotrigine on the GC electrode under physiological conditions

In the present study, the electrochemical behavior of LMT was investigated at physiological pH (PBS, pH 7.4) for understanding the LMT-DNA interaction, which is the main aim of this study. Extensive studies on the electrochemical behavior of LMT have been performed previously by many research groups to identify the optimal experimental conditions for lamotrigine determination [33,35,38,39,46,47]. Depending on the type of the electrode used or the observed electrochemical processes (oxidation and/or reduction), various types of supporting electrolytes were used. For LMT reduction, the most popular supporting electrolytes were buffers of pH 5.0 [35,39], which can be explained by changes in the protonation of acid-base functionalities in the LMT molecules [35]. For the oxidation process of LMT, the most intensive analytical signal was observed in acidic buffers [39]. Hence, there is a high probability of observing the reduction process of LMT at pH 7.4; therefore, in the present study, LMT reduction was performed at the unmodified GCE. The reduction process of LMT was first investigated by cyclic voltammetry. Fig. 2 shows the CV curves of LMT recorded within the potential window from − 0.5 to − 1.6 V at different scan rates. Lamotrigine exhibited only one reduction peak at − 1.1 V in PBS at pH 7.4 in the examined potential range. No peaks were observed in the reverse scan, which suggested that the reduction of LMT at GCE is irreversible. Analysis of the literature data indicates that the electroreduction process might occur through the reduction of the –N = N − bond present in the triazine ring of LMT [39,46].

To evaluate whether the mass transfer of lamotrigine toward the electrode surface is adsorption- or diffusion-controlled, the effect of the scan rate in the range of 10–600 mV s^{-1} on LMT signal was investigated. The plot of log I_p versus log v yielded a straight
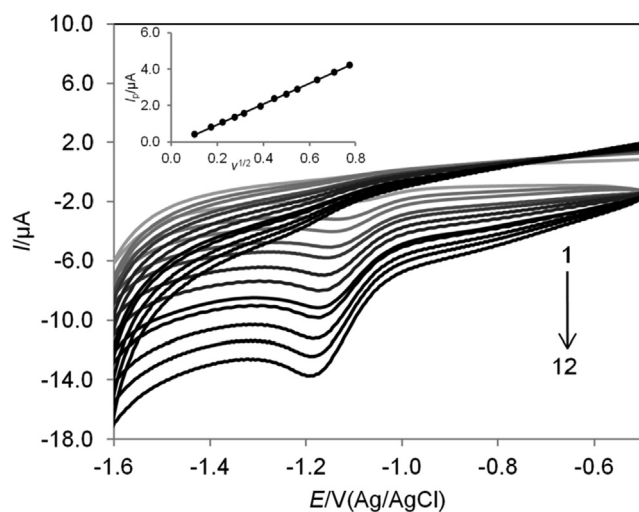
line with a slope of 0.55 (log I_p = 0.550log$v$–5.25). This value was close to the theoretical value of 0.5, which is expected for diffusion characteristics of the registered currents [48]. Next, the linear relationship between the peak current of LMT and the square root of the scan rate was determined (I_p = 5.65$v^{1/2}$ + 0.178, r^2 = 0.9996, Fig. 2, inset), which confirmed that the reduction of LMT occurring on the GCE was a diffusion-controlled process [48].

In the next experimental step, to optimize experimental conditions for the chosen supporting electrolyte, the influence of square wave parameters on LMT signal was examined. Experimental parameters such as amplitude (10–100 mV), step potential (1–10 mV), and frequency (10–100 Hz), were optimized. During these experiments, one of the above-mentioned parameters was changed, while the others were kept constant. The optimized SW parameters, which were selected with respect to the height and shape of LMT signals, were as follows: amplitude of 30 mV, frequency of 25 Hz, and step potential of 6 mV (detailed information is given in Supplementary Material).

To obtain the LMT calibration curve, SWV measurements were performed by measuring the peak current as a function of LMT concentration under optimal conditions. The cathodic peak currents were proportional to lamotrigine concentration in the range of 1.0×10^{-6} to 1.6×10^{-4} mol L^{-1}, with regression equation of I_p (µA) = 0.0182 [µA L µmol^{-1}] $\times$ $c_{(LMT)}$ + 0.0006 [µA] (r^2 = 0.9993) (Fig. 3). By using the plotted calibration curve, the limit of detection (LOD) and limit of quantification (LOQ) were calculated using the following equation: kSD/b (where k = 3 for LOD, k = 10 for LOQ, SD = standard deviation of the intercept, and b = slope of the obtained calibration curve) [49]. The calculated LOD and LOQ values were 2.1×10^{-7} and 7.0×10^{-7} mol L^{-1}, respectively.

The intra-day repeatability of the peak current of LMT was estimated with 10 successive measurements (n = 10) in a solution containing 1.0×10^{-5} mol L^{-1} of LMT. The coefficient of variation (CV) of 4.4% was obtained (the GCE surface was refreshed after each measurement). Moreover, repetitive inter-day measurements (for 5 days) were performed by measuring the peak current response for freshly prepared LMT solutions of the above-mentioned molar concentrations. The CV was 6.9%, which is satisfactory for practical applications. These results confirm the high precision of the proposed methodology.

3.2. Interaction of lamotrigine with dsDNA

The interaction of LMT with dsDNA was investigated by cyclic voltammetry, square wave voltammetry and UV–Vis spectroscopy. The addition of dsDNA to the lamotrigine solution decreased the LMT peak current in both voltammetric techniques (Fig. 4). This confirmed the interaction between LMT and dsDNA. Voltammetric analysis of pure ds/ssDNA showed no cathodic or anodic peak in the used concentrations of ds/ssDNA and potential range from − 0.5 to − 1.5 V vs. Ag/AgCl at GCE in PBS at pH 7.4. Thus, the observed decrease in the peak current of LMT in the presence of dsDNA appeared to be caused by the binding of lamotrigine to the large, slowly diffusing dsDNA, which resulted in a considerable decrease in the diffusion coefficient. To estimate the diffusion coefficient (D_f) value, the formed LMT-dsDNA complexes were studied by cyclic voltammetry at various scan rates. A linear relationship was found between the peak current of the LMT-dsDNA complex and the square root of the scan rate, with the slope of log I_p versus log v equal to 0.49; this finding indicates that the registered currents are diffusion-controlled. After the addition of dsDNA to the LMT solution, there was a decrease in the slope of the linear I_p versus $v^{1/2}$ plots ($r^2 \geq 0.996$); the obtained slope values were 2.23 and 1.85 µA V$^{-1/2}$ s$^{-1/2}$ in the absence and presence of dsDNA, respectively (Fig. 4A inset). From these values, the diffusion coefficient of the free LMT was calculated as 2.32×10^{-6} cm^2 s^{-1}, whereas D_f for

Fig. 2. Cyclic voltammogram of 1.0×10^{-4} mol L^{-1} LMT in PBS at pH 7.4 at scan rates of 10 (1), 30 (2), 50 (3), 75 (4), 100 (5), 150 (6), 200 (7), 250 (8), 300 (9), 400 (10), 500 (11), and 600 (12) mV s^{-1}. Inset: Relationship between the peak current of LMT and the square root of the scan rate (y = 5.65x − 0.178, r^2 = 0.9996).
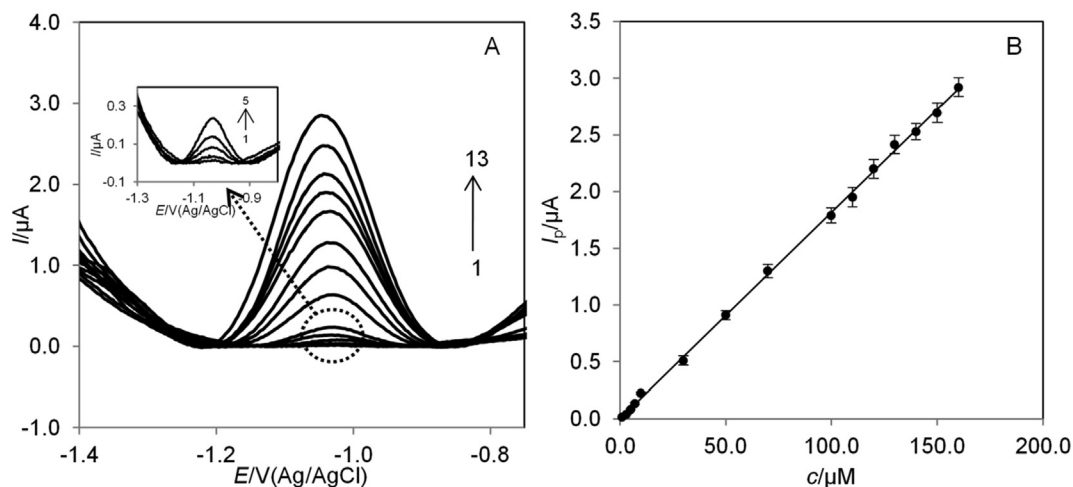
Fig. 3. (A) SW voltammograms for various concentrations of LMT (1.0 (1), 3.0 (2), 5.0 (3), 7.0 (4), 10.0 (5), 30.0 (6), 50.0 (7), 70.0 (8), 100 (9), 110 (10), 120 (11), 140 (12), and 160 (13) μmol L^{-1}); supporting electrolyte: PBS pH 7.4. The other experimental conditions were as follows: amplitude 30 mV, frequency 25 Hz, and step potential 6 mV. (B) A corresponding calibration curve (y = 0.0182x + 0.0006, r^2 = 0.9993).
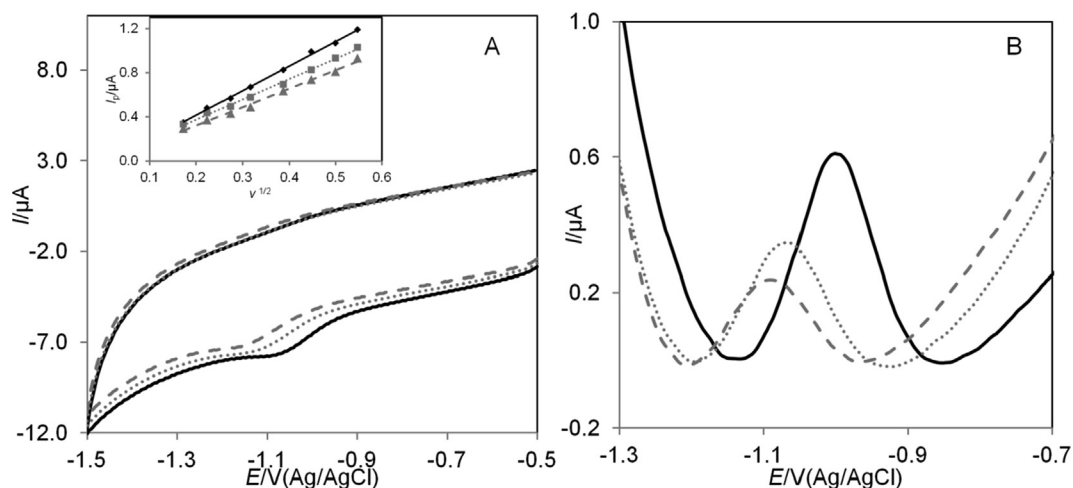

Fig. 4. (A) Cyclic voltammograms of lamotrigine recorded in the absence (straight, black line) and presence of dsDNA (dotted, gray line) and ssDNA (dashed, gray line), c $_{(LMT)}$ = 5.0 $\times$ 10^{-5} mol L^{-1}, c$_{(ds/ssDNA)}$ = 40 mg L^{-1}, supporting electrolyte: PBS at pH 7.4; inset: Corresponding dependence between the lamotrigine peak current and the square root of the scan rate in the absence (y = 2.2344x – 0.0337) and presence of dsDNA (y = 1.8476x + 0.0021) and ssDNA (y = 1.6751x – 0.0132). (B) SW voltammograms of lamotrigine recorded in the absence (straight black line) and presence of dsDNA (dotted, gray line) and ssDNA (dashed, gray line), $c_{(LMT)}$ = 3.0 $\times$ 10^{-5} mol L^{-1}, $c_{(ds/ssDNA)}$ = 40 mg L^{-1}.

the bound LMT (LMT-dsDNA) was 1.76 $\times$ 10^{-6} cm^2 s^{-1} [50]. As can be seen, a decrease in the diffusion coefficient was observed; thus, the obtained results confirmed the earlier assumption that decrease in the LMT peak currents in the presence of dsDNA was caused by the binding of lamotrigine to slowly diffusing DNA molecules. By using the estimated values, the heterogeneous rate constants (k^o) were calculated to deduce whether the interaction between LMT and dsDNA influenced the kinetics of LMT reduction. From the slopes of E_p *vs.* ln$v$ plots, the values of k^o were 1.10 $\times$ 10^{-2} s^{-1} (LMT) and 9.00 $\times$ 10^{-3} s^{-1} (LMT in the presence of dsDNA); thus, we inferred that as assumed, the rate of electron transfer was decreased for LMT in the form of the LMT-DNA complexes.

The changes in the peak current after the addition of dsDNA can be used to quantify the binding of LMT to dsDNA (the influence of the addition of ssDNA is described in section 3.4). The SWV technique provides higher sensitivity and better peak resolution than CV; hence, to evaluate the binding constant, we used the square wave technique. In this context, current titrations were performed by keeping the concentration of lamotrigine constant while vary-

ing the concentration of double stranded DNA. The addition of dsDNA to LMT decreased the peak current of lamotrigine, and no new reduction peaks were noted. Further, it was observed that the level of interaction depends on time; thus, the influence of incubation time on lamotrigine signals after the addition of a constant amount of dsDNA was studied. To determine the appropriate interaction time, the voltammograms of LMT were recorded in the presence of dsDNA at different time intervals elapsed since the addition of dsDNA. A significant decrease in the LMT peak currents was observed up to 8 min, following which the peak currents of LMT became constant (detailed information is given in Supplementary Material, Fig. S1). Thus, an interaction time of 8 min was chosen for further studies and maintained thoroughly after each addition of dsDNA. SW voltammograms of lamotrigine in the absence and presence of increasing concentration of dsDNA in PBS at pH 7.4 are shown in Fig. 5. As can be seen, in the presence of dsDNA, the LMT peak current height decreased and the peak potential shifted to more negative values. The current titration can be illustrated by the following equation [2],[26,51]:
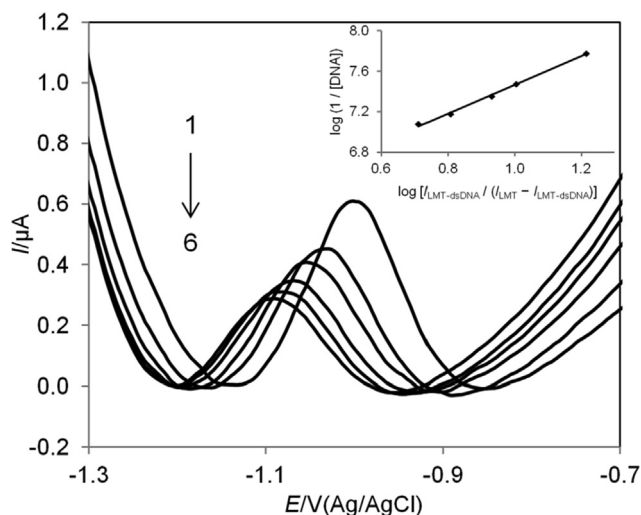
Fig. 5. SW voltammograms of LMT ($c_{(\text{LMT})}$ = 3.0 × 10^{-5} mol L^{-1}) recorded in the absence. (1) and presence of dsDNA ($c_{(\text{dsDNA})}$ = 10.0 (2), 20.0 (3), 40.0 (4), 60.0 (5), 80.0 (6) mg L^{-1}; supporting electrolyte: PBS pH 7.4. Inset: relationship between log [$I_{\text{LMT-dsDNA}}$ / (I_{LMT} − $I_{\text{LMT-dsDNA}}$)] and log (1 / $c_{(\text{DNA})}$) (r^2 = 0.9965).

$$\log(1/c(DNA)) = \log K + \log [I_{LMT-dsDNA}/(I_{LMT} - I_{LMT-dsDNA})] \quad (1)$$

where K is the apparent binding constant and I_{LMT} and $I_{\text{LMT-dsDNA}}$ are the peak current of the free guest (LMT) and the formed complex (LMT-dsDNA), respectively. The constructed plot of log(1 / $c_{(\text{DNA})}$) vs. log [$I_{\text{LMT-dsDNA}}$/(I_{LMT} − $I_{\text{LMT-dsDNA}}$)] was linear (Fig. 5 inset) with the intercept of log K. The binding constant of the LMT-dsDNA complex was evaluated according to Eq. (1) and is listed in Table 1. This result indicates the formation of a stable complex at the physiological pH with intensive attraction between lamotrigine and double stranded DNA. The change in the Gibbs free energy ($\Delta G°$), which reflects the stability of the formed complexes, was estimated by converting the binding constant value. $\Delta G°$ was calculated using the following equation:

$$\Delta G° = -RT \ln K \quad (2)$$

where K is the binding constant and other symbols have their usual meaning. The obtained $\Delta G°$ value is negative (Table 1), which suggests that the interaction process was spontaneous and favorable.

As can be seen, a change in the peak current of the drug in the presence of DNA could be used to evaluate binding constant, whereas the shift in the peak potential could be used to estimate the mode of interaction. In our study, the peak potential of LMT after the addition of an increasing amount of dsDNA shifted to more negative values (Fig. 5), indicating the high probability of the predominant occurrence of the electrostatic binding mode [4,31,52,53]. To determine the binding mode, the analysis of the ionic strength effect may also be useful [1,2,51,54]. When the ionic strength of the analyzed solution is increased by the addition of salt, charge compensation of the nucleotide phosphates caused by the salt cations will hinder the electrostatic binding effect. Therefore, the effectiveness of the complex formation through electrostatic binding would decrease, whereas the binding based

on the intercalation mode would remain virtually unaffected [51,54]. Thus, the influence of ionic strength on the interaction between LMT and dsDNA was also investigated. The ionic strength was varied by changing NaCl concentration from 2.5 to 25 mM in an electrochemical cell containing fixed concentrations of LMT and dsDNA in PBS at pH 7.4. The obtained results suggest that the reaction process is highly dependent on NaCl concentration. As the salt concentration increased, there was an apparent decrease in the peak current of the LMT-dsDNA complex, varying from approximately 0.42 μA at 0.0 M of NaCl to 0.18 μA at 25 mM NaCl (Fig. 6). For low-ionic strength conditions, it may be assumed that the reaction mechanism of LMT-dsDNA interaction included the electrostatic attraction of the negative phosphate groups on the exterior of the dsDNA to lamotrigine molecules [55]. Concomitantly, the peak potential of LMT shifted to more negative values with increasing NaCl concentration, thus confirming the dominance of the electrostatic interactions between lamotrigine and dsDNA. Thus, it can be assumed that the observed interaction occurred mainly through the electrostatic binding mode.

Because no new electrochemical signals appeared after LMT-dsDNA interaction, it could be presumed that during LMT-dsDNA interaction, only one complex is formed [dsDNA(LMT)$_m$], according to the following equation [51,56–58]:

$$dsDNA + m(LMT) \leftrightarrow dsDNA(LMT)_m \quad (3)$$
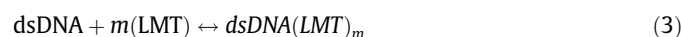
where m represents the binding ratio. Therefore, the following equations can be used to express the association equilibrium constant (β):

$$\beta = [dsDNA(LMT)_m]/[dsDNA][LMT]^m \quad (4)$$

$$\log[\Delta I_p/(\Delta I_{p,max} - \Delta I_p)] = m\log\beta + m\log(c(LMT)) \quad (5)$$

In such cases, $\Delta I_p = I_{p,0} - I_p$, may be used to evaluate the variation in the SW peak current recorded at varying lamotrigine but fixed dsDNA concentration. The plot of log[ΔI_p / ($\Delta I_{p,max}$ − ΔI_p)] vs. log($c_{(\text{LMT})}$) was linear with the slope of m and the intercept of $m\log \beta$. Thus, the values of the binding ratio and the association equilibrium constant were obtained from the slope and intercept, respectively. These values were 0.98 and 2.48 × 10^5 M^{-1}, respectively. The stoichiometry of the cooperative LMT binding is thus at least 1 per base pair unit.

3.3. UV–Vis absorption studies

UV–Vis absorption spectroscopy is perhaps the most widely used instrumental technique to study DNA interactions with drug molecules. As a rule, when a drug molecule interacts with a nucleic acid, some changes occur in absorbance and in the position of the band [52,59]. The magnitude of these changes is associated with the strength of interaction. The extent of hypochromism and red shift generally indicates binding through intercalation [60]. The red shift is associated mainly with the decrease in the energy gap between HOMO and LUMO molecular orbitals after the binding of drug molecules to DNA, while hypochromicity is usually attributed to the interaction between the electronic states of the drug

Table 1
Values of binding constant (K) and Gibbs free energy ($\Delta G°$) for LMT-dsDNA and LMT-ssDNA calculated from the results of voltammetry and UV–vis spectroscopy under physiological conditions.

	LMT-dsDNA		LMT-ssDNA	
	Voltammetry	UV spectroscopy	Voltammetry	UV spectroscopy
K (M^{-1})	6.46 × 10^5	6.93 × 10^5	1.81 × 10^6	1.19 × 10^6
$\Delta G°$ (kJ mol^{-1})	−32.59	−32.76	−35.70	−34.08

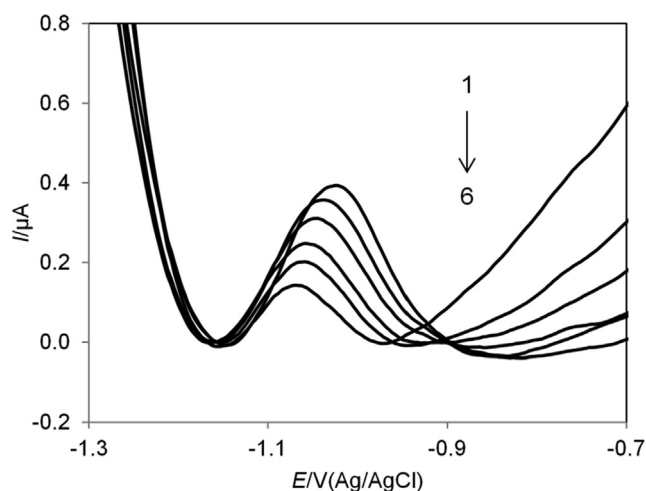**Fig. 6.** SW voltammograms of lamotrigine incubated with dsDNA ($c_{(LMT)}$ = 3.0×10^{-5} mol L^{-1}, $c_{(dsDNA)}$ = 50 mg L^{-1}) in PBS (pH 7.4) with increasing NaCl concentration: 0.0 (1), 5.0 (2) 10.0 (3), 15.0 (4), 20.0 (5), 25.0 (6) mmol L^{-1}.

molecules and those of the nucleic acid bases [52,60,61]. Hyperchromism results from the presence of synergistic noncovalent interactions such as electrostatic binding or groove binding (major or minor) along the exterior of DNA helix surface, and it might be ascribed to partial uncoiling of the helix structure, which exposes more bases of DNA [61].

To validate the interaction between lamotrigine and DNA, the UV–Vis absorption spectra of LMT in the absence and presence of dsDNA were studied. In the absence of dsDNA, lamotrigine showed a sharp absorption band at 306 nm. With the addition of various concentrations of dsDNA into the LMT solution, the absorption band of LMT at 306 nm increased without a shift in the wavelength of maximum absorption; simultaneously, a new band developed at approximately 256 nm with increasing concentration of dsDNA, which may be assigned to the LMT-dsDNA complex (Fig. 7). The observed changes indicate the predominant occurrence of electrostatic interactions, which is in agreement with the electrochemical results. Similar investigations were performed in the presence of ssDNA (Supplementary Material, Fig. S2), and the obtained results also indicated the electrostatic mode of binding.
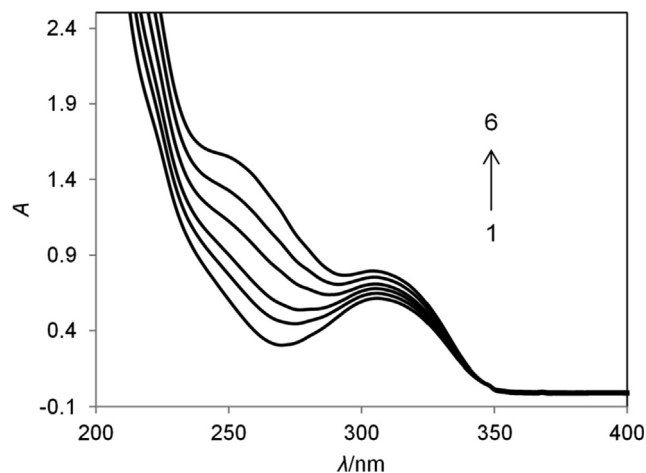

Fig. 7. UV–Vis spectra of LMT (1) ($c_{(LMT)}$ = 1.0×10^{-4} mol L^{-1}) with increasing concentration of dsDNA ($c_{(dsDNA)}$ = 2.0 (2), 6.0 (3), 10.0 (4), 14.0 (5), 18.0 (6) mg L^{-1}); supporting electrolyte: PBS pH 7.4.

On the basis of the variations in the absorbance spectra of LMT upon binding to DNA (both ds- and ssDNA), the binding constant values were calculated according to the following equation [2,52]:

$$A_0/(A - A_0) = \varepsilon_{LMT}/(\varepsilon_{LMT-dsDNA} - \varepsilon_{LMT}) + \varepsilon_G/(\varepsilon_{LMT-dsDNA} - \varepsilon_{LMT}) \times 1/K_f c(DNA) \qquad (6)$$

where A_0 and A are the absorption spectra at 306 nm of the free and complexed LMT, respectively and ε_{LMT} and $\varepsilon_{LMT-dsDNA}$ are the absorption coefficients of the free drug and complexed drug, respectively. Table 1 shows the obtained values of the binding constant, which are in good agreement with those obtained from the electrochemical studies.

3.4. Interaction of lamotrigine with ssDNA

The binding of the antiepileptic drug lamotrigine to single stranded DNA was investigated by CV and SWV in the presence and absence of ssDNA. When ssDNA was added to the LMT solution, a marked decrease in the peak current height was observed, and the peak potential was shifted to more negative value (Fig. 4A,B). As noted in the previous investigation, the decrease in LMT peak current after the addition of ssDNA appeared to be caused by the electrostatic attraction of LMT to the slowly diffusing ssDNA, which resulted in decrease in the apparent diffusion coefficient value. This was apparent from the decrease in the slope of the linear I_p versus $v^{1/2}$ ($r^2 \geq 0.993$) plots; the obtained slope values were 2.23 and 1.68 μA $V^{-1/2}$ $s^{-1/2}$ in the absence and presence of ssDNA, respectively (Fig. 4A inset). From the obtained value, the diffusion coefficient of the bound LMT (LMT-ssDNA) was calculated to be 1.44×10^{-6} cm^2 s^{-1}. By using the estimated value of D_f, the heterogeneous rate constant (k^o) was also calculated. The k^o value in the presence of ssDNA was 9.11×10^{-3} s^{-1}; thus, as assumed, the rate of electron transfer was decreased in the presence of ssDNA.

Current titration was performed with SWV by keeping LMT concentration fixed while varying the concentration of ssDNA (Supplementary Material, Fig. S3). As the LMT-ssDNA interaction also depends on time, voltammograms for the adequate interaction time voltammograms were recorded in the presence of ssDNA at different time intervals. An interaction time of 6 min was found to be sufficient; therefore, this time period was maintained constant after the addition of each concentration of ssDNA. The binding constant was evaluated according to Eq. (1), and the obtained result is shown in Table 1. Consequently, the change in the Gibbs free energy was also estimated (Table 1). The ionic strength influence was examined as previously described, and similar results were obtained.

The effect of a fixed ssDNA concentration on the SW response of a series of increasing concentration of LMT was studied. From Eq. (5), the plot of $\log[\Delta I_p/(\Delta I_{p,max} - \Delta I_p)]$ vs. $\log(c_{(LMT)})$ was found to be linear with the slope of m and the intercept of $m\log \beta$. The values for β and m were 5.37×10^5 M^{-1} and 1.18, respectively. Summarizing, bearing in mind the decrease in the LMT peak current in the presence of ssDNA and a negative shift in the peak potential, it can be assumed that the observed interaction occurred mainly through the electrostatic binding mode. In addition, no intercalative interactions are expected if the binding occurs with single stranded DNA.

Comparison of the electrochemical behavior of LMT after the addition of dsDNA and ssDNA indicated that the peak currents decrease and the peak potentials shift to more negative values in both cases. Nonetheless, the LMT peak current obtained in the presence of dsDNA was slightly higher than that obtained in the presence of ssDNA (Fig. 4). This result indicates that lamotrigine interacts with single stranded DNA more strongly, which also con-

firms the values of the calculated binding constants. The decrease in the LMT peak current after the addition of ssDNA was due to an increase in the electrostatic binding of lamotrigine to single stranded DNA or due to a decrease in the electron transfer of LMT through ssDNA or probably both.

4. Conclusion

The interaction of LMT with double and single stranded DNA at the physiological pH value of 7.4 was investigated for the first time. Electrochemical and spectroscopic studies revealed that LMT interacted with both dsDNA and ssDNA mainly through electrostatic interaction. After the addition of dsDNA or ssDNA, the LMT peak current decreased and shifted to more negative potential values. UV–Vis spectroscopic studies showed a hyperchromic effect without a shift in the wavelength of maximum absorption after the addition of the nucleic acid to the LMT solution. A good correlation was observed between the binding constant values obtained through both techniques. The described approach shows the usefulness of the voltammetric methods for simple investigation of drug-DNA interactions; moreover, electrochemical techniques offer great advantages such as rapidity, relatively low cost, and adequate sensitivity for such analyses. The obtained results are of potential importance for understanding the mechanisms of interaction of drugs with DNA in living organisms.

Declaration of Competing Interest

None.

Appendix A. Supplementary data

Supplementary data to this article can be found online at https://doi.org/10.1016/j.bioelechem.2020.107630.

References

[1] Y. Temerk, M. Ibrahim, H. Ibrahim, W. Schuhmann, Comparative studies on the interaction of anticancer drug irinotecan with dsDNA and ssDNA, RSC Adv. 8 (2018) 25387–25395, https://doi.org/10.1039/C8RA03231A.

[2] Y. Temerk, M. Ibrahim, H. Ibrahim, M. Kotb, Interactions of an anticancer drug Formestane with single and double stranded DNA at physiological conditions, J. Photochem. Photobiol., B 149 (2015) 27–36, https://doi.org/10.1016/j.jphotobiol.2015.05.009.

[3] S. Rauf, J.J. Gooding, K. Akhtar, M.A. Ghauri, M. Rahman, M.A. Anwar, A.M. Khalid, Electrochemical approach of anticancer drugs-DNA interaction, J. Pharm. Biomed. Anal. 37 (2005) 205–217, https://doi.org/10.1016/j.jpba.2004.10.037.

[4] S. Shahzad, B. Dogan-Topal, L. Karadurmus, M.G. Caglayan, T. Taskin Tok, B. Uslu, A. Shah, S.A. Ozkan, Electrochemical, spectroscopic and molecular docking studies on the interaction of calcium channel blockers with dsDNA, Bioelectrochemistry 127 (2019) 12–20, https://doi.org/10.1016/j.bioelechem.2018.12.007.

[5] M. Sirajuddin, S. Ali, A. Badshah, Drug–DNA interactions and their study by UV–Visible, fluorescence spectroscopies and cyclic voltametry, J. Photochem. Photobiol., B 124 (2013) 1–19, https://doi.org/10.1016/j.jphotobiol.2013.03.013.

[6] R. Eckel, R. Ros, A. Ros, S.D. Wilking, N. Sewald, D. Anselmetti, Identification of Binding Mechanisms in Single Molecule–DNA Complexes, Biophys. J . 85 (2003) 1968–1973, https://doi.org/10.1016/S0006-3495(03)74624-4.

[7] A.R. Bahrami, M.J. Dickman, M.M. Matin, J.R. Ashby, P.E. Brown, M.J. Conroy, G.J.S. Fowler, J.P. Rose, Q.I. Sheikh, A.T. Yeung, D.P. Hornby, Use of fluorescent DNA-intercalating dyes in the analysis of DNA via ion-pair reversed-phase denaturing high-performance liquid chromatography, Anal. Biochem. 309 (2002) 248–252, https://doi.org/10.1016/S0003-2697(02)00306-8.

[8] S.T. Saito, G. Silva, C. Pungartnik, M. Brendel, Study of DNA-emodin interaction by FTIR and UV-Vis spectroscopy, J. Photochem. Photobiol., B 111 (2012) 59–63, https://doi.org/10.1016/j.jphotobiol.2012.03.012.

[9] A.H. Hegde, S.N. Prashanth, J. Seetharamappa, Interaction of antioxidant flavonoids with calf thymus DNA analyzed by spectroscopic and electrochemical methods, J. Pharm. Biomed. Anal. 63 (2012) 40–46, https://doi.org/10.1016/j.jpba.2012.01.034.

[10] S. Agarwal, D.K. Jangir, R. Mehrotra, Spectroscopic studies of the effects of anticancer drug mitoxantrone interaction with calf-thymus DNA, J. Photochem. Photobiol., B 120 (2013) 177–182, https://doi.org/10.1016/j.jphotobiol.2012.11.001.

[11] R. Hajian, T. Guan Huat, Spectrophotometric studies on the thermodynamics of the DS-DNA interaction with irinotecan for a better understanding of anticancer drug-DNA interactions, J. Spectrosc. 1 (2013), https://doi.org/10.1155/2013/380352.

[12] K. Sandström, S. Wärmländer, M. Leijon, A. Gräslund, 1H NMR studies of selective interactions of norfloxacin with double-stranded DNA, Biochem. Biophys. Res. Commun. 304 (2003) 55–59, https://doi.org/10.1016/S0006-291X(03)00504-7.

[13] N. Shi, V.M. Ugaz, Using Microchip Gel Electrophoresis to Probe DNA–Drug Binding Interactions, in: J. Stockert, J. Espada, A. Blázquez-Castro (Eds.), Functional Analysis of DNA and Chromatin, Humana Press, Totowa, NJ, 2014, pp. 13–24, https://doi.org/10.1007/978-1-62703-706-8_2.

[14] D. Maciejewska, I. Szpakowska, I. Wolska, M. Niemyjska, M. Mascini, M. Maj-Zurawska, DNA-based electrochemical biosensors for monitoring of bis-indoles as potential antitumoral agents, chemistry, X-ray crystallography, Bioelectrochemistry 69 (2006) 1–9, https://doi.org/10.1016/j.bioelechem.2005.09.003.

[15] J. Yuan, W. Guo, X. Yang, E. Wang, Anticancer Drug−DNA Interactions Measured Using a Photoinduced Electron-Transfer Mechanism Based on Luminescent Quantum Dots, Anal. Chem. 81 (2009) 362–368, https://doi.org/10.1021/ac801533u.

[16] S. Bi, C. Qiao, D. Song, Y. Tian, D. Gao, Y. Sun, H. Zhang, Study of interactions of flavonoids with DNA using acridine orange as a fluorescence probe, Sens. Actuat., B 119 (2006) 199–208, https://doi.org/10.1016/j.snb.2005.12.014.

[17] Y. Ni, D. Lin, S. Kokot, Synchronous fluorescence, UV–visible spectrophotometric, and voltammetric studies of the competitive interaction of bis(1,10-phenanthroline)copper(II) complex and neutral red with DNA, Anal. Biochem. 352 (2006) 231–242, https://doi.org/10.1016/j.ab.2006.02.031.

[18] R. Rohs, H. Sklenar, R. Lavery, B. Röder, Methylene blue binding to DNA with alternating GC base sequence: A modeling study, J. Am. Chem. Soc. 122 (2000) 2860–2866, https://doi.org/10.1021/ja992966k.

[19] V.G. Vaidyanathan, B.U. Nair, Oxidative cleavage of DNA by tridentate copper (II) complex, J. Inorg. Biochem. 93 (2003) 271–276, https://doi.org/10.1016/S0162-0134(02)00593-7.

[20] S.S. Kalanur, U. Katrahalli, J. Seetharamappa, Electrochemical studies and spectroscopic investigations on the interaction of an anticancer drug with DNA and their analytical applications, J. Electroanal. Chem. 636 (2009) 93–100, https://doi.org/10.1016/j.jelechem.2009.09.018.

[21] F. Wang, Y. Xu, J. Zhao, S. Hu, Electrochemical oxidation of morin and interaction with DNA, Bioelectrochemistry 70 (2007) 356–362, https://doi.org/10.1016/j.bioelechem.2006.05.003.

[22] M. Catalán, A. Álvarez-Lueje, S. Bollo, Electrochemistry of interaction of 2-(2-nitrophenyl)-benzimidazole derivatives with DNA, Bioelectrochemistry 79 (2010) 162–167, https://doi.org/10.1016/j.bioelechem.2010.02.002.

[23] Y.M. Temerk, M.S. Ibrahim, M. Kotb, W. Schuhmann, Interaction of antitumor flavonoids with dsDNA in the absence and presence of Cu(II), Anal. Bioanal. Chem. 405 (2013) 3839–3846, https://doi.org/10.1007/s00216-012-6675-2.

[24] B. Dogan-Topal, B. Bozal-Palabiyik, S.A. Ozkan, B. Uslu, Investigation of anticancer drug lapatinib and its interaction with dsDNA by electrochemical and spectroscopic techniques, Sens. Actuators, B 194 (2014) 185–194, https://doi.org/10.1016/j.snb.2013.12.088.

[25] Y. Temerk, H. Ibrahim, Binding mode and thermodynamic studies on the interaction of the anticancer drug dacarbazine and dacarbazine–Cu(II) complex with single and double stranded DNA, J. Pharm. Biomed. Anal. 95 (2014) 26–33, https://doi.org/10.1016/j.jpba.2014.02.010.

[26] K. Morawska, T. Popławski, W. Ciesielski, S. Smarzewska, Electrochemical and spectroscopic studies of the interaction of antiviral drug Tenofovir with single and double stranded DNA, Bioelectrochemistry 123 (2018) 227–232, https://doi.org/10.1016/j.bioelechem.2018.06.002.

[27] L. Hlavata, K. Benikova, V. Vyskocil, J. Labuda, Evaluation of damage to DNA induced by UV-C radiation and chemical agents using electrochemical biosensor based on low molecular weight DNA and screen-printed carbon electrode, Electrochim. Acta 71 (2012) 134–139, https://doi.org/10.1016/j.electacta.2012.03.119.

[28] A. Hájková, J. Barek, V. Vyskočil, Voltammetric Determination of 2-Aminofluoren-9-one and Investigation of Its Interaction with DNA on a Glassy Carbon Electrode, Electroanalysis 27 (2015) 101–110, https://doi.org/10.1002/elan.201400427.

[29] E. Horakova, J. Barek, V. Vyskocil, Voltammetry at a Hanging Mercury Drop Electrode as a Tool for the Study of the Interaction of Double-stranded DNA with Genotoxic 4-Nitrobiphenyl, Electroanalysis 28 (2016) 2760–2770, https://doi.org/10.1002/elan.201600241.

[30] V. Svitková, M. Hanzelyová, H. Macková, J. Blaškovičová, V. Vyskočil, D. Farkašová, J. Labuda, Behaviour and detection of acridine-type DNA intercalators in urine using an electrochemical DNA-based biosensor with the protective polyvinyl alcohol membrane, J. Electroanal. Chem. 821 (2018) 87–91, https://doi.org/10.1016/j.jelechem.2017.11.028.

[31] M.T. Carter, A.J. Bard, Voltammetric studies of the interaction of tris(1,10-phenanthroline)cobalt(III) with DNA, J. Am. Chem. Soc. 109 (1987) 7528–7530, https://doi.org/10.1021/ja00258a046.

[32] M. Fojta, A. Daňhel, L. Havran, V. Vyskočil, Recent progress in electrochemical sensors and assays for DNA damage and repair, TrAC, Trends Anal. Chem. 79 (2016) 160–167, https://doi.org/10.1016/j.trac.2015.11.018.

[33] A. Hanawa, K. Asai, G. Ogata, H. Hibino, Y. Einaga, Electrochemical measurement of lamotrigine using boron-doped diamond electrodes, Electrochim. Acta 271 (2018) 35–40, https://doi.org/10.1016/j.electacta.2018.03.112.

[34] K. Beattie, G. Phadke, J. Novakovic, H.G. Brittain, Chapter 6 - Lamotrigine, in: H.G. Brittain, Profiles of Drug Substances, Excipients and Related Methodology, Academic Press, 2012, pp. 245-285. https://doi.org/10.1016/B978-0-12-397220-0.00006-4.

[35] H. Wang, D. Qian, X. Xiao, S. Gao, J. Cheng, B. He, L. Liao, J. Deng, A highly sensitive and selective sensor based on a graphene-coated carbon paste electrode modified with a computationally designed boron-embedded duplex molecularly imprinted hybrid membrane for the sensing of lamotrigine, Biosens. Bioelectron. 94 (2017) 663–670, https://doi.org/10.1016/j.bios.2017.03.055.

[36] R.T. Wechsler, R. Leroy, A. Van Cott, A.E. Hammer, A. Vuong, R. Huffman, K. VanLandingham, J.A. Messenheimer, Lamotrigine extended-release as adjunctive therapy with optional conversion to monotherapy in older adults with epilepsy, Epilepsy Res. 108 (2014) 1128–1136, https://doi.org/10.1016/j.eplepsyres.2014.04.009.

[37] F. Li, Z.-D. Lin, Y. Hu, W. Li, C.-C. Xue, N.D. Poonit, Lamotrigine monotherapy for paroxysmal kinesigenic dyskinesia in children, Seizure 37 (2016) 41–44, https://doi.org/10.1016/j.seizure.2016.02.009.

[38] R.-S. Saberi, S. Shahrokhian, Highly sensitive voltammetric determination of lamotrigine at highly oriented pyrolytic graphite electrode, Bioelectrochemistry 84 (2012) 38–43, https://doi.org/10.1016/j.bioelechem.2011.10.008.

[39] S. Smarzewska, D. Guziejewski, A. Leniart, W. Ciesielski, Nanomaterials vs Amalgam in Electroanalysis: Comparative Electrochemical Studies of Lamotrigine, J. Electrochem. Soc. 164 (2017) B321–B329, https://doi.org/10.1149/2.0221707jes.

[40] A.F. Cohen, G.S. Land, D.D. Breimer, W.C. Yuen, C. Winton, A.W. Peck, Lamotrigine, a new anticonvulsant: Pharmacokinetics in normal humans, Clin. Pharmacol. Ther. 42 (1987) 535–541, https://doi.org/10.1038/clpt.1987.193.

[41] K. Barel-Cohen, L.S. Shore, M. Shemesh, A. Wenzel, J. Mueller, N. Kronfeld-Schor, Monitoring of natural and synthetic hormones in a polluted river, J. Environ. Manage. 78 (2006) 16–23, https://doi.org/10.1016/j.jenvman.2005.04.006.

[42] N.M. El-Enany, D.T. El-Sherbiny, A.A. Abdelal, F.F. Belal, Validated Spectrofluorimetric Method for the Determination of Lamotrigine in Tablets and Human Plasma Through Derivatization with o-phthalaldehyde, J. Fluorescence 20 (2010) 463–472, https://doi.org/10.1007/s10895-009-0568-6.

[43] K.K. Hotha, S.S. Kumar, D.V. Bharathi, V. Venkateswarulu, Rapid and sensitive LC-MS/MS method for quantification of lamotrigine in human plasma: application to a human pharmacokinetic study, Biomed. Chromatogr. 26 (2012) 491–496, https://doi.org/10.1002/bmc.1692.

[44] L. Antonilli, V. Brusadin, F. Filipponi, R. Guglielmi, P. Nencini, Development and validation of an analytical method based on high performance thin layer chromatography for the simultaneous determination of lamotrigine, zonisamide and levetiracetam in human plasma, J. Pharm. Biomed. Anal. 56 (2011) 763–770, https://doi.org/10.1016/j.jpba.2011.07.018.

[45] J. Zheng, M.W. Jann, Y.Y. Hon, S.A. Shamsi, Development of capillary zone electrophoresis-electrospray ionization-mass spectrometry for the determination of lamotrigine in human plasma, Electrophoresis 25 (2004) 2033–2043, https://doi.org/10.1002/elps.200305823.

[46] M.B. Gholivand, G. Malekzadeh, M. Torkashvand, Determination of lamotrigine by using molecularly imprinted polymer–carbon paste electrode, J. Electroanal. Chem. 692 (2013) 9–16, https://doi.org/10.1016/j.jelechem.2012.12.016.

[47] O. Domínguez-Renedo, M.E.B. Calvo, M.J. Arcos-Martínez, Determination of lamotrigine in pharmaceutical preparations by adsorptive stripping voltammetry using screen printed electrodes, Sensors 8 (2008) 4201–4212, https://doi.org/10.3390/s8074201.

[48] D.K. Gosser, Cyclic Voltammetry, VCH, New York, 1994. https://doi.org/10.1080/00945719408001398.

[49] L.B.O. dos Santos, G. Abate, J.C. Masini, Determination of atrazine using square wave voltammetry with the Hanging Mercury Drop Electrode (HMDE), Talanta 62 (2004) 667–674, https://doi.org/10.1016/j.talanta.2003.08.034.

[50] A.J. Bard, L.R. Faulkner, Electrochemical Methods: Fundamentals and Applications, John Wiley & Sons, New York, 2000.

[51] Y. Temerk, H. Ibrahim, Electrochemical studies and spectroscopic investigations on the interaction of an anticancer drug flutamide with DNA and its analytical applications, J. Electroanal. Chem. 736 (2015) 1–7, https://doi.org/10.1016/j.jelechem.2014.10.019.

[52] E. Jabeen, N.K. Janjua, S. Ahmed, I. Tahiri, M. Kashif, A. Javed, DNA binding interaction studies of flavonoid complexes of Cu(II) and Fe(II) and determination of their chemotherapeutic potential, Inorg. Chim. Acta 496 (2019), https://doi.org/10.1016/j.ica.2019.119048.

[53] X. Wang, L. Sun, N. Zou, Z. Yu, Electrochemical study on the interaction between dopamine and deoxyribonucleic acid using a glassy carbon electrode modified with silver-doped poly cysteine membrane, Int. J. Electrochem. Sci. 10 (2015) 7320–7330.

[54] M.V. del Pozo, C. Alonso, F. Pariente, E. Lorenzo, DNA Biosensor for Detection of Helicobacter pylori Using Phen-dione as the Electrochemically Active Ligand in Osmium Complexes, Anal. Chem. 77 (2005) 2550–2557, https://doi.org/10.1021/ac0489263.

[55] A.-E. Radi, A. Eissa, H.M. Nassef, Voltammetric and spectroscopic studies on the binding of the antitumor drug dacarbazine with DNA, J. Electroanal. Chem. 717–718 (2014) 24–28, https://doi.org/10.1016/j.jelechem.2014.01.007.

[56] X. Tian, Y. Song, H. Dong, B. Ye, Interaction of anticancer herbal drug berberine with DNA immobilized on the glassy carbon electrode, Bioelectrochemistry 73 (2008) 18–22, https://doi.org/10.1016/j.bioelechem.2008.02.005.

[57] K. Morawska, K. Jedlińska, S. Smarzewska, R. Metelka, D. Guziejewski, Analysis and DNA interaction of the profluralin herbicide, Environ. Chem. Lett. 17 (2019) 1359–1365, https://doi.org/10.1007/s10311-019-00865-1.

[58] D. Guziejewski, K. Morawska, T. Popławski, R. Metelka, W. Ciesielski, S. Smarzewska, Lactofen – Electrochemical Sensing and Interaction with dsDNA, Electroanalysis 30 (2018) 94–100, https://doi.org/10.1002/elan.201700472.

[59] M.T. Carter, M. Rodriguez, A.J. Bard, Voltammetric studies of the interaction of metal chelates with DNA. 2. Tris-chelated complexes of cobalt(III) and iron(II) with 1,10-phenanthroline and 2,2'-bipyridine, J. Am. Chem. Soc. 111 (1989) 8901–8911, https://doi.org/10.1021/ja00206a020.

[60] N. Shahabadi, S. Kashanian, M. Khosravi, M. Mahdavi, Multispectroscopic DNA interaction studies of a water-soluble nickel(II) complex containing different dinitrogen aromatic ligands, Transition Met. Chem. 35 (2010) 699–705, https://doi.org/10.1007/s11243-010-9382-x.

[61] N. Shahabadi, S. Amiri, H. Zhaleh, Spectrophotometric and physicochemical studies on the interaction of a new platinum(IV) complex containing the drug pregabalin with calf thymus DNA, J. Coord. Chem. 73 (2020) 35–51, https://doi.org/10.1080/00958972.2019.1710743.

Interactions of lamotrigine with single- and double-stranded DNA under physiological conditions

Kamila MORAWSKA*[a], Tomasz POPŁAWSKI[b], Witold CIESIELSKI[a], Sylwia SMARZEWSKA[a],

[a] University of Lodz, Faculty of Chemistry, Department of Inorganic and Analytical Chemistry, 12 Tamka Str, 91-403 Lodz, Poland

[b] University of Lodz, Faculty of Biology and Environmental Protection, Department of Molecular Genetics, 141/143 Pomorska Str, 90-237 Lodz, Poland

Corresponding author: kamila.morawska@chemia.uni.lodz.pl, Tel.: +48 42 635 5810

S1. Optimization study

S1.1 Selection of optimal square wave voltammetric parameters
As SW voltammetric parameters are interrelated and exert a combine effect on the registered peak current, to establish the optimum conditions for chosen supporting electrolyte, the influence of amplitude, frequency and step potential was studied. Amplitude was evaluated in the range of 10–100 mV. The peak current increased from 10 mV to 30 mV and was well-defined. For amplitude values higher than 30 mV non-linear growth of the peak (plateau) was observed. The best results were obtained at 30 mV, and thus those value was adopted in subsequent studies. Next the influence of frequency (10–100 Hz) on LMT peak current was studied. The strongest analytical signal and the best-shaped peak were obtained at 25 Hz, with a plateau at higher frequency values. Consequently, 25 Hz was selected for further investigations. Finally, the step potential was evaluated in the range of 1–10 mV. At a whole examined range of step potential, the LMT peak current increased with the increasing of step potential value, but it was angularly shaped above 6 mV, thus in further studies a step potential of 6 mV was applied.

S1.2 Selection of optimal interaction time
To establish the optimal interactions conditions, the influence of the interaction time on LMT signals upon the addition of a fixed amount of ds- or ssDNA was investigated. The LMT voltammograms in the presence of both types of nucleic acids were recorded at different time intervals (from 2 to 40 min) which elapsed since the addition of DNA. In the case of presence of dsDNA, LMT peak currents significantly decreased and shifted to more negative potential values up to 8 min, after that time value, no significant changes in peak current and peak potential were observed (Fig. S1). Similar changes were observed in the case of presence of ssDNA, i.e. lamotrigine signals decreased and shifted to more negative potentials, however 6 min was found to be sufficient time for LMT-ssDNA interaction. Thus in further studies an interaction time of 8 min and 6 min in case of interaction with dsDNA and ssDNA, respectively was applied.
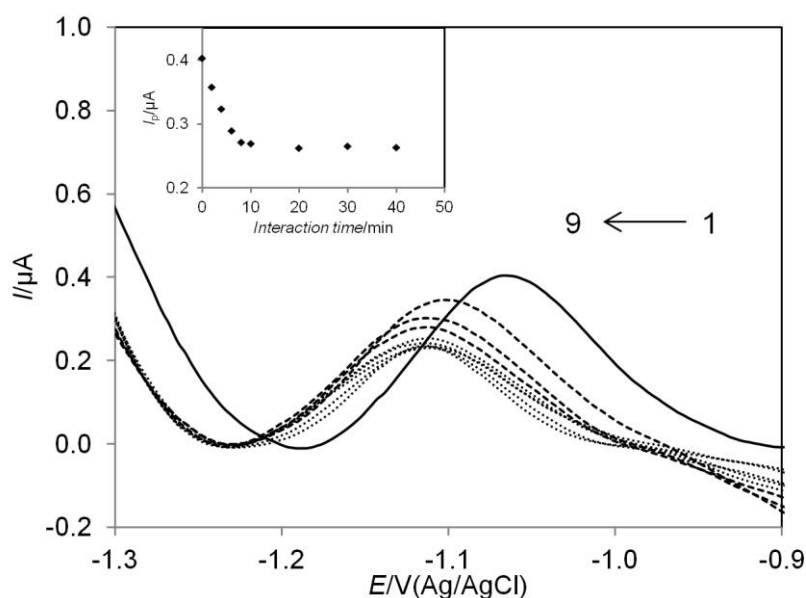

Fig. S1 SW voltammograms of lamotrigine incubated with dsDNA ($c(_{LMT}) = 2.0 \times 10^{-5}$ mol L^{-1}, $c(_{dsDNA}) = 50$ mg $^{L-1}$) in PBS (pH 7.4) with increasing incubation time: 0.0 (1, straight line), 2,

4, 6 (2-4, dashed lines) 8, 10, 20, 30, 40 (5-9, dotted lines) min. Inset: Relationship between the peak current of LMT in presence of fixed concentration of dsDNA and interaction time.
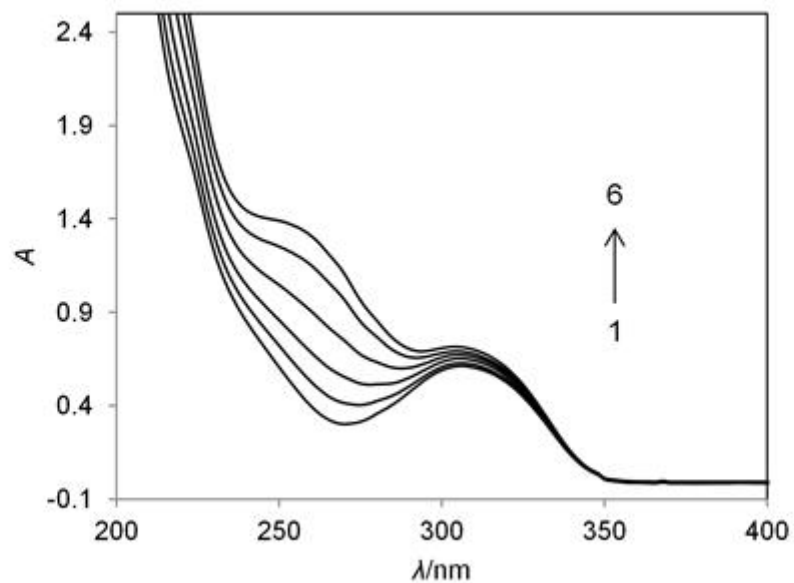
Fig. S2 UV-Vis spectra of LMT (1) (c_{LMT}) = 1.0×10^{-4} mol L^{-1}) with increasing concentration of ssDNA (c_{ssDNA}) = 2.0 (2), 6.0 (3), 10.0 (4), 14.0 (5), 18.0 (6) mg L^{-1}); supporting electrolyte: PBS pH 7.4.

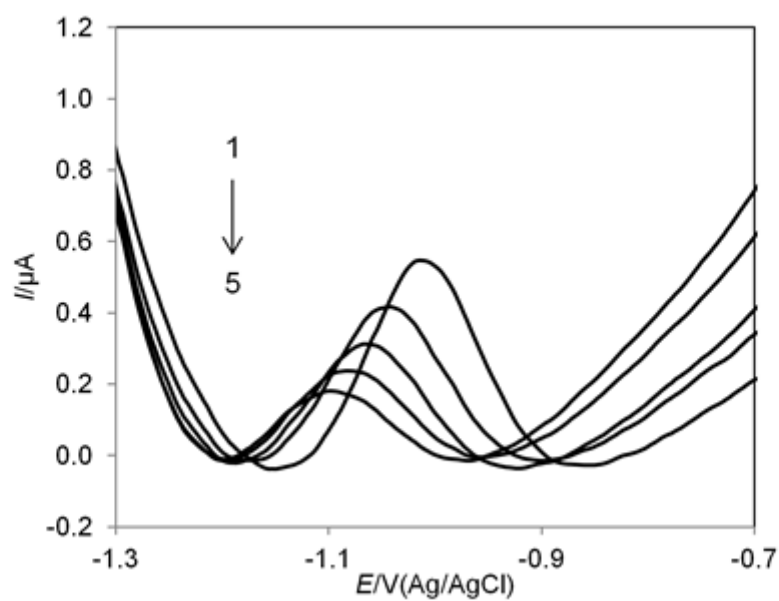Fig. S3 SW voltammograms of LMT (c_{LMT}) = 3.0×10^{-5} mol L^{-1}) recorded in the absence (1) and presence of ssDNA (c_{ssDNA}) = 10.0 (2), 20.0 (3), 40.0 (4), 60.0 (5), mg L^{-1}); supporting electrolyte: PBS pH 7.4.

4

First electroanalytical studies of methoxyfenozide and its interactions with dsDNA

Kamila Morawska *, Witold Ciesielski, Sylwia Smarzewska *

University of Lodz, Faculty of Chemistry, Department of Inorganic and Analytical Chemistry, Tamka 12, 91-403 Lodz, Poland

ARTICLE INFO

ABSTRACT

The widespread use of pesticides is one of the major health and environmental concerns. There is an urgent need to develop improved analytical methodologies as well as for a deep insight into the mechanism behind the interaction between pesticides and the nucleic acids of living organisms. In the present work, the electrochemical behavior of the diacylhydrazine insecticide methoxyfenozide (*Met*) on a boron-doped diamond electrode and its interaction with double-stranded DNA (dsDNA) were investigated for the first time by applying cyclic voltammetry and square-wave (SW) voltammetry. The influence of numerous factors, such as composition of the supporting electrolyte, its pH, and voltammetric parameters, was analyzed. Under the optimized conditions, a simple and sensitive SW voltammetric procedure was developed for the determination of *Met*. Quantification was found to be linear from 5.0×10^{-7} to 7.0×10^{-5} mol L^{-1}, with a detection limit of 1.4×10^{-7} mol L^{-1}. The application of the developed voltammetric methodology for the analysis of tap water, river water and grape juice was tested with spiked samples. Studies on the interaction between methoxyfenozide and double-stranded salmon sperm DNA were conducted using both voltammetric and spectroscopic techniques. The results obtained indicated the dominance of the intercalative binding mode between *Met* and dsDNA. The binding constants of the formed complex were calculated based on the changes in the electrochemical and spectroscopic behaviors of *Met* in the presence of dsDNA.

1. Introduction

Pesticides are broadly defined as substances or mixtures used to prevent, destroy, or reduce pests including insects, weeds, and rodents [1,2]. According to their functions, pesticides can be categorized into several groups, such as insecticides, which are the second largest pesticide category used worldwide [1]. Methoxyfenozide (N-tert-butyl-N′-(3-methoxy-o-toluoyl)-3,5-xylohydrazide, Scheme 1) is a diacylhydrazine insecticide, which was first identified as the most efficacious member of the diacylhydrazine group by Le et al. [3]. The mechanistic aspects of *Met's* insecticidal activity are based on its high-affinity binding to the ecdysone receptor complex in lepidopteran insects, where it induces premature molting and thereby the death of insects by mimicking their specific hormone [4,5]. *Met* exhibits very high insecticidal efficacy against a broad range of caterpillar pests, at all feeding larval stages of the target Lepidoptera, mainly the members of the family *Noctuidae, Pyralidae, Pieridae,* and so on. It is the most effective when ingested by the caterpillar however, it also displays some ovicidal and topical properties [5].

Methoxyfenozide is used for a variety of crops such as grapes, sweet corn, tomato, aubergine, pepper, and leafy vegetables (spinach, herbs, lettuce and other salad plants) [6]. It is a colorless and odorless solid, and is characterized by low aqueous solubility and very low volatility. Based on its physical and chemical properties, it is associated with a real risk of leaching to groundwater [6], and under anaerobic conditions, it may be persistent in soil systems. *Met* shows low oral toxicity toward mammals, birds, or honeybees, but no significant risks to human health have been identified. However, it is relatively more toxic to earthworms and aquatic species [6]. Therefore, a simple, fast, and sensitive method for the determination of methoxyfenozide is vital to protect the ecology and environment. Literature data show that the number of methods available for the quantitative determination of *Met* is scarce; only a few analytical methodologies have been reported, which are mainly based on liquid chromatography [4,7–10]. Although the liquid chromatographic methodologies are among the most sensitive and selective ones, they are quite expensive, time-consuming, and labor-intensive. Furthermore, their generate high quantities of waste, and require a huge volume of toxic organic solvents. The aforementioned features may lead to some important issues in terms of the ecological impact or operator safety. Therefore, there is a need to develop a simple, rapid, inexpensive, and simultaneously sensitive and environmentally friendly method for the assessment of methoxyfenozide. Nowadays, electrochemical techniques, as an interesting alternative to chromatographic techniques, are often used for the determination of a

* Corresponding authors.
 E-mail addresses: kamila.morawska@chemia.uni.lodz.pl (K. Morawska), witold.ciesielski@chemia.uni.lodz.pl (W. Ciesielski), sylwia.smarzewska@chemia.uni.lodz.pl (S. Smarzewska).
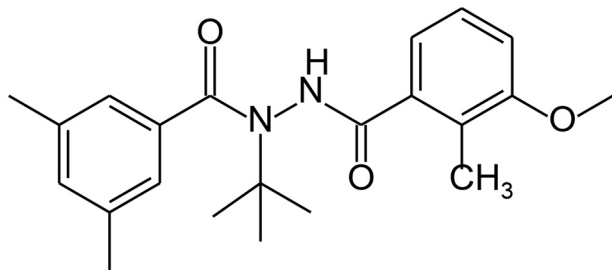
Scheme 1. Chemical structure of methoxyfenozide.

broad range of biologically significant compounds, including pesticides, drugs, and related substances [11–14]. Electrochemical techniques have numerous advantages such as high sensitivity and reproducibility, low instrumentation cost, short analysis time, and possibility of miniaturization [14,15]. The fact that electrochemical techniques may provide valuable information on kinetic and thermodynamic features of the studied system is an added advantage [16,17]. Moreover, there has been an expanding interest in electrochemical investigation of the interactions between small molecules (drugs, pesticides) and DNA [18–24]. Electrochemical techniques are especially promising in such interaction studies, because of the existing similarity between the redox reactions occurring at the working electrodes and the processes occurring in living organisms [25]. Electrochemical signals reflecting the interactions of analyzed molecules with DNA allow evaluating the binding constants, examining the nature of the formed complexes, and studying the interaction mechanisms [19,21,22,26–28]. Over the past few years, the interactions of DNA with small molecules have been extensively investigated using various methods, including the most commonly used spectroscopic techniques [18,29,30]. The electrochemical approach to interaction studies can complement the results obtained through spectroscopic techniques; hence, these techniques are very often combined in order to obtain enhanced results [18,25,28].

Thus, in the present study, electrochemical techniques were applied for the development of a simple methodology for the quantitative determination of methoxyfenozide as well as for the characterization of the interactions occurring between *Met* and double-stranded DNA obtained from salmon sperm. To the best of our knowledge, until now, there are no reports on the electrochemical properties of *Met* and its interaction with DNA. It is noteworthy that the use of a working electrode is particularly significant in electroanalysis. Therefore, in this study, a boron-doped diamond electrode (BDDE) was used. Boron-doped diamond is an electrode material that has attracted a great deal of interest because of its outstanding electrochemical features. Furthermore, it has a low background current, a very wide potential window, and the highest electrochemical stability, and thereby allows highly sensitive detection [13,31].

The current study of methoxyfenozide and its interaction with dsDNA on BDDE was conducted by using cyclic voltammetry (CV) and square-wave voltammetry (SWV). Moreover, the binding mechanism through which *Met* interacts with dsDNA was also investigated by using UV–vis spectroscopy. In the context of analytical chemistry, the work aimed to first develop a sensitive electrochemical procedure for methoxyfenozide determination in spiked juice samples (grape juice) and spiked water samples (river water and tap water). Bearing in mind that many plant protection products may interact with DNA, the aim of this study was also the characterization of the interactions occurring between *Met* and dsDNA.

2. Experimental

2.1. Instrumentation

All voltammetric experiments were conducted using a μAutolab type III potentiostat (run by GPES software, version 4.9; Metrohm-EcoChemie, The Netherlands) combined with an M164 electrode stand (mtm-anko Instruments, Cracow, Poland). A conventional three-electrode system was used,

which consisted of a boron-doped diamond electrode as a working electrode (Windsor Scientific Ltd., UK), saturated Ag/AgCl (3 mol L^{-1} KCl) as a reference electrode, and a platinum wire as a counter electrode. Electrochemical experiments were conducted using a standard voltammetric cell of 10 mL volume. A digital pH-meter (Elmetron, Poland) in conjunction with a glassy electrode, was used for preparing all of the buffer solutions. The PURELAB UHQ (ELGA LabWater, UK) was used for the demineralization of water. Spectrophotometric measurements were performed using a Cary 100 Bio UV–vis Spectrophotometer (Agilent, USA). All the measurements were carried out at the ambient temperature.

2.2. Chemicals and reagents

Methoxyfenozide was purchased from Merk (Poland). A stock standard *Met* solution was prepared weekly by dissolving an appropriate amount of the compound in methanol; the prepared solution was refrigerated at 4 ˚C when not used. Working solutions of lower concentrations were prepared by appropriately diluting the stock *Met* solution. Double-stranded DNA (low-molecular-weight from salmon sperm; Sigma-Aldrich, Germany) standard solution was prepared in phosphate-buffered saline (PBS, Sigma-Aldrich, Poland) at pH 7.4. Various supporting electrolytes, namely Britton–Robinson (BR), phosphate, citrate, and citrate-phosphate buffers, were used for the analysis. Britton Robinson buffers of different pH values were prepared by adding sodium hydroxide to a mixture of phosphoric, acetic, and boric acid, containing 0.04 mol L^{-1} of each acid. Buffer components were purchased from Avantor (Poland). All the chemical reagents were of analytical grade. The aqueous solutions were prepared using distilled and deionized water. Grape juice (Hellena, Poland) was purchased from a local grocery shop.

2.3. Measurement procedures

Cyclic and square-wave voltammetry were applied for the general characterization of the electrochemical properties of methoxyfenozide. *Met* was quantified using SWV after optimizing the SW parameters, such as frequency, step potential, and amplitude. Calibration curve was constructed by succeeding additions of the standard *Met* solution into the voltammetric cell containing the supporting electrolyte. Voltammograms of *Met* were recorded after each aliquot addition of the analyte. All voltammetric measurements of *Met* were performed in the potential range from 0.5 to 1.8 V. Before adding each new sample, BDDE was cleaned by polishing on an alumina slurry to obtain a mirror-shine surface. After polishing, the electrode surface was thoroughly washed with distilled water.

The adequacy of the developed SWV method was evaluated by quantifying *Met* in environmental samples of tap and river water (Ljubljanica river) but also in grape juice samples. The samples containing methoxyfenozide were analyzed using the method of standard addition. The juice, tap and river water samples were analyzed without any preconcentration or pre-separation. Spiked water/juice solutions were prepared using the following procedure: 1 mL *Met* of appropriate concentration was transferred into a 10 mL volumetric flask and then made up to the mark with water samples (tap water or Ljubljanica river water) or juice samples (grape juice). The final concentration of methoxyfenozide in the water samples was equal to 1.0×10^{-5}, 5.0×10^{-5}, and 1.0×10^{-4} mol L^{-1}, in the juice samples was equal to 2.5×10^{-5}, 5.0×10^{-5}, and 1.0×10^{-4} mol L^{-1}.

The selectivity of the proposed method was investigated by analyzing 5.0×10^{-6} mol L^{-1} *Met* in the presence of potential interferent compounds found in the environment; the concentration ratios of compounds ($c_{(Int)}:c_{(Met)}$) were of 1:10, 1:5, 1:1, 5:1, and 10:1.

The interaction of *Met* with dsDNA was investigated using cyclic voltammetry, square wave voltammetry and also UV–vis spectroscopy. Voltammetric measurements at fixed concentration of *Met* were recorded in the absence and presence of dsDNA in phosphate buffer at pH 4.5.

Similarly, the absorption spectra of *Met* were observed in phosphate buffer at pH 4.5 in the absence and presence of an increasing amount of

double-stranded DNA in the wavelength range from 200 to 500 nm. All the voltammetric and spectroscopic measurements were obtained in triplicate.

3. Results and discussion

3.1. Electrochemical studies of methoxyfenozide on BDDE

The type of supporting electrolyte and its pH are known as one of the main factors affecting the electrode reaction of a variety of electroactive compounds [14,20,32]. Thus, the electrochemical behavior of methoxyfenozide was initially investigated at a broad pH range (1.5–9.0) offered by the Britton-Robinson buffer. As can be seen in Fig. 1, the highest *Met* signal was recorded at a pH value of 3.0. At higher pH values, a marked decrease of the peak current was observed. Furthermore, there were no *Met* oxidation signals noticed at pH higher than 6.0. Because the highest *Met* signals were recorded at acidic pH, the effect of other supporting electrolytes (citrate and citrate-phosphate buffers) on *Met* signals was also examined. However, the best shape and height of methoxyfenozide signal was achieved in the BR buffer at pH 3.0, which was selected for further studies. With increasing pH, *Met* signals shifted toward more negative potential values. The plot of E_p *versus* pH was linear with slope equal to 10 mV pH^{-1}. Based on the obtained E_p – pH data, it can be stated that the oxidation of methoxyfenozide is a pH-dependent process [33]; nonetheless, from this result, it is difficult to determine the ratio between transferred protons and electrons, which indicates a complex electrode process with presumably multi-step oxidation reaction [34,35].

Next, cyclic voltammetry was applied to study the electrochemical behavior of *Met* with the chosen supporting electrolyte. The CV curves of *Met*, recorded in the potential window from 1.2 to 1.8 V at different scan rates (25–1000 mV s^{-1}) are shown in Fig. 2. *Met* exhibited only a single oxidation peak at a potential of approximately +1.5, which was related to the irreversible process as there was no corresponding reduction signal. When a broader potential range was tested, no additional peaks or different behavior was observed. As typical for irreversible oxidative electrochemical processes, the *Met* peak potential slightly shifted toward more positive values with an increase in scan rate value. Furthermore, the effect of the scan rate on *Met* peak current was investigated. A linear dependence was observed between peak current of *Met* and the square root of the scan rate (I_p = 8.899 $\nu^{1/2}$ + 0.190, R^2 = 0.995, Fig. 2 inset), suggesting a diffusion-controlled process, which was confirmed by constructing the plot of log I_p *vs.* log ν. The slope of this dependence was equal to 0.49, which is close to the theoretical value of 0.5 for diffusion-controlled processes [36].

Based on these results and the available literature data [37,38], it can be stated that under the measurement conditions utilized, *Met* is first oxidized
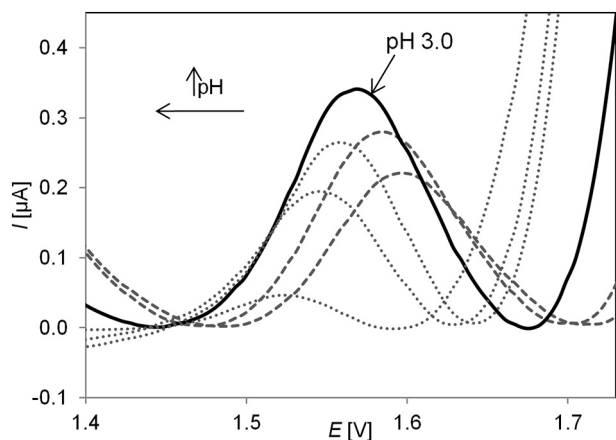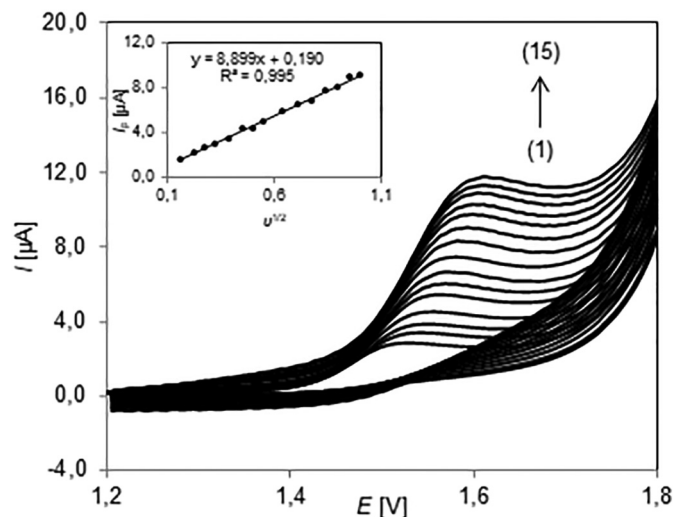

Fig. 2. Cyclic voltammograms of methoxyfenozide (c($_{Met}$) = 1.0 × 10^{-4} mol L^{-1}) in BR, pH 3.0, at different scan rates (mV s^{-1}): (1) 25, (2) 50, (3) 75, (4) 100, (5) 150, (6) 200, (7) 250, (8) 300, (9) 400, (10) 500, (11) 600, (12) 700, (13) 800, (14) 900, and (15) 1000. Inset: the dependence of *Met* peak current (I_p) *versus* the square root of the scan rate.

to a neutral radical. Subsequently, the radical probably undergoes dismutation, and the resulting cationic product loses a proton; however the second step of the oxidation is more complicated, and a detailed investigation of the electrode reaction mechanism is beyond the scope of this study.

In the next step, the parameters of the SWV technique, such as amplitude (10–100 mV), frequency (10–100 Hz), and step potential (1–10 mV), were optimized by sequentially changing one of them, and keeping the others constant. The result showed a significant effect of the aforementioned parameters on the *Met* signal. The optimum peaks with respect to the shape and height were obtained at an amplitude of 30 mV, a step potential of 4 mV, and a frequency of 25 Hz. Further experimental procedures, such as the construction of calibration curve and analysis of water samples, were performed with these optimized parameters.

The robustness of the proposed method was evaluated using SW voltammetric experiments at different pH values of Britton-Robinson buffer considering positive and negative deviations in optimal pH value (2.8–3.2). Such deviation correspond to mistakes in calibration procedures of a pH meter. A small variation in the pH of the supporting electrolyte did not significantly affect *Met* voltammetric response, indicating a suitable robustness of the proposed procedure.

3.2. Analytical application

Quantitative measurements of *Met* were obtained using square-wave voltammetry, under previously optimized conditions. A calibration curve was constructed by plotting the obtained peak currents against the corresponding methoxyfenozide concentration. The anodic peak current increased linearly with *Met* concentration from 5.0 × 10^{-7} to 7.0 × 10^{-5} mol L^{-1} (Fig. 3A). From the calibration curve (Fig. 3B), the limit of detection (LOD) and the limit of quantification (LOQ) for *Met* were calculated as kSD/b, where k = 3 for LOD, and k = 10 for LOQ, b is the slope of the curve, SD is the standard deviation of the intercept [39]. The calculated values of LOD and LOQ were equal to 1.4 × 10^{-7} and 4.8 × 10^{-7} mol L^{-1}, respectively. Subsequently, the intra-day repeatability of the *Met* peak current was assessed with 10 successive measurements in a solution containing 5.0 × 10^{-6} mol L^{-1} of the analyzed compound (n = 10), with the BDDE surface refreshed before each measurement. The obtained coefficient of variation (CV) was 3.1%. In addition, repetitive inter-day measurements, over a period of 5 days, were performed by measuring the obtained peak currents for similarly prepared *Met* solutions of

Fig. 1. SW voltammograms of *Met* (c($_{Met}$) = 1.0 × 10^{-5} mol L^{-1}), recorded in Britton-Robinson buffers at different pH values (1.5, 2.0, 3.0, 4.0, 5.0, 6.0); voltammograms are presented with background subtraction.
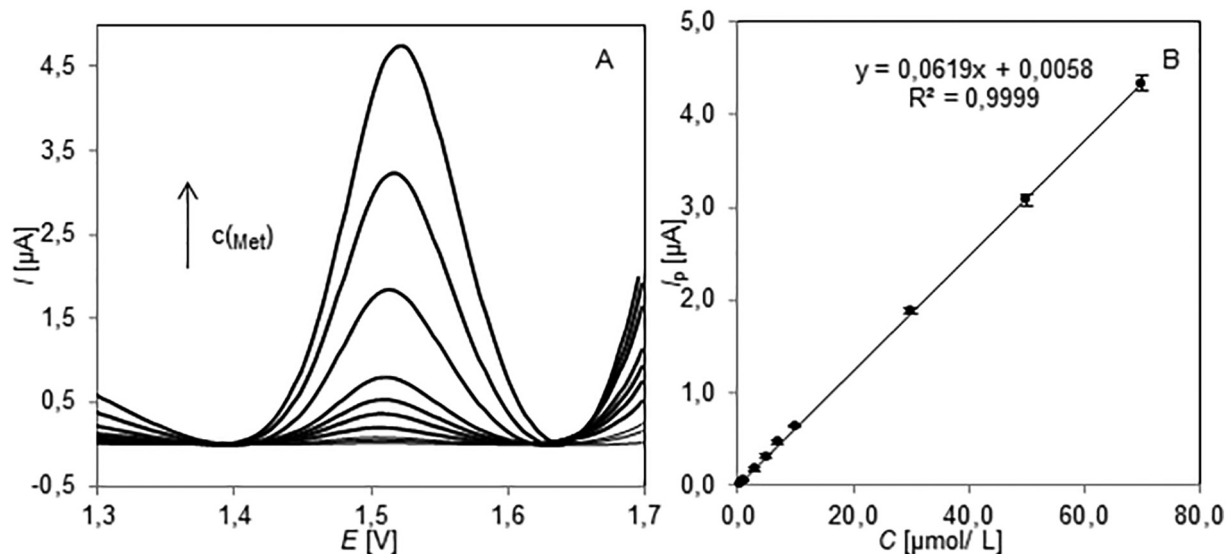
Fig. 3. (A) SW voltammograms recorded in BR, buffer pH 3.0, with increasing methoxyfenozide concentration c($_{Met}$) = 0.5, 0.7, 1.0, 3.0, 5.0, 7.0, 10.0, 30.0, 50.0, and 70.0 μmol L^{-1}; voltammograms are presented with background subtraction. (B) Corresponding calibration curve. The other measurement conditions were as follows: amplitude 30 mV, step potential 4 mV, and frequency 25 Hz.

the same molar concentrations. The CV was found to be 5.7%, which is highly satisfactory for practical applications.

The reliability of the proposed SW voltammetric methodology was investigated by assaying *Met* in tap water, river water (Ljubljanica river) and grape juice. As *Met* was not detectable in the used water and juice samples, a series of spiked samples were used for evaluating the accuracy of the developed method. The standard addition method was used to determine methoxyfenozide in spiked samples. The data related to the recovery curves for the river water, tap water and grape juice samples are shown in Table 1. The presented values of recovery indicated that the components of the water and juice matrices did not affect the analytical sensitivity. Thus, it can be concluded that the developed procedure can effectively determine *Met* in river water, tap water and juice samples.

The selectivity of the method was investigated using SWV by measuring 5.0 × 10^{-6} mol L^{-1} of methoxyfenozide in the presence of 11 interfering species such as pesticides (profluralin, lactofen, mandipropamid, metam sodium, fenthion) and metal ions (Ca^{2+}, Mg^{2+}, Cu^{2+}, Cd^{2+}, Zn^{2+}, Pb^{2+}). The interferent concentration was altered in the range from 5.0 × 10^{-7} to 5.0 × 10^{-5} mol L^{-1}, corresponding to the interferent/analyte ratios of 1:10, 1:5, 1:1, 5:1, and 10:1. The presence of Ca^{2+}, Mg^{2+}, Cd^{2+}, Zn^{2+}, lactofen, mandipropamid and metam sodium was not found to interfere with *Met* voltammetric response in the studied concentration range (percentage of the *Met* peak current change was less than 10% in comparison to the peak current value for uncontaminated *Met* solutions). The presence of lead and copper ions precluded proper determination of *Met* at a

concentration of 2.5 × 10^{-5} mol L^{-1} and higher, whereas the presence of fenthion and profluralin precluded proper determination of *Met* at 5.0 × 10^{-6} mol L^{-1} and above.

3.3. Interaction of methoxyfenozide with dsDNA

It has been widely recognized that the biological activities of a large number of biologically active compounds are related to their ability to interact with DNA [40]. Interactions between DNA and agents present in the environment often result in mutations of the DNA nucleotide sequence [41,42]. Plant protection products such as herbicides, insecticides, and fungicides are some examples of chemicals that may interact with nucleic acids [43]. Since methoxyfenozide is toxic to aquatic species and earthworms, double-stranded DNA, isolated from salmon sperm was selected to examine the interaction between *Met* and DNA. The interaction study was conducted using square wave voltammetry, cyclic voltammetry and UV–Vis spectroscopy. Because the oxidation signals of *Met* were not observed at a pH of the supporting electrolyte higher than 6.0, studies on the *Met*-dsDNA interaction were conducted at pH 4.5 (phosphate buffer). It should be mentioned that phosphate-buffered saline (PBS) of physiological pH value is the most commonly used buffer in such studies however, buffers of pH close to 4.5 are also used in interaction studies [26,44,45]. In the phosphate buffer of pH 4.5, *Met* also exhibited one oxidation peak, related to the irreversible anodic process. In the presence of double-stranded DNA, methoxyfenozide signals decreased and shifted to more positive potential values in both voltammetric techniques (Fig. 4), which indicated the occurrence of interaction between *Met* and dsDNA. Generally, the differences observed in the electrochemical behavior of the analyzed compound upon the addition of nucleic acid can be investigated by tracking the shift in the peak potential and by observing the changes occurring in the peak current [26]. The observed shift in the *Met* peak potential can be employed to estimate the interaction mode, whereas the peak current change can be used to evaluate the binding constant value. For peak potential shift, Carter and Bard [26,46] have reported that a positive shift is characteristic of the intercalative mode of interaction. Thus, the obtained results indicate the dominance of the intercalative mode for binding between methoxyfenozide and dsDNA. Subsequently, to confirm the intercalative binding mode, the ionic strength effect was studied, which is also a highly efficient parameter to distinguish the modes of binding between small molecules and DNA [18,45,47]. While the ionic strength of the reaction medium increased with the addition of salt (NaCl), charge compensation of the present

Table 1
Results obtained from *Met* determination in spiked juice and water samples with SWV technique.

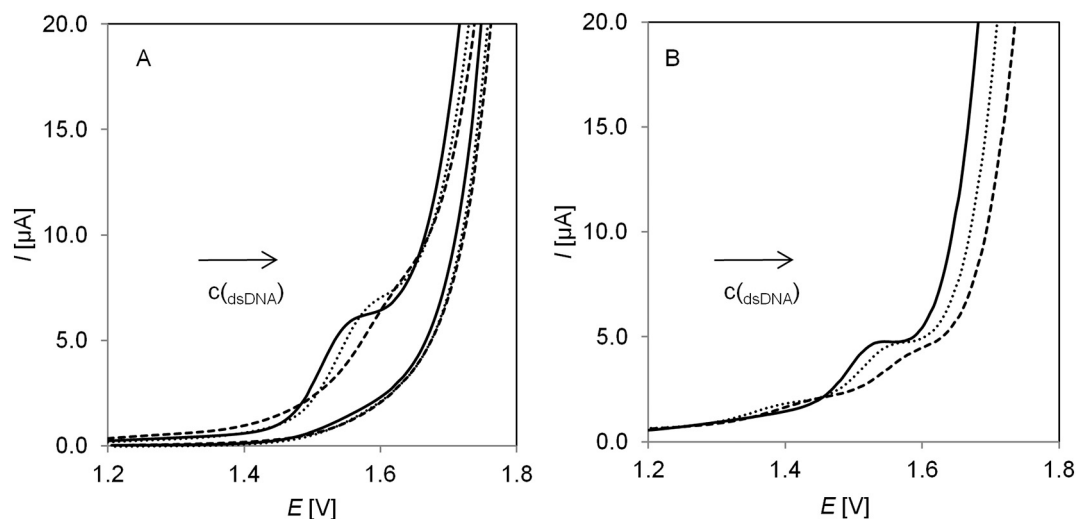| Added [μmol L^{-1}]	Found [μmol L^{-1}]	Precision [%]	Recovery [%]
Ljubljanica river water			
10.0	10.5	4.71	105
5.00	5.09	6.95	102
1.00	1.05	6.68	104
Tap water			
10.0	10.4	1.03	103
5.00	5.18	4.99	104
1.00	0.96	3.68	95.6
Grape juice			
10.0	10.5	8.62	105
5.00	5.19	2.76	104
2.50	2.57	2.46	103

Fig. 4. (A) Cyclic voltammograms of methoxyfenozide (c(Met) = 1.0×10^{-4} mol L^{-1}) recorded in the absence (straight line) and presence of dsDNA, c($_{dsDNA}$) = 20 mg L^{-1} (dotted line), and c($_{dsDNA}$) = 100 mg L^{-1} (dashed line). (B) SW voltammograms of Met (c(Met) = 3.0×10^{-5} mol L^{-1}) recorded in the absence (straight line) and presence of dsDNA, c($_{dsDNA}$) = 10 mg L^{-1} (dotted line), and c($_{dsDNA}$) = 50 mg L^{-1} (dashed line); supporting electrolyte: phosphate buffer, pH 4.5.

nucleotide phosphate by Na$^+$ would hinder the effect of electrostatic binding. Thus, complex formation throughout the electrostatic mode would decrease, whereas binding based on intercalation should remain virtually unaffected [18,47]. In the present study, the ionic strength was varied by gradually changing the NaCl concentration from 5.0 to 40.0 mmol L^{-1} in a voltammetric cell containing fixed concentrations of Met (c(Met) = 3.0×10^{-5} mol L^{-1}) and dsDNA c($_{dsDNA}$) = 30 mg L^{-1}) in phosphate buffer at pH 4.5. Square wave signals were recorded after the addition of each salt. As the NaCl concentration increased, no significant change was observed in the peak current of the Met-dsDNA complex. Consequently, the obtained result indicated that the interaction of Met with dsDNA is independent of the salt concentration, which confirms the intercalative binding mode.

The observed loss of methoxyfenozide signal upon the addition of dsDNA is apparently due to the formation of Met–dsDNA adduct with a large molecular weight, which should result in a decrease in the apparent diffusion coefficient. Thus, to evaluate the diffusion coefficient value, the formed Met-dsDNA adducts were examined by CV technique at various scan rates. In all the obtained cyclic voltammograms, a single anodic signal was observed. A linear dependence was noted between the peak current of

the Met-dsDNA adduct and the square root of the scan rate, whereas the slope of log I_p $vs.$ log v was equal to 0.47; such a finding indicates the diffusion-controlled nature of the observed phenomena. Most importantly, upon the addition of dsDNA to the methoxyfenozide solution, a significant decrease was observed in the slope of the I_p versus $v^{1/2}$ plot ($R \geq 0.990$) in comparison with the results obtained for free Met. The slope values obtained were 4.73 and 2.57 μA V$^{-1/2}$ s$^{-1/2}$ for Met in the absence and presence of DNA, respectively. Based on aforementioned data, the diffusion coefficient value of the free Met was calculated as 6.91×10^{-6} cm^2 s^{-1}, whilst for the bound Met (Met-dsDNA), the diffusion coefficient was equal to 2.09×10^{-6} cm^2 s^{-1} [48]. The decrease observed in the diffusion coefficient values confirmed the assumption that a decrease in the methoxyfenozide peak currents in the presence of double-stranded DNA was due to the binding between Met and slowly diffusing nucleic acid molecules. Furthermore, to verify whether the interaction between Met and dsDNA affected the kinetics of Met oxidation, the heterogeneous rate constants (k^o) were estimated by using calculated diffusion coefficient values. From the slopes of E_p versus ln($v^{1/2}$) plots [49], the values of the rate constants were determined as 2.1×10^{-3} s^{-1} (Met) and 1.1×10^{-3} s^{-1} (Met in the presence of double-stranded DNA); therefore, based on the
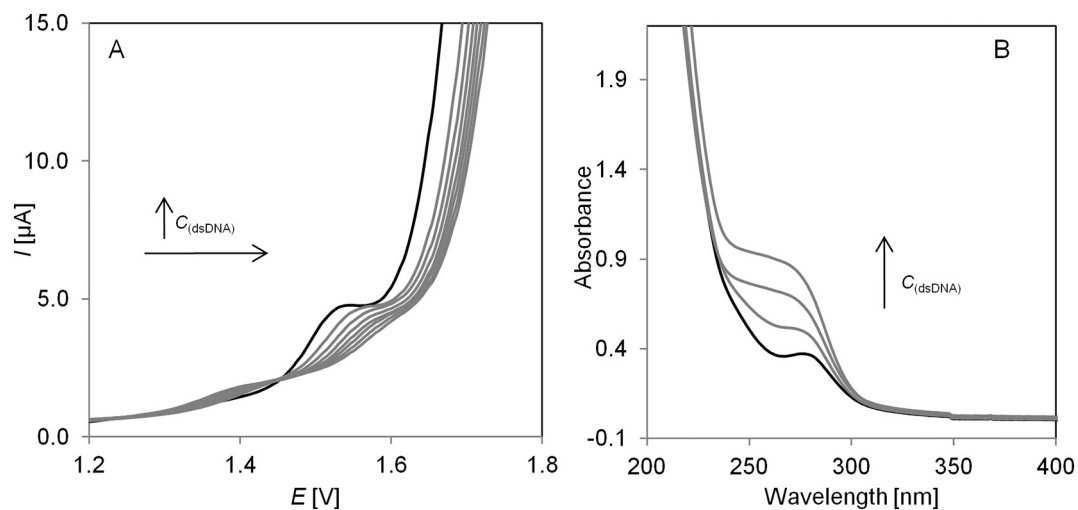
Fig. 5. (A) SW voltammograms of methoxyfenozide (c(Met) = 3.0×10^{-5} mol L^{-1}) recorded in the absence (blank line) and presence of DNA (c($_{dsDNA}$) = 10.0, 20.0, 40.0, 60.0, 80.0, and 100.0 mg L^{-1}, gray lines). (B) UV–vis spectra of Met (c(Met) = 1.0×10^{-4} mol L^{-1}) recorded in the absence (black line) and presence of dsDNA (c($_{dsDNA}$) = 8.0, 16.0, and 24.0 mg L^{-1}, gray lines); supporting electrolyte: phosphate buffer, pH 4.5.

Table 2

Values of calculated binding constant (K), and Gibbs free energy ($\Delta G°$) for *Met*-dsDNA interaction.

	SW voltammetry	UV–vis spectroscopy
K (M^{-1})	3.47×10^7	2.34×10^7
$\Delta G°$ (kJ mol^{-1})	-42.29	-41.34

obtained results it can be concluded that as presumed, the rate of electron transfer was lowered for *Met* in the form of the *Met*-dsDNA adducts.

Subsequently, SW voltammetry was used to evaluate the binding constant values of *Met*-dsDNA complexes. The reason for selecting the SWV technique for this purpose was its better peak resolution, and higher sensitivity in comparison to CV. As the *Met* signals decreased upon the addition of dsDNA, titrations were performed at the fixed *Met* concentration while changing the concentration of dsDNA (Fig. 5A). As can be seen in Fig. 5A, in the presence of an increasing amount of dsDNA, the *Met* peak current height gradually decreased. Thus, the following equation was used for the evaluation of the binding constant value [18,50].

$$\log\left(1/c_{(dsDNA)}\right) = \log K + \log\left[I_{Met}-_{dsDNA}/(I_{Met}-I_{Met}-_{dsDNA})\right] \qquad \text{Eq.(1)}$$

where K is the apparent binding constant, and I_{Met} and $I_{Met}-_{dsDNA}$ are the peak currents of the free guest (*Met*) and the formed adduct (*Met*–dsDNA), respectively. The binding constant calculated for the *Met*–dsDNA complex is listed in Table 2.

For a more detailed investigation of the *Met*-dsDNA interaction, a spectrophotometric study was also performed. Generally, spectral properties such as hypo- or hyperchromic shift may indicate the interactions occurring between an analyte and DNA. In the UV–vis spectra *Met* showed an absorption band at 276 nm (Fig. 5B). This absorption band increased and slightly shifted (blue shift ~10 nm) with the addition of increasing concentrations of DNA into the solution. The observed changes confirmed the occurence of interactions between *Met* and dsDNA. For comparison purpose, the binding constant value of the *Met*-dsDNA complex was estimated spectrophotometrically by applying the Benesi-Hildebrand equation [27,51].

$$A_0/(A-A_0) = \varepsilon_{Met}/(\varepsilon_{Met-dsDN}A-\varepsilon_{Met}) + \varepsilon_{Met}/(\varepsilon_{Met-dsDNA}-\varepsilon_{Met})$$
$$\times 1/K_f \; c_{(dsDNA)} \qquad \text{Eq.(2)}$$

where A_0 and A are the absorbances of the free and complexed *Met*, respectively, ε_{Met} and $\varepsilon_{Met-dsDNA}$ are the absorption coefficients of the free analyte and complexed analyte, respectively, and K_f is the binding constant. Table 2 shows the calculated binding constant value, which is in good agreement with the electrochemically obtained value.

The obtained K values proved the formation of a stable complex resulting from the close interaction between methoxyfenozide and dsDNA. To reflect the stability of the *Met*-dsDNA complex, the change in the Gibbs free energy ($\Delta G°$) was estimated with the equation Guziejewski et al. [16].

$$\Delta G° = -RT \ln K \qquad \text{Eq.(3)}$$

where K is the binding constant value; the other variables used have their usual meaning. The calculated $\Delta G°$ values were found to be negative (Table 2), which suggested that the *Met*-dsDNA interaction process was favorable and spontaneous.

4. Conclusion

The electrochemical behavior of methoxyfenozide was examined for the first time. The tested insecticide was found to be electrochemically active at a boron-doped diamond electrode and its oxidation was irreversible and diffusion-controlled. The obtained results clearly demonstrated the potential utility of a bare BDDE for square wave voltammetric determination of *Met*, which is of considerable significance owing to the fact that electrode

surface modification is a time-consuming process, and simultaneously, its repeatability is much worse. The proposed methodology is fast, has high precision, and can therefore be employed for the quantification of *Met* in water and juice samples. Furthermore, the simplicity, low apparatus cost, and environmental friendliness are the other main advantages of the presented voltammetric procedure, and thus, it can serve as an attractive alternative to very expensive and time-consuming chromatographic techniques. As methoxyfenozide is toxic to aquatic organisms, its interaction with double-stranded salmon sperm DNA was also examined. Both voltammetric and spectrophotometric techniques revealed the interaction between *Met* and dsDNA. Upon the addition of dsDNA, the peak current of *Met* decreased and also shifted to more positive potential values, while its absorption band increased and slightly shifted in the wavelength. Based on these correlations and the binding constant values calculated (a good correlation was found between the binding constants estimated through both techniques), it can be stated that strong interactions occur between *Met* and dsDNA, and the interaction mode is mainly intercalative.

Declaration of Competing Interest

The authors declare that they have no known competing financial interests or personal relationships that could have appeared to influence the work reported in this paper.

References

[1] D.B. Barr, L.L. Needham, Analytical methods for biological monitoring of exposure to pesticides: a review, J. Chromatogr. B 778 (2002) 5–29.

[2] E.R. Laws, W.J. Hayes, Handbook of Pesticide Toxicology, Academic Press, San Diego, 1991.

[3] D.P. Le, M. Thirugnanam, Z. Lidert, G.R. Carlson, RH-2485: a new selective insecticide for caterpillar control, Brighton Crop Protection Conference, Pests & Diseases, Farnham, Surrey Brighton, England 1996, pp. 481–486.

[4] D. Lin, X. Jin-Zhong, D. Tao, Z. Jun-Jie, W. Bin, S. Chong-Yu, J. Yuan, Determination of tebufenozide and methoxyfenozide residues in vegetables using liquid chromatography-electrospray tandem mass spectrometry, Chin. J. Anal. Chem. 36 (2008) 87–90.

[5] G.R. Carlson, T.S. Dhadialla, R. Hunter, R.K. Jansson, C.S. Jany, Z. Lidert, R.A. Slawecki, The chemical and biological properties of methoxyfenozide, a new insecticidal ecdysteroid agonist, Pest Manag. Sci. 57 (2001) 115–119.

[6] A. European Food Safety, M. Arena, D. Auteri, S. Barmaz, G. Bellisai, A. Brancato, D. Brocca, L. Bura, H. Byers, A. Chiusolo, D. Court Marques, F. Crivellente, C. De Lentdecker, M. De Maglie, M. Egsmose, Z. Erdos, G. Fait, L. Ferreira, M. Goumenou, L. Greco, A. Ippolito, F. Istace, S. Jarrah, D. Kardassi, R. Leuschner, C. Lythgo, J.O. Magrans, P. Medina, I. Miron, T. Molnar, A. Nougadere, L. Padovani, J.M. Parra Morte, R. Pedersen, H. Reich, A. Sacchi, M. Santos, M. Serafimova, R. Sharp, A. Stanek, F. Streissl, J. Sturma, C. Szentes, J. Tarazona, A. Terron, A. Theobald, B. Vagenende, A. Verani, L. Villamar-Bouza, Peer review of the pesticide risk assessment of the active substance methoxyfenozide, EFSA J. 15 (2017), e04978, .

[7] J.H. Choi, M.I.R. Mamun, E.H. Shin, H.K. Kim, A.M.A. El-Aty, J.H. Shim, Determination of methoxyfenozide residues in water and soil by liquid chromatography: evaluation of its environmental fate under laboratory conditions, Toxicol. Res. 24 (2008) 207–212.

[8] S. Song, C. Zhang, Z. Chen, F. He, J. Wei, H. Tan, X. Li, Simultaneous determination of neonicotinoid insecticides and insect growth regulators residues in honey using LC–MS/ MS with anion exchanger-disposable pipette extraction, J. Chromatogr. A 1557 (2018) 51–61.

[9] J.D. Berset, S. Mermer, A.E. Robel, V.M. Walton, M.L. Chien, J.A. Field, Direct residue analysis of systemic insecticides and some of their relevant metabolites in wines by liquid chromatography – mass spectrometry, J. Chromatogr. A 1506 (2017) 45–54.

[10] A. Morales, I. Ruiz, J. Oliva, A. Barba, Determination of sixteen pesticides in peppers using high-performance liquid chromatography/mass spectrometry, J. Environ. Sci. Health Part B Pestic. Food Contam. Agric. Wastes 46 (2011) 525–529.

[11] K. Zarei, A. Khodadadi, Very sensitive electrochemical determination of diuron on glassy carbon electrode modified with reduced graphene oxide–gold nanoparticle–Nafion composite film, Ecotoxicol. Environ. Saf. 144 (2017) 171–177.

[12] A. Sunyer, A. González-Navarro, M.P. Serra-Roig, N. Serrano, M.S. Díaz-Cruz, J.M. Díaz-Cruz, First application of carbon-based screen-printed electrodes for the voltammetric determination of the organic UV filters oxybenzone and octocrylene, Talanta 196 (2019) 381–388.

[13] H.S. Ali, A.A. Abdullah, P.T. Pınar, Y. Yardım, Z. Şentürk, Simultaneous voltammetric determination of vanillin and caffeine in food products using an anodically pretreated

boron-doped diamond electrode: its comparison with HPLC-DAD, Talanta 170 (2017) 384–391.

[14] S. Smarzewska, A. Jasińska, W. Ciesielski, D. Guziejewski, First electroanalytical studies of profluralin with square wave voltammetry using glassy carbon electrode, Electroanalysis 29 (2017) 244–248.

[15] M. Brycht, K. Konecka, K. Sipa, S. Skrzypek, V. Mirčeski, Electroanalysis of the anthelmintic drug bithionol at edge plane pyrolytic graphite electrode, Electroanalysis 31 (2019) 2246–2253.

[16] D. Guziejewski, V. Mirceski, D. Jadresko, Measuring the electrode kinetics of surface confined electrode reactions at a constant scan rate, Electroanalysis 27 (2015) 67–73.

[17] V. Mirceski, D. Guziejewski, M. Bozem, I. Bogeski, Characterizing electrode reactions by multisampling the current in square-wave voltammetry, Electrochim. Acta 213 (2016) 520–528.

[18] Y. Temerk, H. Ibrahim, Electrochemical studies and spectroscopic investigations on the interaction of an anticancer drug flutamide with DNA and its analytical applications, J. Electroanal. Chem. 736 (2015) 1–7.

[19] K. Morawska, K. Jedlińska, S. Smarzewska, R. Metelka, W. Ciesielski, D. Guziejewski, Analysis and DNA interaction of the profluralin herbicide, Environ. Chem. Lett. 17 (2019) 1359–1365.

[20] A. Hájková, J. Barek, V. Vyskočil, Voltammetric determination of 2-aminofluoren-9-one and investigation of its interaction with DNA on a glassy carbon electrode, Electroanalysis 27 (2015) 101–110.

[21] M. Ibrahim, H. Ibrahim, N.B. Almandil, M.A. Sayed, A.-N. Kawde, A new hybrid nanocomposite electrode based on Au/CeO$_2$-decorated functionalized glassy carbon microspheres for the voltammetric sensing of quercetin and its interaction with DNA, Anal. Methods 12 (2020) 2846–2857.

[22] M. Ibrahim, H. Ibrahim, N.B. Almandil, M.A. Sayed, A.-N. Kawde, Y. Aldaqdouq, A novel platform based on Au$-$CeO$_2$@MWCNT functionalized glassy carbon microspheres for voltammetric sensing of valrubicin as bladder anticancer drug and its interaction with DNA, Electroanalysis 32 (2020) 2146–2155.

[23] Y. Temerk, M. Ibrahim, H. Ibrahim, W. Schuhmann, Comparative studies on the interaction of anticancer drug irinotecan with dsDNA and ssDNA, RSC Adv. 8 (2018) 25387–25395.

[24] Y. Temerk, H. Ibrahim, Binding mode and thermodynamic studies on the interaction of the anticancer drug dacarbazine and dacarbazine–Cu(II) complex with single and double stranded DNA, J. Pharm. Biomed. Anal. 95 (2014) 26–33.

[25] S.S. Kalanur, U. Katrahalli, J. Seetharamappa, Electrochemical studies and spectroscopic investigations on the interaction of an anticancer drug with DNA and their analytical applications, J. Electroanal. Chem. 636 (2009) 93–100.

[26] S. Shahzad, B. Dogan-Topal, L. Karadurmus, M.G. Caglayan, T. Taskin Tok, B. Uslu, A. Shah, S.A. Ozkan, Electrochemical, spectroscopic and molecular docking studies on the interaction of calcium channel blockers with dsDNA, Bioelectrochemistry 127 (2019) 12–20.

[27] Y. Temerk, M. Ibrahim, H. Ibrahim, M. Kotb, Interactions of an anticancer drug lomustine with single and double stranded DNA at physiological conditions analyzed by electrochemical and spectroscopic methods, J. Electroanal. Chem. 769 (2016) 62–71.

[28] K. Morawska, T. Popławski, W. Ciesielski, S. Smarzewska, Interactions of lamotrigine with single- and double-stranded DNA under physiological conditions, Bioelectrochemistry 136 (2020) 107630.

[29] S.T. Saito, G. Silva, C. Pungartnik, M. Brendel, Study of DNA-emodin interaction by FTIR and UV-vis spectroscopy, J. Photochem. Photobiol. B Biol. 111 (2012) 59–63.

[30] G. Tyagi, S. Charak, R. Mehrotra, Binding of an indole alkaloid, vinblastine to double stranded DNA: a spectroscopic insight in to nature and strength of interaction, J. Photochem. Photobiol. B Biol. 108 (2012) 48–52.

[31] M. Brycht, A. Leniart, J. Robak, B. Burnat, K. Kaczmarska, K. Sipa, S. Skrzypek, First electrochemical study of the fungicide oxycarboxin, Int. J. Environ. Anal. Chem. 97 (2017) 1298–1314.

[32] K. Morawska, N. Festinger, G. Chwatko, R. Głowacki, W. Ciesielski, S. Smarzewska, Rapid electroanalytical procedure for sesamol determination in real samples, Food Chem. 309 (2020) 125789.

[33] D. Stanković, E. Mehmeti, L. Svorc, K. Kalcher, New electrochemical method for the determination of β-carboline alkaloids, harmalol and harmine, in human urine samples and in Banisteriopsis caapi, Microchem. J. 118 (2015) 95–100.

[34] P. Manjunatha, Y. Arthoba Nayaka, B.K. Chethana, C.C. Vidyasagar, R.O. Yathisha, Development of multi-walled carbon nanotubes modified pencil graphite electrode for the electrochemical investigation of aceclofenac present in pharmaceutical and biological samples, Sens. Bio Sens. Res. 17 (2018) 7–17.

[35] M. Brycht, A. Leniart, J. Zavašnik, A. Nosal-Wiercińska, K. Wasiński, P. Półrolniczak, S. Skrzypek, K. Kalcher, Synthesis and characterization of the thermally reduced graphene oxide in argon atmosphere, and its application to construct graphene paste electrode as a naptalam electrochemical sensor, Anal. Chim. Acta 1035 (2018) 22–31.

[36] D.K. Gosser, Cyclic Voltammetry, VCH, New York, 1994.

[37] S. Horrobin, D.W. Ramsay, L.F.A. Mason, Phenidone (1-phenyl-3-pyrazolidone): oxidation, J. Photogr. Sci. 11 (1963) 145–149.

[38] J. Grimshaw, Electrochemical Reactions and Mechanisms in Organic Chemistry, Elsevier, 2000.

[39] L.B.O. dos Santos, G. Abate, J.C. Masini, Determination of atrazine using square wave voltammetry with the Hanging Mercury Drop Electrode (HMDE), Talanta 62 (2004) 667–674.

[40] L.S. Lerman, Structural considerations in the interaction of DNA and acridines, J. Mol. Biol. 3 (1961) 18–IN14.

[41] Q. Zhang, C. Wang, W. Liu, X. Zhang, S. Zhuang, Evidence for DNA-diquat interaction and cytotoxicity in in vitro rat cells, Environ. Chem. Lett. 10 (2012) 35–39.

[42] M. Blackburn, M. Gait, Nucleic Acids in Chemistry and Biology, IRL Press, New York, 1990.

[43] D. Guziejewski, K. Morawska, T. Popławski, R. Metelka, W. Ciesielski, S. Smarzewska, Lactofen – electrochemical sensing and interaction with dsDNA, Electroanalysis 30 (2018) 94–100.

[44] X. Tian, Y. Song, H. Dong, B. Ye, Interaction of anticancer herbal drug berberine with DNA immobilized on the glassy carbon electrode, Bioelectrochemistry 73 (2008) 18–22.

[45] Y. Temerk, M. Ibrahim, H. Ibrahim, M. Kotb, Interactions of an anticancer drug Formestane with single and double stranded DNA at physiological conditions, J. Photochem. Photobiol. B Biol. 149 (2015) 27–36.

[46] M.T. Carter, A.J. Bard, Voltammetric studies of the interaction of tris(1,10-phenanthroline)cobalt(III) with DNA, J. Am. Chem. Soc. 109 (1987) 7528–7530.

[47] M.V. del Pozo, C. Alonso, F. Pariente, E. Lorenzo, DNA biosensor for detection of helicobacter pylori using Phen-dione as the electrochemically active ligand in osmium complexes, Anal. Chem. 77 (2005) 2550–2557.

[48] A.J. Bard, L.R. Faulkner, Electrochemical Methods: Fundamentals and Applications, John Wiley & Sons, New York, 2000.

[49] R.S. Nicholson, Theory and application of cyclic voltammetry for measurement of electrode reaction kinetics, Anal. Chem. 37 (1965) 1351–1355.

[50] N. Shahabadi, N.H. Moghadam, Determining the mode of interaction of calf thymus DNA with the drug sumatriptan using voltammetric and spectroscopic techniques, Spectrochim. Acta A Mol. Biomol. Spectrosc. 99 (2012) 18–22.

[51] Z. Tian, Z. Zhao, F. Zang, Y. Wang, C. Wang, Spectroscopic study on the interaction between naphthalimide–polyamine conjugates and DNA, J. Photochem. Photobiol. B Biol. 138 (2014) 202–210.

Łódź, dn. 9 kwietnia 2021 r.

Prof. dr hab. Witold Ciesielski

Wydział Chemii UŁ

Niniejszym oświadczam, że mój udział w każdej z publikacji wchodzących w skład pracy doktorskiej mgr Kamili Morawskiej:

Kamila Morawska* Witold Ciesielski ,Sylwia Smarzewska*
"First electroanalytical studies of methoxyfenozide and its interactions with dsDNA"
Journal of Electroanalytical Chemistry (2021), 882, 115030.

Kamila Morawska*, Tomasz Popławski, Witold Ciesielski, Sylwia Smarzewska
"Interactions of lamotrigine with single- and double-stranded DNA under physiological conditions"
Bioelectrochemistry (2020), 136, 107630

Kamila Morawska*, Natalia Festinger, Grażyna Chwatko, Rafał Głowacki, Witold Ciesielski, Sylwia Smarzewska*
"Rapid electroanalytical procedure for sesamol determination in real samples"
Food Chemistry (2020), 309, 125789.

Dariusz Guziejewski*, Kamila Morawska, Tomasz Popławski, Radovan Metelka, Witold Ciesielski, Sylwia Smarzewska*
"Lactofen – electrochemical sensing and interaction with dsDNA"
Electroanalysis (2018), 30 (1), 94-100.

polegał na inicjacji tematycznej i udziale w końcowym opracowywaniu tekstu. Całkowity wkład w każdej z powyższych publikacji oceniam na 5%

Witold Ciesielski

**WYDZIAŁ
CHEMII**

Uniwersytet Łódzki

dr Sylwia Smarzewska
adiunkt
Zakład Analizy Instrumentalnej
Katedra Chemii Nieorganicznej i Analitycznej

Łódź, dnia 09.04.2021 r.

Oświadczam, iż:

-mój udział w pracy

Kamila Morawska, Witold Ciesielski, Sylwia Smarzewska "First electroanalytical studies of methoxyfenozide and its interactions with dsDNA" Journal of Electroanalytical Chemistry (2021), 882, 115030

oceniam na 15%;

-mój udział w pracy

Kamila Morawska, Tomasz Popławski, Witold Ciesielski, Sylwia Smarzewska "Interactions of lamotrigine with single- and double-stranded DNA under physiological conditions" Bioelectrochemistry (2020), 136, 107630
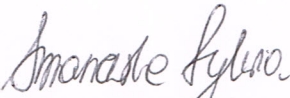
oceniam na 20%;

-mój udział w pracy

Kamila Morawska, Natalia Festinger, Grażyna Chwatko, Rafał Głowacki, Witold Ciesielski, Sylwia Smarzewska "Rapid electroanalytical procedure for sesamol determination in real samples" Food Chemistry (2020), 309, 125789

oceniam na 20%;

-mój udział w pracy

Dariusz Guziejewski, Kamila Morawska, Tomasz Popławski, Radovan Metelka, Witold Ciesielski, Sylwia Smarzewska "Lactofen – electrochemical sensing and interaction with dsDNA" Electroanalysis (2018), 30 (1), 94-100

oceniam na 25%.

Dr Sylwia Smarzewska

tel.:48 42 635 58 08
ul. Pomorska 163, 90-236 Łódź
e-mail: sylwia.smarzewska@chemia.uni.lodz.pl

www.chemia.uni.lodz.pl/kai

WYDZIAŁ
CHEMII
Uniwersytet Łódzki

dr Dariusz Guziejewski
adiunkt
Zakład Analizy Instrumentalnej

Oświadczam, że mój udział w pracy:

Dariusz Guziejewski, Kamila Morawska, Tomasz Popławski, Radovan Metelka, Witold Ciesielski,
Sylwia Smarzewska;
"Lactofen – electrochemical sensing and interaction with dsDNA";
Electroanalysis, (2018), 30 (1), 94-100

polegał na dyskusji przy opracowywaniu wyników i redakcji manuskryptu. Swój wkład
oceniam na 25%.

Materiał tej publikacji nie będzie wchodził w skład mojej rozprawy habilitacyjnej.

/Dariusz Guziejewski/

prof. dr hab. Tomasz Popławski
Katedra Genetyki Molekularnej

Oświadczam, iż mój udział w każdej z poniższych publikacji wchodzących w skład pracy doktorskiej mgr Kamili Morawskiej:

Kamila Morawska*, Tomasz Popławski, Witold Ciesielski, Sylwia Smarzewska;
"Interactions of lamotrigine with single- and double-stranded DNA under physiological conditions" Bioelectrochemistry (2020), 136, 107630.

Dariusz Guziejewski*, Kamila Morawska, Tomasz Popławski, Radovan Metelka, Witold Ciesielski, Sylwia Smarzewska* "Lactofen – electrochemical sensing and interaction with dsDNA" Electroanalysis (2018), 30 (1), 94-100.

oceniam na 5%.

**WYDZIAŁ
CHEMII**
Uniwersytet Łódzki

dr hab. Grażyna Chwatko, prof. UŁ
Katedra Chemii Środowiska
tel. 042-635-58-43

Oświadczenie

Oświadczam, że mój udział w pracy:

Kamila Morawska, Natalia Festinger, Grażyna Chwatko, Rafał Głowacki, Witold Ciesielski, Sylwia Smarzewska, *Rapid electroanalytical procedure for sesamol determination in real samples*, Food Chemistry (2020), 309, 125789.

polegał na zaplanowaniu i wykonaniu eksperymentu chromatograficznego oraz opisie tej części wyników badań w manuskrypcie i późniejszej korekcie. Udział ten oceniam na 15%.

Grażyna Chwatko

Katedra Chemii Środowiska
ul. Pomorska 163, 90-236 Łódź
e-mail: grazyna.chwatko@chemia.uni.lodz.pl

www.uni.lodz.pl

**FACULTY OF
CHEMISTRY**

University of Lodz

prof. dr hab. Rafał Głowacki
Department of Environmental Chemistry
163 Pomorska Str.
90-236 Łódź
Poland
Phone: +48 42 635 58 35

Oświadczam, że mój udział w pracy:

Kamila Morawska*, Natalia Festinger, Grażyna Chwatko, Rafał Głowacki, Witold Ciesielski, Sylwia Smarzewska* "Rapid electroanalytical procedure for sesamol determination in real samples", Food Chemistry (2020), 309, 125789,

polegał na konsultacjach na etapie eksperymentu chromatograficznego oraz pisania manuskryptu, która dotyczyła tej części wyników. Całkowity wkład oceniam na 5%.

Łódź, 08.04.2021.

Department of Environmental Chemistry
Faculty of Chemistry, University of Łódź
163 Pomorska Str., 90-236 Łódź, tel/fax (+48) (42) 635-58-32,
http://www.chemia.uni.lodz.pl/kchs,
tel. (+48) (42) 635-58-35, e-mail: glowar@uni.lodz.pl

Ing. Radovan Metelka, Ph.D.

University of Pardubice, Faculty of Chemical Technology,
Department of Analytical Chemistry
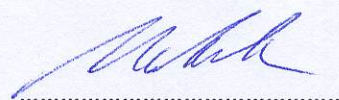Studentská 95, 532 10 Pardubice 2

radovan.metelka@upce.cz

Publication co-author statement

I hereby confirm that M.Sc. Kamila Morawska has significantly contributed to the below mentioned publication. She was involved in all stages pertaining to publication preparation.

The publication together with percentage contribution can be found below:

1. Dariusz Guziejewski* (25%), Kamila Morawska (35%), Tomasz Popławski (5%), Radovan Metelka (5%), Witold Ciesielski (5%), Sylwia Smarzewska* (25%), "Lactofen – electrochemical sensing and interaction with dsDNA", Electroanalysis (2018), 30 (1), 94-100.

Signature

WYDZIAŁ CHEMII
Uniwersytet Łódzki

Łódź, dnia 15.04.2021r.

mgr Natalia Festinger
doktorant
Zakład Analizy Instrumentalnej

Oświadczam, iż mój udział w poniższej publikacji wchodzącej w skład pracy doktorskiej mgr Kamili Morawskiej

Kamila Morawska*, Natalia Festinger, Grażyna Chwatko, Rafał Głowacki, Witold Ciesielski, Sylwia Smarzewska* "Rapid electroanalytical procedure for sesamol determination in real samples"

oceniam na 5%.

Materiał tej publikacji nie będzie wchodził w skład mojej rozprawy doktorskiej.

Natalia Festinger